

Lib

93

STUDIES OF THE ELECTRONIC PROPERTIES OF SOME  
TRANSITION METAL ION GLASSES

BY

SADEGH FERIDOONIAN, M.Phil.

Ph.D.

This thesis is submitted in fulfilment  
of the requirements for the degree of  
Doctor of Philosophy at  
Brunel University Uxbridge, 1991.

**PAGE**  
**NUMBERING**  
**AS ORIGINAL**

### ACKNOWLEDGEMENTS.

I would like to express my deep and sincere appreciation and gratitude to my research supervisor Professor C.A. Hogarth, for his valuable discussions, suggestions, and constructive criticisms and from whose ideas this thesis has been developed. He never failed in providing adequate assistance at all the difficult stages, theoretical or practical.

I extend my most sincere thanks to the following people:

i) Mr. R. Bulpett and technical staff of the Experimental Technique Centre;

ii) Dr. K.A.K. Lott and Mr. P. Hemming of the Department of Chemistry, for their guidance and encouragement given willingly at all times for the ESR, Atomic Absorption, Ultraviolet and IR measurements.

iii) The teaching staff and technical staff who have always been available when help and advice were needed, and to all colleagues in the Glasses, and the Thin-Films Groups for useful discussion during this work.

Finally I wish to express my profound feeling of indebtedness to my parents for their financial support and to my wife for her continuous encouragement and patience.

## ABSTRACT

Three series of glasses were prepared and studied. They include the barium -vanadate , the barium-tellurite series and a series of tellurium-vanadate glasses, the first two series being modified by the inclusion of barium chloride and the third by the addition of barium oxide. It was found for each series that glasses could be obtained within well-defined limits of composition. Properties studied included a detailed investigation using electron paramagnetic resonance (electron spin resonance) which enables reduced valency states to be evaluated and measurements of density, electrical conductivity and optical absorption measurements in the vicinity of the absorption edge and in the infra-red region were made. X-ray diffraction was used to establish the non-crystalline character of the samples. Standard wet chemical analysis and atomic absorption analysis were used to determine the total vanadium ion content for comparison with values inferred from the e.s.r. measurements . All samples were studied after the glass forming and initial annealing process but a number of samples were given longer periods of annealing. The semiconducting properties of the glass systems without halogen or BaO addition were typical of many similar glass systems. The e.s.r. results gave useful estimates of the normal and reduced valency constituents and these compared reasonably with the results of chemical analysis. The replacement of oxygen by chlorine gave results, which although comparable with earlier reports on copper- phosphate glasses containing chlorine, nevertheless presented problem of interpretation. As the BaCl<sub>2</sub> content was increased, the electrical conductivity and concentration of the paramagnetic ions decreased steadily up to about 7mole% but with further addition of BaCl<sub>2</sub>, the DC conductivity and spin concentration increased again. The possible reasons for this observation were discussed and involved a change in the behaviour of chlorine ion bonding or possibly a clustering of chlorine ions for samples with higher chlorine content. The results are discussed in terms of recent ideas on the science of amorphous materials.

## CONTENTS.

	Page No.
ABSTRACT:	i
ACKNOWLEDGEMENTS:	ii
LIST OF TABLES AND FIGURES:	iii
<u>CHAPTER 1. INTRODUCTION:</u>	1
1.1 Electronic transport in crystalline solids	1
1.2 Theory of glassy amorphous semiconductors	2
1.3 Preparation of glasses and amorphous solids	3
1.3.1 Thermal evaporation	4
1.3.2 Cooling from the melt	4
1.3.3 Other methods	5
1.4 Glass formation	6
1.5 Classification of semiconducting glasses	8
1.6 Glass-formers and modifiers	9
 <u>CHAPTER 2. THEORETICAL BACKGROUND OF ELECTRONIC CHARACTERISTIC OF DISORDERED MATERIALS:</u>	
2.1 Introduction	11
2.2 The electronic structure of amorphous solids	14
2.3 Band structure of non-crystalline solids	16
2.3.1 Basic band model	16
2.3.2 The Cohen, Fritzsche and Ovshinsky model(CFO)	17
2.3.3 The Davis and Mott model	19
2.3.4 Marshall and Owen model	19
2.4 Electrical conduction of - amorphous semiconductors	20
2.5 Temperature dependence of d.c. conductivity	23
2.6 Hopping conduction	24
2.7 Optical properties of amorphous materials	27
2.8 Polaron formation and transport	30
2.9 Experimental data on conduction in - transition-metal oxide crystal	32
 <u>CHAPTER 3. REVIEW OF PREPARATION, STRUCTURE AND CONDUCTIVITY MECHANISM OF TRANSITION METAL OXIDE GLASSES:</u>	
3.1 Preparation of amorphous transition - metal oxides.	35
3.2 Classification of transition metal - oxide glasses.	35
3.3 Binary glass systems containing transition- metal ions.	36

3.4	Ternary glass systems containing transition-metal ions.	37
3.5	The transition metal ion valence state.	39
3.6	The influence of vanadium valence states- on glass formation.	41
3.7	The chemical structure on vanadate glasses	42
3.8	Phase separation.	42
3.9	Conduction in transition metal oxides	43
3.10	Conduction in vanadate glasses.	45

#### CHAPTER 4                      GLASS PREPARATION AND STRUCTURAL INVESTIGATIONS:

4.1	Glass preparation	50
4.2	X-ray diffraction investigation	53
4.3	Density measurements	53
4.4	Molar volume	54
4.5	Results and discussion	55
4.6	Electron spin resonance (E.S.R)	55
4.7	Wet chemical analysis	58
4.8	Atomic absorption analysis	58
4.9	Electron Spin resonance measurements	59
4.10	Results and discussion	61

#### CHAPTER 5.                      OPTICAL PROPERTIES:

5.1	Infrared spectroscopy	64
5.1.1	Basic principle	64
5.1.2	Experimental methods	68
5.1.3	Results and discussions	69
5.2	Ultra-violet and visible spectroscopy	72
5.2.1	Introduction	72
5.2.2	Experimental methods	74
5.2.3	Results and discussion	75

#### CHAPTER 6                      ELECTRICAL PROPERTIES:

6.1	D.C. conductivity	77
6.2	Preparation of specimens	80
6.3	Electrical circuit and measuring methods	81
6.4	Results	82
6.5	Discussion.	85

#### CHAPTER 7.                      SUMMARY AND CONCLUSION:                      88

#### REFERENCES:                      95

## CHAPTER 1.

### 1.0. INTRODUCTION.

#### 1.1. ELECTRONIC TRANSPORT IN CRYSTALLINE SOLIDS.

In metals and crystalline semiconductors such as silicon, germanium, III-V and II-IV compounds, the electronic charge transport can be described by the free-electron approach within the limits of the effective mass approximation. Carriers have relatively wide bands of allowed energy and the mobility is high implying a large mean free path. In this situation charge transport is limited by scattering of the carriers by a range of processes. There is also large number of crystalline materials for which these concept are not valid because they have narrow bands of allowed energies. This implies that curvature of the parabolic relation between the energy  $E$  and the wave number  $K$  become small and the effective mass  $m^* = \hbar^2/4\pi^2(d^2E/dk^2)^{-1}$  become larger. As a consequence carriers have low mobilities and short mean-free-paths resulting effectively in their localisation. In some instances conduction takes place by hopping between localised states when the conditions of temperature and pressure allow. Examples of materials which show this kind of behaviour are certain transition metal oxides and some organic compounds such as anthracene. The essential feature is a small overlap of the wave function forming the conduction and valence bands as in a molecular crystal. However as will be described below there is a wide range of non-crystalline materials having low free carrier densities, low carrier mobilities, and therefore

low conductivities, in which electronic conduction is by a hopping process. The subject of this thesis is electronic transport in transition-metal oxide glasses.

## 1.2. THEORY OF GLASSY AMORPHOUS SEMICONDUCTORS.

The current theoretical status is similar to that of crystalline semiconductors some fifty years ago when the first major advances in the band theory of crystals were made. Band theory was built on the universal features of the electronic structure of crystals. Amorphous semiconductors by contrast are examples of disordered materials (see Fig. 1.1). They should also possess some features related to those of crystals. Experiments on amorphous semiconductors have probed just those aspects of the electronic structure of disordered material, that differ most from the corresponding aspects of crystals. Theory and experiment on amorphous semiconductors are therefore very illuminating with respect to the larger subject of the electronic structure of disordered materials. In an amorphous material the atoms may have some local organisation or short range order, but lack the periodic structure, that is, the long range order of crystals over a distance greater than a few atomic radii. The most important elements that exhibit such behaviour are silicon and germanium from group IV of the Periodic Table, arsenic, antimony and bismuth from group V and sulphur, selenium and tellurium from group VI (the chalcogenides) all in thin film form, although sulphur, tellurium and selenium can form bulk glassy structures. Other elements drawn from all over the Periodic Table



may be present as well, usually as minority constituents. These elements form a variety of covalent amorphous structures that have excellent short range but no long-range order. They may be single elements such as bulk selenium, tellurium or films of silicon or germanium, and may be multi-component alloys that form glasses over a broad range of compositions. In crude outline the arrangements of atoms or molecules vary from those that are primarily linear in character for the group VI elements towards planar structure as group V elements are added and then towards three-dimensional network structures as group IV elements are added. It is convenient to represent such a wide variety of material and structures by a single model. Sir Nevil Mott<sup>1</sup> first defined an ideal covalent glass as a one, two or three-dimensional random network with excellent short-range and no long-range order.

Glasses of a more conventional kind have been prepared for many centuries from oxide materials (traditionally silicates). In recent years a variety of glass-forming oxides e.g.  $B_2O_3$ ,  $V_2O_5$ ,  $MoO_3$ ,  $P_2O_5$  and  $TeO_2$  have emerged, and these are normally heated with other oxides particularly those of transition metals to form a range of useful and interesting glasses.

### 1.3. PREPARATION OF GLASSES AND AMORPHOUS SOLIDS.

Amorphous solids are prepared by methods which inhibit crystallisation. There are various methods of preparing amorphous solids from the solid, liquid or vapour phases. Each method is appropriate for certain groups of materials. The

vitreous solids or glasses are prepared by cooling their melts and are structurally continuous with the parent phase whereas amorphous thin films are prepared by other methods. The following are the most commonly used methods.

#### 1.3.1. Thermal evaporation.

Many of the tetrahedral elemental films and other amorphous semiconductors are prepared by vacuum evaporation in the thin film form. Thermal evaporation is carried out in high vacuum. The material is put in a suitable boat or directly under an electric filament and is evaporated by simple heating or by electron beam bombardment. The evaporated material is allowed to condense on a substrate, forming films of the required thickness by the adjustment of the various factors involved. This technique involves several experimental variables such as filament temperature, source to substrate separation, substrate cleaning and residual gas pressure. It is difficult to control all these parameters.

#### 1.3.2. Cooling from the melt.

Glasses which are needed in bulk form are generally prepared by this method. Preparation of the glass from its melt should be rapid enough to avoid crystallisation. The cooling rate required depends upon the viscosity of the liquid. If the glass is cooled at a faster rate than a critical value, there are fewer chances of nucleation, growth and crystallisation. The most rapid technique is that of super-cooling which can involve quenching rates higher than  $10^7$  deg./sec. However, silicate glasses and most of the

chalcogenides require very small cooling rates and can be readily prepared by this method. Most of the glasses in the chalcogenide group and transition metal oxide glasses can be readily obtained by cooling the melt. Materials which can be formed from liquids after supercooling are known to have structures similar to the liquid phase and show the features of glass transformation. When glasses are made from more than one component, the melt is kept for a longer time before cooling in order to achieve a homogeneous mixture.

#### 1.3.3. Other methods.

There are some other methods used in making amorphous solids, for example R.F sputtering and glow discharge decomposition. The glow discharge method is used to obtain amorphous films from mixtures of the elements by decomposition, e.g.  $\text{SiO}_2$  can be obtained from triethyl silicate. In the sputtering method, either direct current(d.c.) or radio frequency(R.F) fields can be employed to obtain thin films. High energy ions are accelerated and directed onto a target of the material to be sputtered. The atoms knocked out of the materials are collected on the substrate. The sputtering technique is preferred over the glow discharge method and other methods to produce thin films as the sputtering yields are uniform for different elements. This makes it suitable for mixed chalcogenides and other glasses with several constituents. Examples of compounds prepared by this technique are Ge-Se-Te-As with different compositions.

#### 1.4. GLASS FORMATION.

Zachariasen<sup>2</sup> pointed out that the ultimate condition for glass formation is an extended three-dimensional network lacking periodicity, with an energy content comparable with that of the corresponding crystalline network. He discussed the structure of glasses and proposed some rules in predicting new glass-forming oxides. The development of further understanding of the structure was provided by Rawson<sup>3</sup>. In general, substances are more stable in a crystalline than that in a glassy state, i.e. the free energy is less for a crystal than for a glass of similar chemical composition. Therefore, to form a glass, crystallization must be bypassed. In making a glass by the method of cooling from the melt, a set of factors such as cooling rate, the viscosity and the density have to be considered. The method of obtaining amorphous solids by cooling the melt can yield homogeneous amorphous solids only when cooled above a minimum critical rate. The critical rate ( $dT/dt$ ) is closely related to the viscosity ( $\eta$ ) and the melting point  $T_m$  of the materials and is given by Sarjeant and Roy<sup>4</sup> as:

$$dT/dt = 2 \times 10^{-6} \cdot (T_m)^2 \cdot R / V \eta$$

where  $V$  is the molar volume and  $R$  is the gas constant.

When the melt is cooled, the glass formation sets in at a transformation temperature  $T_g$ , which is characteristic of the glass. Figure 1.2 shows a typical volume-temperature curve for a material in its liquid, glassy and crystalline forms. As the temperature of its liquid is reduced through its freezing

point,  $T_f$ , it may either freeze into a crystalline solid, with a continuous change in volume, or if the cooling is rapid enough to prevent nucleation, it may continue as a super-cooled liquid below  $T_f$  until a temperature  $T_g$ , at which there is a change in slope to that of the crystalline one. This temperature ( $T_g$ ) known as the glass transformation temperature, defines the transition between the super-cooled liquid state and the solid glassy state. It should be noted that  $T_g$  is dependent upon the cooling during the glass-formation process. It rises with increasing cooling rate so it is not a uniquely defined temperature for a given composition (unlike the melting and boiling points). The glassy state is unstable and the ease with which it reverts to the crystalline form is dependent upon the composition, temperature and thermal history of the glass. The first order thermodynamic properties of glass such as volume, heat content, entropy, resistivity and dielectric constant are discontinuous at the change of state. The properties of a glass depend upon the rate of cooling during manufacture e.g. a rapidly cooled glass has a greater tendency to contract as it ages than one which has been cooled slowly. The physical properties in different regions of a glass ingot tend to vary. This results to difficulties in ensuring an even cooling rate throughout the bulk and can give rise to undesirable mechanical stress in the glass. These effects can be virtually eliminated by an annealing treatment in which the glass is heated for a long period at a temperature below the transformation temperature and then cooled slowly. This procedure relieves the mechani-

cal stress on cooling and also encourages the development of uniform properties throughout the glass.

#### 1.5. CLASSIFICATION OF SEMICONDUCTING GLASSES.

Materials known as semiconducting glasses (related to amorphous semiconductors) are very different in their electrical properties from the conventional crystalline semiconductors such as germanium, silicon or compounds such as indium antimonide. However, they fall within one, though not an exclusive, definition of a semiconductor as materials exhibiting electronic conductivity and having a positive temperature coefficient of conductivity. The semiconducting glasses can be subdivided as follows:-

##### (i) Chalcogenide glasses:

The chalcogenide based glasses have one or more of the elements from group VI (S, Se, or Te) combined with one or more of the elements of group V (P, As, Sb, Tl or Bi), e.g. As-S, As-Se, P-Se, etc. More complex glasses can be made by adding other sulphides and selenides to these binary systems. According to Mott and Davies<sup>5</sup> (1971), they can be put into two groups: (a) the elements and compounds which have chain or layer structures with considerable order extending locally in one or two dimensions, e.g. Se, S, Te, As<sub>2</sub>S<sub>3</sub>.

##### (b) the three-dimensional network structures, e.g.:

Ge-Sb-Se

Si-Ge-As-Te

Ge-As-Se

As<sub>2</sub>Se<sub>3</sub>-As<sub>2</sub>Te

As-Se-Te

Tl<sub>2</sub>Se-As<sub>2</sub>Te<sub>3</sub>.

However, type (a) glass can be prepared as thin films while

type(b) can be prepared both by quenching and by thin film techniques.

(ii) Halide glasses:

Halides do not commonly form glasses as the oxides do. Only  $\text{ZnCl}_2$  and  $\text{BeF}_2$  are known as halide glass formers. The bonds in halides are in general more ionic than in the oxides.

(iii) Elemental glasses:

This kind of glass contains only one kind of atom and is known to form a vitreous network when these are mixed or chemically bonded to each other, and are known to be very viscous in the liquid state and to under cool very easily. Elements of group VI of the Periodic Table, S, Se and Te can form such glasses.

(iv) The transition metal oxide based glasses:

The transition metal oxide is combined with one or more other oxides, providing a network, capable of conducting an electric current via a charge exchange among the transition metal ions of different valence states as in the case of hopping of electrons. They can be prepared by cooling from the melt. This thesis is mainly concerned with glasses based on the transition metal oxide vanadium pentoxide ( $\text{V}_2\text{O}_5$ ), and the relationship between structural change and vanadium valence state.

#### 1.6. GLASS-FORMERS AND MODIFIERS.

Glass formers have the capability to form glasses on their own when cooled from the melt and include materials such as  $\text{SiO}_2$ ,  $\text{P}_2\text{O}_5$  and  $\text{B}_2\text{O}_3$ . They can also form glass when

mixed with each other using two or more oxides. The strong bonding between oxygen and the positive ions facilitates the formation of a 3-dimensional network of atoms. On the other hand elements such as sodium which normally form ionic bonds are referred to as "modifiers". In the case of sodium, for example, the introduction of sodium oxide into silica is thought to cause a breakdown of the Si-O network through the formation of non-bridging oxygen ions. The sodium ions occupy the interstices, between the non-bridging oxygen ions in the Si-O network. Van Wazer<sup>6</sup> and Stevels<sup>7</sup> predicted that, as the proportion of modifier is gradually increased, the network breaks down, first to cross-linked and branched chains and finally to unbranched chains.

The oxides of metals such as aluminium, magnesium and lead are known as "intermediate oxides", as they do not form glasses on their own but can be incorporated in large amounts into the network of glasses.



## CHAPTER 2.

### THEORETICAL BACKGROUND OF ELECTRONIC CHARACTERISTICS OF DISORDERED MATERIALS.

#### 2.1. INTRODUCTION:

The matter which surrounds us may be conveniently divided into three categories, gases, liquids and solids. In the gaseous state the constituent atoms or molecules move freely about inside the container, experiencing very little influence on each other, but they do collide with one another elastically. If the kinetic energy is removed from the gas atoms, for example by cooling, a point will be reached at which the atoms, after a collision process, do not have enough energy to move apart as a result of the attractive force that atoms or molecules exert on each other when they come close together. The gas is said to have condensed to form a liquid. In the liquid state the atoms have sufficient thermal energy to slide and twist around each other, but not enough to move apart. This is the reason why liquids have the familiar characteristics that they take on the shape of the containing vessel, but have a fixed volume at a given temperature. The third category is the solid state. A solid may be formed when a liquid is further cooled. Once enough of the thermal energy is removed, the attractive forces between the atoms dominate over the disruptive effects of the temperature. When this happens the atoms are capable of being held at fixed positions. The result is the very rigid structure known as a

solid. With this in mind materials that may be regarded as solids can generally be divided into two categories, crystalline and amorphous. Crystalline substances are characterised by a perfect (or almost perfect) periodicity of atomic arrangement. This regularity of structure provides a very simple conceptual picture of a crystal and simplifies the task of understanding and calculating its physical properties. For this reason, crystalline solids are better understood physically than amorphous solids and liquids. On the other hand in amorphous substances, the atoms or molecules may be bound quite strongly to one another, but there is little if any long-range geometric regularity or periodicity in the way in which the atoms are arranged in space. Such substances are usually viscoelastic and are sometimes regarded as super-cooled liquids. To gain more insight into the structure we must plot the so-called radial distribution function. If we take a particular atom in the solid and determine the probability  $P(r)$  of finding an atom at some distance  $r$ , the curve obtained is the radial distribution function, illustrated in Fig. 2.1. If the solids were crystalline this function would be given by the shaded areas.

The important conclusion derived from this curve is that although the long range periodic structure does not exist, a short range order does. This is why there is a strong peak in the curve. This also suggests that the number of nearest neighbours to any atom does not vary greatly from the single crystal result and the postulated local order exists in all parts of the solid. Sometimes the local density is greater

and sometimes less than the crystalline value, but on average it is much the same. In this chapter the main purpose is to consider the theoretical concept of electronic properties in amorphous solids, particularly electrical conductivity and optical properties. Although a rigorous, quantitative theory of amorphous semiconductor does not exist at present and there is little hope of obtaining from first principles unique solutions of the Schrodinger equation for a disordered system in the near future, nevertheless, great strides have been made in the formulation of a semi-quantitative approach, since Anderson's<sup>8</sup> paper published in 1958 which enables us to analyse the experimental results in a consistent manner. Among non-crystalline materials are liquid metals, glasses and amorphous evaporated films. Despite the disordered configuration of amorphous solids, their electron energy band structure can be described in terms of quantum mechanics. It has been shown that the energy spectrum of a semi-conductor changes little on melting, where the short range-order does not change. This means that the loss of the periodicity of the lattice had little influence on the band structure and that the major features of the band structure are determined by the short-range order. The study of the electrical properties of glasses began with work of Kolomiets and his colleagues<sup>9</sup>, on the chalcogenide glasses. They showed that these glasses behave as intrinsic semiconductors with a band gap of typically less than 2eV and they also showed that, in contrast to crystalline materials, the conductivity depends little on purity and for them acceptor and donor

impurities do not seem to behave as they do in crystals.

## 2.2. THE ELECTRONIC STRUCTURE OF AMORPHOUS SOLIDS.

For crystalline materials the band theory is based on the work of Bloch and Wilson in the early 1930's. The energies of electrons in the crystalline solid are distributed among the so-called valence and conduction bands and there exists a gap of energy between these two bands. Confining our attention then to a rigid array of atoms, we have to consider first which of the concepts appropriate to crystalline solids may be used for non-crystalline materials. The first concept equally valid for crystalline and non-crystalline materials, is the density of states, which we denote by  $N(E)$  and is defined so that  $N(E)dE$  is the number of states available in unit volume for an electron in the system with given spin direction and with energy between  $E$  and  $E + dE$ . Whatever the nature of the states (empty or occupied), this density function must exist. Then at a temperature  $T$  the number of electrons in the energy range  $dE$  for each spin direction is:

$$g(E) = N(E)f(E)dE \quad \text{.....(2.1)}$$

where  $f(E)$  is the Fermi distribution function given by:

$$f(E) = 1/e^{(E-E_F)/kT} + 1 \quad \text{.....(2.2)}$$

The available evidence confirms that the form of the density of states function in an amorphous material does not differ greatly from the corresponding form in the crystal, except that the finer features of the energy band structure may be smeared out, and some localized states may appear in the normally forbidden energy band of the semiconductor. From the above equation, the Fermi energy  $E_F$  is a function of  $T$  and

tends to a limiting value as  $T \rightarrow 0$ ,  $E_f$  separating occupied from non-occupied states.

Due to the presence of phonons or impurities, scattering takes place and the concept of a mean free path  $L$  is introduced. In non-crystalline materials two possibilities arise for investigating the form and the value of  $N(E)$  and the corresponding wave function. One is that the mean free path  $L$  is large between the carrier scattering events compared with the interatomic distance and scattering of the electrons by each atom is weak. In this case, the energy  $E$  of each electron to a first approximation (assuming that electrons are confined in a rigid container) a parabolic function of the wave vector  $\underline{k}$ , so that :

$$E = \hbar^2 \underline{k}^2 / 2m^* \quad \dots\dots(2.3)$$

where  $\hbar$  is the reduced Planck constant and  $m^*$  is the electron effective mass of the electron. As the mean free path  $L$  is large, the deviation of the density of the states is given for each spin direction by the free electron formula assuming that the Fermi surface is spherical so that,

$$\begin{aligned} N(E) &= \{4\pi \underline{k}^2 / 8\pi^3\} / dE/d\underline{k} \\ &= \underline{k}m / 2\pi^2 \hbar^2 \quad \dots\dots(2.4) \end{aligned}$$

Another possibility is that the interaction between scattered electrons by each atom is strong. Thus the mean free path  $L$  is short  $\underline{k}L \sim 1$ . (i.e.localisation) and the deviation of  $N(E)$  from the free electron value is large. This is the most important difference between the theories of crystalline and non-crystalline materials. In the latter case, phenomena frequently occur in which electrons have energies for which

$kL \approx 1$ . This is so, for the carriers in most amorphous and liquid semiconductors. It was first emphasised by Ioffe and Regel<sup>10</sup> that values of  $L$  such that  $kL < 1$  are impossible, this leads us to expect that when the interaction of the carrier with an atom is sufficiently strong, something different ought to happen. It was first conjectured by Gubanov<sup>11</sup> that near the edges of conduction or valence bands in most non-crystalline materials the states are localized. The existence of tails of localized state in disordered materials has been argued with mathematical rigour.

## 2.3. BAND STRUCTURE OF NON-CRYSTALLINE SOLIDS.

### 2.3.1 Basic band model.

A quantitative interpretation of the experimental data requires a detailed model of the electronic structure of disordered materials. We start by noting that in all crystalline materials the electronic structure has certain universal features that is the individual electrons are described by Bloch wave function that are extended, with long-range order in both phase and amplitude, and the corresponding energies fall into bands of allowed levels that are separated by gaps and have sharp edges. We assume that disordered materials also possess such universal features. The basic band model, introduced by Mott out of earlier work, is the simplest possible representation of such universal features. The model assumes a band of extended states with long-range order in their amplitudes but only short-range order in their phases. Figure 2.2 illustrates the model for a single isolated band.

The band has tails of localized states, which have only short-range order. There are sharp transition at the energies  $E_C$  and  $E'_C$  from localized to extended states and vice versa. As the disordered character of the material increases, more and more localized states are created and the mobility edges move further into the band gap. When the disorder reaches a certain critical value, the two mobility edges merge, and, for any degree of disorder greater than this critical value, virtually all the states in the band are localized. This is known as the Anderson<sup>12</sup> transition. No single band model can describe the essential features of all amorphous materials, because of large differences in the nature of various groups of amorphous materials. Various band models have been put forward to explain the different behaviour of such materials. All of these models use the concept of localized states and the mobility gap but vary in the extension of the edges of localized states in the gap. Here we shall describe a few models briefly.

### 2.3.2 The Cohen, Fritzsche and Ovshinsky model (CFO).

Cohen<sup>13</sup>, Fritzsche<sup>14</sup>, and Ovshinsky<sup>15</sup> proposed a band model based on extension of the basic band model. Before the basic band model can be applied to a discussion of amorphous or liquid semiconductors it must be extended to include the band structure illustrated in Figure 2.3.

There is a valence band with a tail of localized states above the valence band energy  $E_V$  and a conduction band with a tail below the conduction band energy  $E_C$ . They suggested that

Fig. 2.3 is not adequate for concentrated amorphous covalent alloys, such as those based on the chalcogenides Se and Te. Such alloys contain atoms of varying valency in large concentration. They suggested that in this case, it is possible that the valence and conduction band tails actually overlap in what formerly was the forbidden energy gap, as shown in Figure 2.4. Such a situation preserves a gap between the valence and conduction bands, at the mobility edges, and it is the existence of this mobility gap,  $E_C - E_V$ , which leads to semiconductivity rather than metallic behaviour. The overlapping bands will moreover lock the Fermi energy near the centre of the gap, where the total density of states is near to its minimum. But even in this overlapping region, the individual conduction band and valence band states retain their identity. The states corresponding to the conduction band tail are considered to be neutral when empty and the states corresponding to the valence band tail are assumed to be neutral when occupied and the Fermi level is pinned near the centre of the gap. According to the CFO model, at higher temperatures the material behaves as an intrinsic semiconductor and at low temperatures conduction will take place by electrons at or near the Fermi energy, hopping from one site to another. The points corresponding to  $E_C$  and  $E_V$  are called mobility edges and the gap between  $E_C$  and  $E_V$  is referred to as the mobility gap and contains localized states.



### 2.3.3 The Davis and Mott model.

Davis and Mott<sup>11</sup> proposed a band model as shown in Figure 2.5. A fairly narrow ( $<0.1$  eV) band of localized states is assumed to exist near the centre of the gap, of sufficiently high density to effectively pin the Fermi energy over a wide temperature range. Thus conduction is extrinsic rather than intrinsic. The origin of the states is speculative, but they could conceivably arise from some specific defect characteristics of the material, for example dangling bonds, interstitials etc., whose number will be dependent on the conditions of sample preparation and subsequent annealing treatment. This model seems more compatible with the high transparency shown by many glasses at photon energies below the fundamental absorption edge. This model was later extended by Mott<sup>17</sup> as shown in figure 2.6. The shaded region is due to the mobility gap in which only localized states exist. Charge transport in these states is only possible by phonon-assisted tunnelling or hopping. The two peaks of  $N(E)$  are supposed to be due to dangling bonds which may either act as acceptors or as donors as indicated by capital letters A and D in fig.2.6.

### 2.3.4 Marshall and Owen model.

Marshall and Owen<sup>18</sup> proposed a model as shown in Figure 2.7. In this model for complete compensation the Fermi energy lies halfway between the sets of states at all temperatures. The band states of donors and acceptors relate to the upper and lower halves of the mobility gap. The upper half contains

compensated donor-like states below the conduction band, and the lower half contains the uncompensated and compensated acceptors states above the valence band.

#### 2.4. ELECTRICAL CONDUCTION OF AMORPHOUS SEMICONDUCTORS.

The quantum mechanics of typical semiconductors (e.g. Si, Ge, group III - V and II- VI compounds) predict that an electron can move through the periodic potential of a perfect crystalline lattice with an energy in certain allowed bands which are separated by forbidden gaps. The typical values of bandgaps in normal crystalline semiconductors lie in the range 0.3 to 2.1 eV. The effect of chemical impurities and imperfections in the crystal structure is to introduce energy states into the forbidden gap. The electrons in these states are localized (i.e. their wave functions are not continuous throughout the lattice) and can not move through the lattice unless:

(i) Sufficient energy is supplied to excite them into the conduction band; OR

(ii) There are a sufficient number of localized states in the forbidden gap for their wave functions to overlap and form an impurity band within the forbidden gap; OR

(iii) The carriers jump or "hop" instantaneously from one localized state to another with the absorption or emission of a photon. This is the situation observed in heavily-doped germanium at low temperatures, or in InSb at temperatures of a few tens of millidegrees. In a non-crystalline semiconductor the effect of disorder is to introduce a high

density of localized states (typically  $10^{25}\text{m}^{-3}$ ) into the forbidden gap. There are several different models which describe the electronic structure of non-crystalline semiconductors, but a common feature is that they postulate tails of states extending into gap from both the valence and conduction bands. Mott and Twose<sup>19</sup> applied Anderson's results to the localization of electrons in non-crystalline materials and they showed that below a certain critical density of states, all the electron states are effectively localized. Since the density of states varies with energy a transition occurs from localized states (i.e. the wave function becomes continuous throughout the solid) at energy  $E_C$ . This known as Anderson localization and  $E_C$  is called the mobility edge because the mobility of electrons in extended states is orders of magnitude greater than in those which are localized. With the concept of localized states and band tails, three distinct mechanisms of electrical conductivity have been recognized as important in a non-crystalline semiconductors. We refer here to figure 2.8.

(a) Carriers having energies above some critical value  $E_C$ . In this case the mean free path ( $L$ ) between carrier scattering events is large compared to the average interatomic spacing. Liquid metals are obvious examples of disordered conductors whose electrical conductivity can be explained by a band model such as the "nearly free electron" (NFE) picture of conduction which regards the electron as forming a degenerate free-electron gas with a spherical Fermi surface. The mobility is typically  $100\text{ cm}^2\text{V}^{-1}\text{sec}^{-1}$  or above, is given by a well

defined expression for band transport, involving the relaxation time  $\tau$  between collisions

$$\mu = e / m^* \langle \tau \rangle \quad \dots\dots(2.5)$$

(b) A diffusion mechanism, in which the mobility of carriers having an energy between  $E_C$  and  $E_D$  is considerably reduced due to the electronic wave function being highly modulated by the disorder in the lattice, which results in regions in the diffusion path where the probability of finding the carrier is extremely small. The behaviour of carriers in such delocalization or extended states (diffusion region), with a mean free-path of the order of the average interatomic spacing is still band-like, in that it is a non-thermal activated process.  $E_D$  and  $E_C$  are temperature dependent, increasing with increasing temperature. The mobility in such a case can be estimated from the Einstein relation;

$$\mu = eD / kT \quad \dots\dots(2.6)$$

where  $D$  is the diffusion constant and given by:

$$D = a^2 \Gamma_{e1} / 6 \quad \dots\dots(2.7)$$

where  $\Gamma_{e1}$  is the electron frequency, thus

$$\mu = e \cdot a^2 \Gamma_{e1} / 6kT \quad \dots\dots(2.8)$$

The estimated drift mobility is about 1 to 10  $\text{cm}^2\text{V}^{-1}\text{sec}^{-1}$ .

(c) Carriers having energies below  $E_C$  will be localized in the lattice, and the transport will take place by a thermally activated hopping process and this means that a carrier can move from one localized state to another with the emission or absorption of a phonon. For such cases the mobility can be very low indeed, possibly in the range  $10^{-2} - 10^{-7} \text{cm}^2/\text{V}^{-1}\text{Sec}^{-1}$ .

## 2.5. Temperature dependence of d.c. conductivity.

Regarding the proposed model for the density of states in an amorphous semi-conductor, the electrical conductivity may be determined by a number of parallel current paths. The energy of the predominant path often depends quite strongly on temperature and this is of considerable help in the interpretation of electrical measurements. Considering the model of Davis and Mott for the density of states, as the temperature increases from absolute zero temperature, there are three basic phenomena for conductivity in amorphous semi-conductors:

(a) Hopping conduction in localized states at the Fermi energy.

(b) Hopping conduction in localized states below the mobility edges.

(c) Extended state conduction above the mobility edges.

Thus the conductivity equation can be written as:

$$\sigma = \sigma_1 \exp(-E_1/kT) + \sigma_2 \exp(-E_2/kT) + \sigma_3 \exp(-W_2/kT) \dots (2.9)$$

The first term defines the conductivity due to the carriers excited beyond the mobility edge (region C in Figure 2.9).

If the main current is carried by electrons, it should be expected that

$$E_1 = E_C - E_f \dots (2.10)$$

In general  $\sigma_1$  lies between  $100$  and  $500 \Omega^{-1} \text{ cm}^{-1}$  in most amorphous materials<sup>20</sup>. The second term is due to carriers

excited into localized band edge (region B in Figure 2.9 ). For an electron,  $E_2 = E_A - E_f + W_1$ , where  $W_1$  is the activation energy for hopping. The value of  $\sigma_2$  is expected to be a factor  $10^2 - 10^4$  less than  $\sigma_1^{20}$ . The third term is due to the hopping of carriers between localized states near the Fermi energy (region A in Figure 2.9). This is the process analogous to impurity conduction in heavily doped semi-conductors.  $W_2$  is the hopping energy and  $\sigma_3 \ll \sigma_2$ . We emphasise here that a straight line in a plot of  $\ln \sigma$  against  $1/T$  is expected only if hopping between nearest neighbours is involved. A particularly important case for electron (or hole) transport is the so called variable-range hopping mechanism which sets in at low temperatures where it can become energetically more favourable for a carrier to hop beyond its nearest neighbour sites in order to find a final site closer in energy to its initial site. Conduction then occurs near the Fermi energy  $E_f$  and Mott has shown that the conductivity is expected to behave as:

$$\ln \sigma = A - BT^{-1/4} \quad \dots\dots(2.11)$$

$$\sigma = \exp (-\text{const. } T^{1/4})$$

In Figure 2.9 this behaviour is shown schematically as region(d). The whole range of the temperature dependence of conductivity is also shown in figure 2.9. If the density of defect states is high, then the second equation will not dominate in any temperature range and a direct transition from (a) to (c) will result, as indicated in figure 2.9.

## 2.6. Hopping conduction.

The presence of a high density of localized states makes

it necessary to consider direct hopping of carriers between traps (localized states) as a probable mechanism of transport. The carrier is regarded as spending most of its time trapped at a particular localized state and making more or less instantaneous transitions to neighbouring empty states. In each hop an electron moves from one localized state to another with the emission or absorption of a phonon. Miller and Abraham<sup>21</sup> were the first to use this kind of conduction mechanism in the theory of impurity conduction. The probability (P) of an electron to jump from one site to other depends on the following factors:

(i) Boltzmann factor  $\exp.(-W/kT)$  where W is the difference between the energies of two sites.

(ii) A factor  $\nu_{ph}$  depending on the phonon spectrum

(iii) A factor depending on the overlap of wave function.

If the localization is very strong, the electron will normally jump to the nearest available state in space because the term  $\exp.(-2 \alpha R)$  falls rapidly with distance,  $\alpha$  is the decay factor and R is the distance taken by each hop. Therefore the jump probability is given by:

$$P = \nu_{ph} \exp(-2 \alpha R) \exp(-W/kT) \quad \dots\dots(2.12)$$

Only electrons of energies within a range of  $kT$  at the Fermi energy are taking part in the conduction process. Those with lower energies will need more energy to hop. Therefore, the number of electrons that will take part in hopping conduction is  $N(E_F)kT$ , where  $N(E_F)$  is the density of states at the Fermi energy. The diffusion coefficient D could be written

as(20,22):

$$D = R^2 P \quad \dots\dots(2.13)$$

and the mobility is given by;

$$\mu = eD/kT = e/kT.R^2 P$$

$$\mu = eR^2/kT \cdot \nu_{ph} \exp(-2\alpha R) \exp(-W/kT) \dots(2.14)$$

As conductivity is related to mobility through

$$\sigma = ne\mu \quad \dots\dots(2.15)$$

where n is the number of carriers then;

$$\begin{aligned} \sigma &= N(E_F)kT e\{eR^2/kT \nu_{ph} \exp(-2\alpha R) - \exp(-W/kT)\} \\ &= e^2 R^2 \nu_{ph} N(E_F) \exp(-2\alpha R - W/kT) \quad \dots\dots(2.16) \end{aligned}$$

The condition  $\alpha R \gg 1$  will not apply near the mobility edge. If  $\alpha R$  is not large, the factor  $\exp(-2\alpha R)$  may be put equal to unity and then:

$$\sigma = e^2 R^2 \nu_{ph} N(E_F) \exp(-W/kT) \quad \dots\dots(2.17)$$

Where R is the distance to the nearest centre.

At sufficiently low temperature as mentioned earlier the phenomenon of variable range hopping is expected<sup>17</sup>

The principle of variable range hopping is shown in Figure 2.10. If sites B and C differed negligibly in energy, hopping proceeded preferentially to site B because of its smaller distance with respect to A. If however,  $W_{AB} > W_{AC}$  then it is evident that at a sufficiently low temperature  $\exp(-W_{AB}/kT) \ll \exp(-W_{AC}/kT)$  and the carrier will prefer to jump to site C. To obtain the temperature dependence of jump probability (P) and the consequent conductivity equation Mott<sup>17</sup> proposed that the jump probability in the case of variable range hopping depends on  $T^{-2.5}$  and the conductivity should follow a general formula of the form;



$$\sigma = B \exp(-A / T^{2.5}) \quad \dots\dots(2.18)$$

Where A and B are constant.

The theoretical basis of the law has been extensively discussed in the literature and it has been used in the interpretation of transport properties of amorphous semiconductors. It is also suggested by Grant and Davis<sup>22</sup> that a variable range hopping behaviour can be expected in the band tails.

## 2.7 OPTICAL PROPERTIES OF AMORPHOUS MATERIALS

Amorphous materials exhibit an absorption edge which is usually situated at approximately the same energy region on the absorption edge of the crystalline form of the material if it exists, having a similar short-range order. Below this edge the transparency of amorphous semiconductors can be remarkably high at least until the frequency of lattice vibrations become important. Absorption edges of amorphous semiconductors may be quite sensitive to the condition of preparation, thermal history and purity. Measurements of the optical absorption coefficient particularly the absorption edge, provide a standard method for the investigation of optical-induced transitions and provide some ideas about the band structure and energy gap in both crystalline and non-crystalline materials. Basically there are two types of optically transition that can occur at the fundamental edge, direct and indirect, both involve the interaction of an electromagnetic wave with an electron in the valence band

which is raised across the fundamental gap to the conduction band. However, indirect transition also involves simultaneous interaction with lattice vibrations. A direct transition is that in which absorption will occur at an energy  $\hbar\omega = E_g$  for a semiconductor in which the lowest minimum of the conduction band and the highest maximum of valence band lie at the same point in  $k$ -space. If this is not the case, the transitions are possible only when phonon assisted and are called non-direct. Since the absorbed photon has negligible momentum, there is no significant change in the momentum  $\hbar k$  when an electron is transported between two bands by indirect optical transitions and the extremes of the energy bands are separated, possibly widely, in  $k$  space. Photons will be involved during the optical transitions to satisfy the conservation of momentum due to the change in the electron wave vector. Optical measurement can determine whether the band gap  $E_g$  is due to direct or indirect transitions. To estimate the value of the optical energy gap  $E_{opt}$  the curve of absorption coefficient versus wavelength needs to be fitted to a theoretical curve. Two such approaches have been given in the literature, one by Urbach<sup>23</sup> and the other by Tauc et al<sup>27</sup>, and by Davis and Mott<sup>16</sup>. In many amorphous semiconductors the absorption edge can be divided into three regions as shown in Figure 2.11. Regions A and B are created by transitions within the fully co-ordinated system, while region C arises from transition involving the defect state directly.

Region A: At very low absorption levels where the absorption coefficient  $\alpha(\omega) < 1$  and a weak absorption tail is observed.

It is normally difficult to observe this absorption tail because of the low absorption level.

Region B: The exponential part B where absorption coefficient  $\alpha(\omega) \leq 10^4 \text{ cm}^{-1}$  there is usually an Urbach tail in which  $\alpha$  depends exponentially on photon energy  $\hbar\omega$  as:

$$\alpha(\omega) = \alpha_0 \exp(\hbar\omega/E_e) \quad \dots\dots(2.19)$$

Where  $\alpha_0$  is a constant,  $\omega$  is the angular frequency of the radiation and  $E_e$  is an energy which is constant or weakly temperature-dependent and is often interpreted as the width of the tails of localized states in the band gap.

Region C: At very high absorption where  $\alpha \geq 10^4 \text{ cm}^{-1}$  and the absorption coefficient  $\alpha$  obeys the following relation:

$$\alpha\hbar\omega = B(\hbar\omega - E_{\text{opt}})^n \quad \dots\dots(2.20)$$

B is a constant,  $E_{\text{opt}}$  is the optical energy gap of the material and the index n may assume one of the values 2, 3, 1/2, 3/2 indicating the type of electronic transitions. Equation (2.20) with  $n = 2$  has been successfully applied to many amorphous semiconductors and insulators suggests absorption by non-direct transition. The relation with  $n = 2$  was derived by Tauc et al<sup>24</sup> who assumed the electron density of states at the band edge in regions of localized state to be a parabolic function of energy. Davis and Mott<sup>16</sup> obtained the same relation by assuming that the density of states is a function of energy and that  $E_{\text{opt}}$  corresponds to indirect transition between a localized state and an extended state in the conduction band or vice versa but considered the various values that n could assume and the associated physical transitions.

## 2.8. POLARON FORMATION AND TRANSPORT.

Polaron formation occurs when the time that a carrier resides on each lattice site is sufficiently long in relation to the lattice vibrational period to relax under the influence of the electrostatic potential of the carrier. Figure (2.12a) shows a simple ionic lattice and figure (2.12b) shows the same lattice with the addition of an electron to a positive site. The surrounding atoms tend to be displaced in response to the presence of the electron and the electron with its surrounding cloud of displaced atoms is known as a polaron. The carrier is self-trapped within its own potential well and behaves as a particle consisting of an electron and a phonon combined. Polarons are usually classified as being large or small. A large polaron is one where electron overlap is large compared to its binding energy, resulting in a lattice distortion which extends over several lattice sites. When the opposite conditions occur the polaron is tightly bound and the extent of the lattice distortion becomes comparable with the lattice spacing resulting in a small polaron. The formation of a small polaron can occur in materials where there are strong electron-lattice interactions and also when the carriers are strongly localized. In materials where polarons are formed, two mechanisms of conduction are possible. Firstly consider that charge carriers and their associated lattice deformations may reside on any site. These configurations are degenerate with each other and the proper states of the system are linear combinations of Bloch waves; consequently they may form a

polaron conduction band. In this case carriers are free to move through the lattice with exact conservation of lattice energy. Thus the conductivity will be expected to be independent of temperature. Secondly, the interaction between lattice waves and the deformation potential of the polaron can give rise to a hopping mechanism of charge transfer. Figure (2.13) shows this schematically. Figure (2.13a) illustrates an excess charge on a lattice site. The length of the vertical line represents the strength of the deformation potential round the carrier. If a lattice wave interacts with this deformation potential causing the wave function of the occupied site and the adjacent one to become the same (Fig.2.13b) the carrier can transfer to the next site as they are momentarily degenerate with each other. Figure 2.13c shows the carrier in equilibrium on the next site. This second method of charge transport can only occur when the lattice vibrations are of sufficient amplitude, i.e. at temperatures above one half the Debye temperature. Holstein<sup>26</sup> makes detailed calculations of this behaviour in a one-dimensional molecular crystal consisting of a linear chain of diatomic molecules. The separation between the nuclei of the molecules is allowed to vary but the distances between the centres of gravity of the molecules is fixed. The temperature dependence of the mobility as predicted from Holstein's small polaron treatment is shown in figure 2.14. A minimum occurs at approximately half the Debye temperature ( $\theta_D / 2$ ), the transition temperature between the two different conduction mechanisms. Above this temperature the main mechanism of

charge transport is that of electron hopping induced by interchange of phonon energy between the carrier and the lattice. Below this temperature charge transport occurs within a polaron band characterised by exact conservation of the lattice energy. The conductivity of a crystalline material where charge transport occurs by the motion of small polarons will have an activation energy ( $W_H$ ), the hopping activation energy above  $\theta_D / 2$ , while below this temperature the conductivity will be un-activated as conduction occurs within a polaron band. It should be noted at this point that the concept of polaron formation is applicable to a wide range of materials not just the transition-metal oxides. The name polaron arises from the early consideration by Mott and Gurney<sup>27</sup> of self-trapping of a carrier in ionic (or polar) materials.

## 2.9 EXPERIMENTAL DATA ON CONDUCTION IN TRANSITION-METAL OXIDE CRYSTALS..

Austin and Mott<sup>28</sup> show data on the variation of resistivity with temperature in crystalline lithium-doped NiO. This is reproduced in figure 2.15. At temperatures above 100K the resistivity has a constant activation energy of 0.2 to 0.4 eV, which is dependent upon the doping level, while below 100K the activation energy drops slowly from approximately 0.05 eV to 0.004 eV at 10K. Austin and Mott interpret the transition to the lower activation energy on the onset of impurity conduction arising from the presence of compensating donor centres (possibly oxygen vacancies) which give up

electrons to the  $\text{Li}^+$ ,  $\text{Ni}^{3+}$  acceptors. It is suggested that the continuous decrease in activation energy to the lowest temperatures is due to the occurrence of variable range hopping in the impurity states.

Bosman and Van Daa1<sup>29</sup> report data on the variation of resistivity with temperature in a number of crystalline transition-metal oxides. Figures 2.16 illustrates their data on lithium doped CoO, MnO, NiO and  $\text{Fe}_2\text{O}_3$ . The samples of MnO and CoO show a constant activation energy to very high resistivity values while NiO and  $\text{Fe}_2\text{O}_3$  show a decrease in activation energy with temperature, which Bosman and Van Daa1 attribute to impurity conduction. This different behaviour stems from the dissimilar properties of impurity centres. In CoO and MnO dielectric loss measurements have shown that the bound hole around the Li ions has a high activation energy for movement (CoO  $\approx 0.2$  eV, MnO  $\approx 0.3$  eV) resulting in very small bound-carrier mobilities at low temperature, compared to those of NiO and  $\text{Fe}_2\text{O}_3$ . As a result it is expected that the impurity conduction contribution will be severely limited in CoO and MnO compared with NiO and  $\text{Fe}_2\text{O}_3$ .

Van Daa1<sup>30</sup> concludes that the free charge carriers in NiO and CoO can be successfully described on the basis of a large polaron band model, i.e. one where the extent of the lattice deformation is greater than one lattice spacing, while bound carriers can be described as small polarons. Van Daa1 discounts the possibility of charge transport in NiO and CoO by small polarons on the basis of the behaviour of thermopower at high temperatures ( $\approx 1000\text{K}$ ). At the lower tempera-

tures, he suggests that small polaron band transport is impossible because of energy fluctuations between adjacent sites. Such fluctuations arise from the random distribution of charge majority and minority centres and effectively prevent the formation of a polaron band.



### CHAPTER 3.

#### REVIEW OF PREPARATION, STRUCTURE AND CONDUCTIVITY MECHANISM OF TRANSITION METAL OXIDE GLASSES.

##### 3.1. PREPARATION OF AMORPHOUS TRANSITION METAL OXIDES.

Transition metal oxide glasses are a group of glassy semi-conductors. They consist of inorganic glass forming oxides, together with a significant transition metal content (V, Fe, Cu, Ti, Cr, Mn, Co, Ni, Mo and W) and there may also be some glass-modifying oxide. It has been established that pure transition metal oxides will not form a glass under normal quenching conditions, e.g. casting on to a chilled metal slab, but amorphous films of  $V_2O_5$  have been prepared by , for example, R.F. sputtering and vapour phase deposition. Kennedy et al<sup>31</sup> have reported unsuccessful attempts to prepare  $V_2O_5$  glass by casting the melt onto a slab cooled to liquid nitrogen temperature, but thin films of  $V_2O_5$  were prepared by condensing the vapour onto cold substrates in vacuum and the absence of crystallinity has been confirmed by microscopic examination in polarised light and by electron diffraction.

##### 3.2 CLASSIFICATION OF TRANSITION METAL OXIDE GLASSES.

As mentioned in the above section, pure transition metal oxides will not form glass by normal quenching. Nevertheless, many transition metal oxides are capable of forming glasses when combined with glass-forming oxides and in some cases the glass forming oxide need only be present in small quantities

(e.g. a few mole percent) so that the transition metal oxide is the predominant constituent. The oxides  $\text{TiO}_2$ ,  $\text{V}_2\text{O}_5$ ,  $\text{Fe}_2\text{O}_3$  and  $\text{CuO}$  are known for example to form glasses over a wide range of composition when combined with oxides such as  $\text{P}_2\text{O}_5$ ,  $\text{TeO}_2$ ,  $\text{B}_2\text{O}_3$  and  $\text{GeO}_2$ . Mixtures of  $\text{V}_2\text{O}_5$ - $\text{BaO}$  and  $\text{V}_2\text{O}_5$ - $\text{PbO}$  are known ( ) to form glasses in the composition ranges of 63-73% and 46-62% respectively although the oxides barium and lead are not normally considered to be glass formers.

For the purpose of discussion in the following section the glasses are classified into binary and ternary systems. It must be remembered that this is a slightly artificial representation since the transition metal oxide is usually reduced to some extent and is present, therefore in at least in two states of oxidation. Thus the binary system  $\text{V}_2\text{O}_{(5-x)}\text{P}_2\text{O}_5$  is in reality at least a ternary system, i.e.  $\text{V}_2\text{O}_5$ - $\text{V}_2\text{O}_4$ - $\text{P}_2\text{O}_5$ . Nevertheless it is convenient to regard such systems notionally as binary.

### 3.3 BINARY GLASS SYSTEMS CONTAINING TRANSITION METAL IONS.

The vanadium-phosphate  $\text{V}_2\text{O}_5$ - $\text{P}_2\text{O}_5$  glass system is probably the most closely studied of the transition metal oxide glasses. The first recorded observation of glass formation was by Roscoe<sup>32</sup> who observed that  $\text{P}_2\text{O}_5$  inhibited the crystallisation of  $\text{V}_2\text{O}_5$  if present in quantities exceeding 1% by weight.

Denton et al<sup>33</sup> reported the preparation of a number of vanadate glasses including the  $\text{V}_2\text{O}_5$ - $\text{P}_2\text{O}_5$  system in which the,

found that glasses are readily formed over the range 0 - 95 mole percent  $V_2O_5$ . They also reported making vanadate glasses with the glass formers  $GeO_2$ ,  $TeO_2$  and  $As_2O_3$ . Table 3.1 shows the approximate composition ranges of glass formation for each of the systems investigated by Denton et al. Copper oxide ( $CuO$ ) reported by Malik<sup>34</sup> and Hajian<sup>35</sup> forms a glass in a composition range of 10% - 30% when mixed with a glass former such as  $TeO_2$  or  $P_2O_5$ . Magnetite ( $Fe_2O_3$ ) will form a glass when combined with other glass formers. The preparation of phosphate glass containing 55 molar percent  $FeO_x$  was reported by Hansen<sup>36</sup>, Hansen and Splann<sup>37</sup> and by Kinser<sup>38</sup>. Sayer and Mansingh<sup>39</sup> have described the preparation of phosphate glasses containing 50 mole per cent of each of the 3d transition metal oxides except chromium, i.e.  $TiO_2$ ,  $V_2O_5$ ,  $Mn_3O_4$ ,  $Fe_2O_3$ ,  $CoO$ ,  $NiO$  and  $CuO$ . They also prepared phosphate glasses containing molybdenum and tungsten oxides, i.e.  $MoO_3$  and  $WO_3$ . Ahmed<sup>40</sup> & Moridi<sup>43</sup> also prepared binary vanadate glasses containing barium and tellurium oxides. Mohammad Elahi<sup>42</sup> investigated iron-phosphate glasses and outlined their optical and electrical properties.

### 3.4 TERNARY GLASS SYSTEMS CONTAINING TRANSITION METAL IONS.

A wide variety of three component glasses containing a transition-metal oxide as one component has been prepared. A typical ternary system would be one containing a transition-metal oxide, a glass-forming oxide and a modifier or an intermediate oxide, e.g.  $V_2O_5$ - $P_2O_5$ - $NaO_3$ ,  $V_2O_5$ - $P_2O_5$ - $CaO$  respectively. Kennedy and Mackenzie<sup>31</sup> have prepared glasses in

the systems  $V_2O_5-B_2O_3-CaO$  and  $V_2O_5-P_2O_5-CaO$  and have investigated the effect of network forming oxide on the conductivity of the glass. Mordi and Hogarth<sup>43</sup> reported the preparation of glasses in the certain composition of  $55P_2O_5-xCuO-(45-x) CaO$ . Where  $35 \geq x \geq 0$ , in their studies of electrical memory switching. The alkaline earth oxide  $CaO$  was sometimes included as a glass modifier which made the network more suitable for memory switching. Hogarth and Hosseini<sup>44</sup> also reported the preparation of ternary glass system of vanadium-phosphate-tellurium ( $V_2O_5-P_2O_5-TeO_2$ ) containing 60 mol.%,  $V_2O_5$ , (40-x) mole %  $P_2O_5$ , and x mole %  $TeO_2$ , in which x varies from 5 to 35 under normal cooling from the melt, for their investigation of optical absorption edge.

Malik and Hogarth<sup>45</sup> in their recent work reported the preparation of copper tellurite glasses doped with  $Lu_2O_3$ , and the effect of the addition of lutetium oxide ( $Lu_2O_3$ ) on the optical properties has been investigated. Khan et al<sup>46</sup> have made a comparative study of the effects of rare earth oxides such as  $Ce_2O_3$ ,  $Pr_6O_{11}$ ,  $Eu_2O_3$ ,  $Gd_2O_3$ ,  $Tb_4O_7$ ,  $Yb_2O_3$  and  $CeO_2$  in  $V_2O_5-P_2O_5$  on the physical, optical, electrical and structural properties of vanadium phosphate glasses. The work of Dimitriev et al<sup>47</sup> illustrates the wide range of glass formation in the system of  $V_2O_5-TeO_2-CdO$ . Two regions of glass formation were distinguished, the first at lower ( $< 50$  m.p.c)  $CdO$  contents and the second at high ( $> 75$  m.p.c)  $CdO$  contents. This was attributed to the  $CdO$  acting as a network modifier when present in low concentrations, leading to the break up of the glass network as the proportion of  $CdO$  increased. As

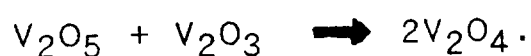
an explanation of the glass forming region at high concentrations of CdO. Dimitriev postulated that CdO can act as a glass former when present in sufficient concentration. Dimitriev<sup>48</sup> also reported formation of glass in the system of  $V_2O_5$ - $TeO_2$ -CaO in the  $V_2O_5$  concentration range of 20 to 65 percent and the incorporation of 25 mole% CaO. Beyond that concentration of CaO the glass devitrified. Grechanik et al<sup>49</sup> investigated the vitrification regions of binary, ternary and quaternary semiconducting glasses and found that as the composition become more complex, more stable glasses can be obtained and possess a greater variety of properties characteristic both of their semiconducting and glassy natures.

### 3.5 THE TRANSITION METAL ION VALENCE STATE.

In transition-metal oxide glasses a proportion of the transition-metal ions are normally reduced to lower valency states during the melting process. The degree of reduction can be controlled either by incorporation of an oxidising or reducing agent to the melt or by controlling the furnace atmosphere. According to the available information the electrical conduction in transition-metal oxide crystals is thought to occur by the hopping of carriers between high and low valence transition-metal ions. The same is true for the transition-metal oxide glasses and obviously an exact measurement of the number, and valence state of the transition-metal ions in the glass is necessary to enable us to estimate the carrier concentration in the glass to be made. Methods by

which this can be done are described later in this chapter.

Electron spin resonance (e.s.r) data on vanadium phosphate glasses shown by Lynch et al<sup>50</sup> suggest that the concentration of vanadium valence states lower than four is small. E.s.r. was used to measure the concentration of  $V^{4+}$  ions in a 80 molar percent  $V_2O_5$ - 20 molar percent  $P_2O_5$  glass by a comparison of the intensity of the resonance due to the  $V^{4+}$  ions with that of a sample of anhydrous copper sulphate of known spin concentration. The predominantly single line resonances observed suggests that the concentration of valence states below the first reduced state is low, since  $V^{3+}$ ,  $V^{2+}$  and  $V^{1+}$  are expected to give signals with appreciable fine structure. Lynch et al<sup>50</sup> also found that the ratio of high to low vanadium valence states measured by e.s.r agreed reasonably well with that obtained from wet chemical analysis, which assuming that the wet chemical analysis data is a measure of the total reduced vanadium content, regardless of valence state, suggests that little vanadium is in valence states other than four and five. It is also worth noting that the simultaneous presence of  $V^{3+}$  and  $V^{5+}$  states is unlikely at high vanadium concentrations and at high temperatures, such as those used for glass melting, since the auto-oxidation reaction:



is likely to occur under such conditions.

### 3.6 THE INFLUENCE OF VANADIUM VALENCE STATES ON GLASS FORMATION .

Consider a glass system such as  $V_2O_5$ - $P_2O_5$  for which the range of glass formation by normal quenching techniques, is usually quoted as 0 to  $\sim 95$  mole%  $V_2O_5$ . The degree of reduction of the vanadium does affect the glass-forming ability of a particular composition and thus is best illustrated by considering the ternary system  $V_2O_5$ - $V_2O_4$ - $P_2O_5$ . The approximate glass-forming region in the appropriate ternary diagram, is shown in Figure 3.1. This was constructed from data given by Linsley<sup>51</sup> and it corresponds to the preparation of glass in quantities of several grams by normal quenching of the melt. Figure 3.1 shows clearly that the greater the total vanadium concentration the smaller is the degree of reduction which can be incorporated in the glass. Linsley's data is based on the probably justifiable assumption - that all the reduced vanadium occurs as  $V^{4+}$ . The presence of lower valence states might be expected to limit glass formation even more. There is insufficient information to construct diagrams similar to figure 3.1. for other vanadium systems but it is almost certainly reasonable to generalise and conclude that in all cases the greater the total vanadium content the smaller is the degree of reduction which can be incorporated without devitrification. In fact, the generalization can probably be broadened to encompass all transition-metal oxide glasses.

### 3.7 THE CHEMICAL STRUCTURE OF VANADATE GLASSES.

The oxides of vanadium and phosphorus are known to form long chain polymeric compounds, both individually and in mixtures, and there is evidence that in  $V_2O_5$ - $P_2O_5$  glasses long chain polymeric vanadophosphate complexes are formed.

The vanadium is regarded as being mostly in the  $V^{5+}$  state but with some  $V^{4+}$  present. Only the  $V^{5+}$  ions can form structural complexes and it has been suggested that the  $V^{4+}$  acts as a network modifier in the form of the vanadyl ion.

### 3.8 PHASE SEPARATION.

Phase separation has been reported in many vanadate glasses where systematic studies have been made of macrostructure. Scanning electron microscopy was used by Kinser and Wilson<sup>52</sup> to study the macrostructural features of the vanadium phosphate glass system and indicated extensive separation into two glassy phases, with maximum phase separation occurring at the extremes of the glass forming region. It also appears that glasses may be structurally more homogeneous near the conductivity maximum while those removed from the conductivity maximum are more heterogeneous. According to Bogomolova et al<sup>53</sup>, their e.s.r and scanning electron microscopy data can be interpreted to show that the  $V_2O_5$ - $P_2O_5$ -CuO glasses are phase separated into regions of high and low conductivity. Scanning electron micrographs reveal two phases which correspond to the high and low conductivity regions. When paramagnetic  $V^{4+}$  ions appear in more than one phase of an inhomogeneous glass, a complex e.s.r spectrum is expected consisting



of the superposition of the spectra of the  $V^{4+}$  ions in the different phases. No such complex spectrum is observed and the conclusion is that all the  $V^{4+}$  ions are contained in only one phase, which is solely responsible for electronic conduction.

### 3.9 CONDUCTION IN TRANSITION METAL OXIDES.

The first series of transition elements comprises those ranging from Sc to Cu in the periodic table. They are characterised by the progressive filling of the 3d electron shell which lies below the outermost 4s electron shell. The characteristic properties of these are well known. The metals themselves have high densities, high melting points and good mechanical and catalytic properties, and in their compounds they show variable valency, colour, complex ion formation and paramagnetism. Most of the first series of transition element oxides fall somewhere between semiconductor and insulators when pure. In order to understand the mechanisms of conduction in these oxides, it is first necessary to have some knowledge of the energy band structure in the first series of transition elements. They are characterised by their partially filled 3d orbitals, and it is not obvious as to whether the 3d wave functions overlap sufficiently to form a 3d band, or whether they are localised energy levels. The location of other energy levels relative to 3d orbital, have been calculated by Morin<sup>54</sup> and usually it is found that the 4s band is very wide and overlaps the 3d band. In nickel, the 3d band is 1/15 of the width of the 4s band, which suggests that elec-

trons in the 3d band have a high effective mass and low mobility as a result of this narrowness. It is considered probable that the 4s band does not overlap the 3d band at all in the oxides and so electronic conduction must be entirely within the 3d band. According to Morin, of the 3d oxides probably only those of scandium, titanium and vanadium are like ordinary semiconductors in that their charge carriers are in energy bands. After vanadium, the band width of oxides of 3d elements goes to zero, as the atomic number increases. Figure 3.2 illustrates the decrease of 3d bandwidth as the atomic weight increases and superimposed on this in a curve showing the increase in reduced effective mass ( $m^*/m$ ) of carriers in the 3d-band as the bandwidth reduces to zero. When the 3d band becomes extremely narrow it is no longer meaningful to assign a width to it and 3d charge carriers can be considered as occupying energy levels localised on the cations. De Boer and Verwey<sup>55</sup> and Mott<sup>56</sup> were the first to suggest that the oxides of Cr, Mn, Fe, Co, Ni and Cu are insulators when pure ( $\sigma < 10^{-10} \text{ ohm}^{-1}.\text{cm}^{-1}$  at room temperature). For conduction to take place, according to De Boer and Verwey, it is necessary that there are ions of the same element but of different valency and present at crystallographically equivalent lattice points. For pure stoichiometric NiO, for example, this can be achieved via a reaction



but at room temperature this cannot occur because of the large energy required ( $\approx 4\text{eV}$ ). Hence NiO is strictly an insulator.

### 3.10 CONDUCTION IN VANADATE GLASSES.

The first reported preparation of vanadate glasses was by Roscoe<sup>32</sup> in the  $V_2O_5$ - $P_2O_5$  system with  $V_2O_5$  contents of more than 90 mole%. Dento et al<sup>33</sup> investigated the electrical properties of vanadium based glasses and found that like  $V_2O_5$  itself, they are semiconductors. The conductivity was shown to be n-type (electron predominant) from thermo-electron e.m.f. measurements. The conductivity was measured over the range 300 to 400 K and showed a temperature dependence of the form;

$$\sigma = \sigma_0 \exp(-W/kT) \quad \text{.....(3.1)}$$

Where  $\sigma_0$  is a pre-exponential constant.

Binary glasses were melted with  $P_2O_5$ ,  $TeO_2$ ,  $PbO$ ,  $GeO_2$ ,  $As_2O_3$  as the other constituents. Baynton et al<sup>57</sup> carried out a more systematic study of the system  $V_2O_5$ - $BaO$ - $P_2O_5$  and  $V_2O_5$ - $BaO$ - $Na_2O$ - $P_2O_5$  with  $V_2O_5$  contents ranging from 50 to 87 mole per cent. The conductivity was found to be strongly dependent on  $V_2O_5$  content. Activation energies for conduction are in the range of 0.35 - 0.40 eV for all glasses. These authors suggested that in comparing the two systems under investigation, the effect of  $Na_2O$  is to increase the conductivity, and in order to do this, the soda must affect the balance of the vanadium valence state, that is,



In extrapolating the curve of  $\log_{10}$  conductivity against  $V_2O_5$  content to 100%  $V_2O_5$ , the value of conductivity so obtained was close to that of pure vanadium pentoxide crystals ( $\sigma \approx$

$5 \times 10^{-3} \text{ ohm}^{-1} \cdot \text{cm}^{-1}$ ). Munakata<sup>58</sup> investigated the effect of varying the valence state of vanadium on the conductivity of the glass system of  $60\text{V}_2\text{O}_5 - (40-x)\text{P}_2\text{O}_5 - x\text{RO}$ , where RO represents a basic metal oxide. The effect of adding  $\text{P}_2\text{O}_5$  at the expense of the third oxide is to increase the  $\text{V}^{4+}$  content. The magnitude of the conductivity was found to depend on the third oxide (RO). For glasses of high  $\text{V}_2\text{O}_5$  content a mechanism involving the exchange of an electron between  $\text{V}^{4+}$  and  $\text{V}^{5+}$  sites is postulated. This mechanism was also postulated by Ioffe et al<sup>59</sup> in work on the system  $\text{V}_2\text{O}_5\text{-P}_2\text{O}_5$  and  $\text{V}_2\text{O}_5\text{-BaO-P}_2\text{O}_5$ . Ioffe states that conductivity and vanadium valence state depend only on the ratio  $\text{P}_2\text{O}_5 / \text{V}_2\text{O}_5$  and that any third oxide acts as a filler of holes in the glass network. Although this opposes the suggestions of Baynton et al<sup>58</sup>, in order to substantiate their statement the authors re-plotted the data of Baynton to show the dependence of conductivity on the  $\text{V}_2\text{O}_5 / \text{P}_2\text{O}_5$  ratio. For ternary systems the work of Munakata<sup>58</sup> illustrating the dependence of magnitude of conductivity on the nature of the third oxide shows that the postulates of Ioffe can not be completely correct. Ioffe estimated the density and mobility of carriers by using conductivity and thermo electric power data. A value was of  $10^{-18} \text{ cm}^{-3}$  was obtained for carrier density and  $10^{-2} - 10^{-3} \text{ cm}^2\text{V}^{-1} \text{ sec}^{-1}$  for mobility at room temperature. The carrier density appeared to be independent of temperature, but the mobility increased with temperature exponentially.

A study of the effects of thermal history on the electrical conductivity of some vanadate glasses is a feature of

the work of Hamblen et al<sup>60</sup>. Conductivity was shown to be dependent on the thermal history above the transformation range. For example, a 72/28 mole %  $V_2O_5/Ba(PO_3)_2$  glass when heat treated, after melting, at 250°C for five hours had a conductivity of  $1.9 \times 10^{-4} \text{ ohm}^{-1}.\text{cm}^{-1}$ . If the same glass was heat treated for the same period of time at 350°C then the conductivity was  $9.1 \times 10^{-2} \text{ ohm}^{-1}.\text{cm}^{-1}$  (conductivity measured when cooled to 27°C). According to this, the rate of change of conductivity increases rapidly as the transformation range is reached. Two possible conduction mechanisms were suggested as follows:-

(1) Conduction by electrons released by partial dissociation of an oxygen anion according to the reaction:



2. Conduction by electron exchange between vanadium cations of different valence occupying equivalent positions in adjacent  $VO_6$  octahedra. Although the idea of valence exchange as suggested seems to be generally accepted, the suggestion that this exchange occurs via the  $VO_6$  octahedra is new. The structure of  $V_2O_5$  was regarded as being of three-dimensional  $VO_6$  octahedra. The effect of dilution, by making a glass with another constituent, is to move progressively from the sheet structure of  $VO_6$  octahedra to ribbon structure and to chain structure, depending on the number of oxygen shared by the  $VO_6$  octahedra. The continuous sheets, ribbons or chain, are then supposed to provide a conduction path for electrons, thus explaining the fall in conductivity as  $VO_6$  octahedra become isolated progressively by the addition of more of the

other glass constituents. At temperatures below 250K Nester and Kingery<sup>61</sup> interpreted a change in slope of reciprocal temperature variation of log conductivity as indicating some change in the conduction process in this temperature region. This was also based upon the gradual decrease in thermoelectric power in the region. They attributed the process to the hopping of electrons in the same way as Ioffe, between the four and five-valent vanadium ions. An important assumption was made, that the number of charge carriers is the same as the number of  $V^{4+}$  ions. It was used in estimating the mobility of charge carrier ( $\mu$ ) using the relation

$$\sigma = ne\mu \quad \dots\dots(3.2)$$

where  $\sigma$  is the conductivity,  $e$  is the electronic charge and  $n$  is the concentration of free carriers.

In the range 90/10 - 50/50 weight per cent  $V_2O_5/P_2O_5$ , the mobility appeared to vary between  $2.5 \times 10^{-6}$  and  $1.0 \times 10^{-8}$   $cm^2.V^{-1}.sec^{-1}$  at  $100^\circ C$  and at higher temperatures increased exponentially with temperature, a result consistent with the predictions of the theory of free carrier hopping.

The theoretical approach of Mott to hopping conduction has been mentioned in chapter 2, but he also developed an equation for conduction in transition metal oxide glasses.

$$\sigma = \nu \cdot c(1-c)(e^2/RkT) \exp(-2aR) \exp(-W/kT) \dots\dots(3.3)$$

where  $\nu$  is a phonon frequency,  $R$  is the mean distance taken by each hop,  $c$  and  $(1-c)$  are the concentrations of the two valence states. The overlap integral  $a$  is a part of the tunnelling term  $\exp(-2aR)$ .

Possible application of vanadate glasses include their use as thermistors and surface junction detectors. The glasses tend to be opaque in the visible range but transparent in the infrared. This property could be useful for signalling and detecting devices at infrared wavelength. Switching between high and low conductivity states is also possible for transition metal oxide glasses<sup>62</sup>. The switching is achieved by electrical pulsing and both states are stable, a memory state being retained when the applied voltage is reduced to zero.

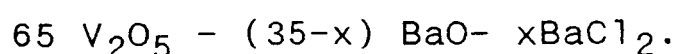
## CHAPTER 4

### 4. GLASS PREPARATION AND STRUCTURAL INVESTIGATIONS.

#### 4.1. GLASS PREPARATION:

Three different series of  $V_2O_5$ -BaO-BaCl<sub>2</sub>,  $V_2O_5$ -TeO-BaO and TeO-BaO-BaCl<sub>2</sub> glasses were prepared. Analytical reagent grades of  $V_2O_5$ , BaO, BaCl<sub>2</sub> and TeO<sub>2</sub> oxides were supplied by B.D.H. Chemicals. The appropriate amounts of oxides were weighed and mixed together in the crucibles using an alumina rod. The melts were stirred from time to time to ensure homogeneity and were then cast as disc-shaped glasses 1.5 to 2.0 cm diameter and 2.5 to 3.0 mm thick on a stainless steel plate. All the series of glasses were annealed to relieve mechanical stress and minimize cracking of glass, and were then allowed to cool down to room temperature by switching off the furnace. It was believed that the annealing temperature, annealing time, melting temperature, melting time, rate of cooling and melting atmosphere could all affect the properties of glasses. So it was decided to keep all these parameters constant for the glasses of the same series. The preparation conditions of the various series of glasses were as follows:

(i) Vanadium pentoxide - barium oxide and barium chloride glasses were prepared from a range of composition given by the general formula :-



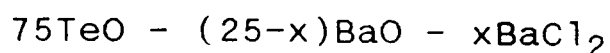


where  $x = 0, 3, 5, 7, 10, 12.5$  and  $15$ .

An attempt was made to melt a glass containing 20 mole%  $\text{BaCl}_2$  but this resulted in crystallization during cooling. Examination by x-ray diffraction revealed that the crystalline phase was  $\text{BaCl}_2$ . Glasses were melted in 30g batches in silica crucibles at  $750^\circ\text{C}$  for 10 minutes. The glasses which were fluid were then cast onto stainless steel plates which were preheated to  $400^\circ\text{C}$ . Each plate was immediately transferred to a preheated furnace held for 2 hours and then allowed to cool to room temperature. Annealing temperatures were based on prior knowledge of the glass transformation temperature. During melting a significant loss of chlorine occurred and it was in order to minimize this loss that a short melting time was used. Measurements of weight loss on melting were made by weighing the crucible before melting and by weighing the crucible and sample after melting. The results are shown in Table 4.1, which indicates that essentially no loss occurred for glasses, containing  $< 10$  mole%  $\text{BaCl}_2$ , whereas a gradually increasing weight loss was observed for glasses containing more  $\text{BaCl}_2$ . It was assumed that chlorine volatilised from the glass. Certainly the glass containing 15 mole%  $\text{BaCl}_2$  was observed to emit vapours during melting and contained many very fine bubbles after casting. Although the weight loss discussed above indicates that the glasses assumed to have the highest chlorine content probably contain less chlorine than that indicated by the batch composition, the trends observed in this study do not depend upon the exact composition. It was therefore decided in the first

instance to plot all data on the basis of the original batch composition. The glasses so obtained were dark and opaque in appearance.

(ii) Tellurium and barium oxides doped with barium chloride: Ternary glass samples of general formula;



where  $x = 0, 3, 5, 6, \text{ and } 7$  (mole%).

An attempt was made to cast a glass containing more than 7%  $\text{BaCl}_2$  resulted in fracture of the bulk samples. The mixture of oxides was kept in an electric furnace at a temperature of  $400^\circ\text{C}$  in an atmosphere of air for one hour. This was believed to serve to minimize the material volatilization during the melting process. The pre-heated batches were then transferred into the second furnace and melted at  $800^\circ\text{C}$  for 15 minutes. During the melting process the melt was stirred by an alumina rod several times to obtain homogeneous samples. Bulk samples were made by pouring the melt into clean steel moulds and quenching the molten materials by a relatively heavy and smooth block of steel to obtain disc-shaped samples. The thickness of the samples was about 3mm and the diameter of the samples, generally between 20 and 30 mm. The glass samples were annealed at  $300^\circ$  for 2 hours. The glasses so obtained were greenish yellow and transparent in appearance.

(iii) Vanadium pentoxide- tellurium and barium oxide glasses were prepared as 30g batches in silica crucibles at  $800^\circ\text{C}$  for one hour. The composition used cover the range



(in mole%). The preparation condition remained the same as those used for other series. The glasses so obtained were dark red and opaque in appearance. All samples,, when not in use, were stored in an evacuated desiccator.

#### 4.2 X-RAY DIFFRACTION INVESTIGATION.

X-ray diffraction is a useful technique since it is readily possible to detect crystals in a glassy matrix if the crystals are of dimensions greater than typically 100nm<sup>64</sup>. The X-ray diffraction pattern of an amorphous material is distinctly different from that of crystalline material and consists of a few broad diffuse haloes rather than sharp rings. All the glass samples were tested and recorded with a Phillips type PW1050 diffractometer, using a copper tube and nickel filter. The experiment was carried out for all glass compositions studied in this work, and the results were found to be identical, demonstrating the absence of crystalline characteristics. The amorphous nature of the annealed glasses was also tested and found no evidence of crystallization on annealing. Figure 4.1 shows typical x-ray diffraction patterns for different glasses.

#### 4.3 DENSITY MEASUREMENTS.

##### Experimental:

The density measurement is based on Archimedes' principle which states that, when a body is immersed in a fluid (liquid or gas), it experience an upthrust equal in magnitude to the

weight of fluid displaced<sup>64</sup>. If the weight of a rigid body is  $M_a$  in the air and  $M_b$  in the fluid, then the weight of fluid displaced is  $M_a - M_b$ , thus we obtain:

$$d_a = M_a / V \quad \text{.....(4.1)}$$

$$d_f = (M_a - M_b) / V \quad \text{.....(4.2)}$$

where  $d_a$  and  $d_f$  are the densities of glass and fluid respectively,  $V$  is the volume of glass. Dividing equation 4.1 by equation 4.2, we obtain:

$$d_a = M_a / (M_a - M_b) \quad \text{.....(4.3)}$$

The densities of glasses were determined with a balance having an accuracy of 0.2 mg using ethyl-methyl-Ketone ( $C_2H_5-CO-CH_3$ ) as the immersion liquid. This has a relative density at 20°C of 0.803 – 0.805. Table 4.2 represents the values of densities of the glasses and Figures 4.2. and 4.3 show how the densities vary with  $BaCl_2$  concentration.

#### 4.4 MOLAR VOLUME.

Molar volume  $V$  is defined as a volume occupied by one gram-molecule of any composition<sup>65</sup>. Suppose a compound contains  $n_A$  gram-molecules of component A,  $n_B$  gram-molecules of component B,  $n_C$  gram-molecules of component C, etc., then the molar volume is given by:

$$V = (n_A + n_B + n_C + \dots) / d \quad \text{.....(4.4)}$$

Where  $d$  is the density of compound. The molar volumes of all three series of glasses were obtained and listed in Table 4.2

#### 4.5 RESULTS AND DISCUSSION.

The density of the ternary  $V_2O_5 - BaO - BaCl_2$  glasses decreases as chlorine replaces oxygen, but the variation of density with  $BaCl_2$  content is not the smooth curve which might have been expected and does not obey the simple additivity rule, since its value goes through a minimum at 7%  $BaCl_2$  content. Further addition of chlorine into the glass system causes the density of glass to increase. Figure 4.2 illustrates the influence of  $BaCl_2$  on the density. The decrease in density was also observed for  $TeO-BaO-BaCl_2$  glass system as oxygen was replaced by chlorine ions.

The density of the glass of composition  $V_2O_5-TeO_2-BaO$  increases as the  $BaO$  is gradually replaced by  $V_2O_5$  as shown in Table 4.2. Figure 4.4 shows the variation of density with  $BaO$  content. The molar volume was found to decrease as the density of glass was increased, which is in agreement with the results of previous workers<sup>43,44,76,77</sup>.

#### 4.6 ELECTRON SPIN RESONANCE (E.S.R).

##### Introduction:

Transition-metal ions characterised by a partially filled d shell can frequently exist in a number of oxidation states and electronic conduction can occur as a result of electron transfer from ions in a lower oxidation state to ones in a higher oxidation state. The relative portion of

transition-metal ions in the different oxidation states has been an important parameter in explaining this electronic conduction in oxide glasses.

ESR is a non-destructive method of measuring the reduced transition-metal ion content of the glass, without altering the structure in any way. It can be defined as a phenomenon observed when paramagnetic substances containing unpaired electrons are subjected to high magnetic fields and microwave radiations. In the case of a vanadate glass for example,  $V^{4+}$  ions are paramagnetic and give strong e.s.r. signals while  $V^{5+}$  ions are diamagnetic. Measurement of the intensity of resonance peak gives an indication of the concentration of  $V^{4+}$  ions. The general concept of this phenomenon is that an unpaired electron has spin and normally its energy due to this spin is independent of the electron's orientation. Electrons possess a magnetic moment due to this inherent spin angular momentum and associated rotation. In the majority of familiar substances, every electron is paired with another in the same spatial orbital. Such paired electrons are always aligned with their spins opposite and thus not have a net magnetic moment. When the sample is in a zero magnetic field, spins and magnetic moments of the unpaired electrons will be pointed in a random directions and will have equal energy. However, an unpaired electron has two observable energy states in an external magnetic field. If an magnetic field  $H$  is applied across the sample, the electrons will align themselves either with their spins and moments parallel or anti-parallel to the field, no intermediate orientation being

allowed by quantum condition since  $S = 1/2$ . Therefore electrons will fall into two groups with different energies. Since those electrons with their spins aligned parallel to the field, will have energy  $(1/2) g\beta H$  less than the zero field value, and those with their spins aligned anti-parallel to the field will have an energy of  $(1/2) g\beta H$  greater than the zero field value. From figure 4.5 it can be seen that the splitting between these two energies increases linearly with increasing magnetic field  $H$  and is equal to  $g\beta H$ . If electromagnetic radiation of frequency  $\nu$ , such that  $h\nu = g\beta H$ , is fed to the molecules, the absorption of this radiation should occur as the electrons are excited from a lower to a higher state of energy. So unpaired electrons in a solid will absorb microwave radiation when the splitting of their two energy states matches the frequency of the incoming microwave. In the case of vanadate glasses hyperfine splitting may be expected in the spectrum and a single absorption line would then be replaced by a hyperfine pattern. Such hyperfine structure arises from the interaction of the unpaired electron with the nucleus around which it is moving<sup>66</sup>. This is the basic principle of e.s.r. E.s.r. analysis has the disadvantage over wet chemical analysis in that it is not accurate in its estimation of the valence ratio. Landsberger and Bray<sup>67</sup> quote an accuracy of  $\pm 20\%$  for their results which is surprisingly good, since they used powdered glass sample for the analysis. To estimate the spin concentration in a powdered glass sample a packing factor must also be determined for the powder. This is difficult to do accurately since it

will be strongly dependent upon the degree to which the sample is compacted into the tube. E.s.r. is probably the only technique to use when a measure of valence ratio is required on solid sample without destroying it, but if accuracy is the prime consideration wet chemical analysis may be the best method.

#### 4.7 WET CHEMICAL ANALYSIS.

The method most commonly used for the measurement of valence ratio is titration of solution prepared from the powdered glass, against standardised acidified potassium permanganate( $\text{KMnO}_4$ ). In a vanadate glass the four-valent vanadium undergoes the reaction:



resulting in the decoloration of the permanganate solution. This permanganate titration gives an estimate of the reduced vanadium content of the solution. In order to measure the total vanadium content, all of the vanadium is reduced to the  $\text{V}^{4+}$  state by bubbling  $\text{SO}_2$  gas through the solution and then titrating against  $\text{KMnO}_4$  as before. This then gives the total vanadium content of the solution.

#### 4.8 ATOMIC ABSORPTION ANALYSIS.

In glasses containing the glass-former  $\text{TeO}_2$  it is not possible to use chemical analysis based on oxidation and



reduction of the transition-metal ions, because it is known that tellurium can also exist in two different valency states in glass. On titration with  $\text{KMnO}_4$ , the lower valence state of tellurium are oxidised along with those of vanadium and interfere with the end point of the titration. To avoid this difficulty a atomic absorption method has been used in the present work. Absorption of electromagnetic radiation in the visible and UV regions of the spectrum by atoms results in changes in electronic structure. Samples were prepared by dissolving powdered glass in dilute acid ( $\text{HNO}_3$ ) and compared against the standard graph. Solution which contain  $\text{V}^{5+}$  ions have an absorption peak at 380nm, while those containing  $\text{V}^{4+}$  ions have an absorption peak at 790nm. The two peaks do not interfere with each other in solutions containing mixtures of the ions. By measuring the optical absorption of a solution containing  $\text{V}^{5+}$  and  $\text{V}^{4+}$  ions at 380nm and 790nm respectively, and comparing these with the absorption of standard solutions of the ions it is possible to determine the concentration of  $\text{V}^{4+}$  and  $\text{V}^{5+}$  ions in the solution prepared from the glass. This method has the disadvantage, common to all wet chemical analysis methods, of requiring dissolution of the glass in dilute acid with the attendant danger of altering the transition-metal ion valence state, but it has the advantage that colourless and insoluble tellurium oxide does not interfere with the result.

#### 4.9 ELECTRON SPIN RESONANCE MEASUREMENTS.

The e.s.r. spectra were recorded on a Varian E3 e.s.r. spectrometer working at x-band (9.5 GHz), using standard Varian accessories. The glasses were finely powdered and placed in 3mm silica sample tubes, packed to a constant length of sample and individually weighed. All settings of the instruments were maintained constant throughout the investigation with the exception of the gain level which was varied according to need with individual samples. Ammonium vanadyl was used as a standard for the spin concentration determination of  $V^{4+}$  in the glasses. The total vanadium in the glasses were determined by standard wet chemical analysis and atomic absorption analysis. The samples were scanned for 2 minutes in a scan range of 1000 G. The spin concentration density for each glass was estimated by the following expression:

$$B = (A_1 / A_2)Y$$

where  $A_1$  and  $A_2$  are the areas under the microwave absorption versus magnetic field strength curves for the glass and the standard sample respectively. The value of  $Y$  which is the number of spins for the standard sample was found by the following relation:

$$Y = (W_S)(N) / (M_S)$$

where  $W_S$  is the weight and  $M_S$  is the molecular weight of the standard. It must be borne in mind that the spin densities are only approximately calculated by double integration of the first derivative of spectra, due to uncertainties regarding the active sample volume which is controlled by the penetration depth of the microwave signal and the assumption

made that proportionality between the e.s.r. signal and the microwave field exists. Given these uncertainties the amount of  $V^{4+}$  in 100g of glass was estimated by using the following equations:

$$Z = 100M_G B / NW_G.$$

Where  $M_G$  is the molecular and  $W_G$  is the weight of glass. The values of spin concentration and  $V^{4+}$  are quoted in Table 4.3 and 4.4.

#### 4.10 RESULTS AND DISCUSSION.

The glasses investigated were those of initial composition  $(65)V_2O_5 - (35-x)BaO - (x)BaCl_2$  and  $(75)TeO_2 - (25-x)V_2O_5 - (x)BaO$ .

Where  $x$  varies from 2-15 and 5-25 mole% respectively.

In all the samples investigated, the existence of Vanadium ion of valence lower than five has been detected. When the contents of the glass, namely  $V_2O_5$ ,  $BaO$ ,  $BaCl_2$  and  $TeO_2$  are mixed up and then dissolved in dilute acid, the solution does not react at all with  $KMnO_4$  solution. However, when the mixture is melted into a glass and then dissolved in acid, the solution reacts strongly, as a reducing agent with  $KMnO_4$ . This reaction must be attributed to lower-valence vanadium ions, since no other reducing ions are likely to exist in the solution. As this effect is only found after the mixture is melted into glassy a state, these lower-valence vanadium ions must have been produced while the materials were melted together into glass. Whether this lower-valence vanadium is

$V^{3+}$  or  $V^{4+}$  can not be determined from this results alone, but the fact that this glass is easily soluble in acid suggest that it is  $V^{4+}$ , as it is known that  $V_2O_4$  is easily soluble in acids while  $V_2O_3$  is not. The extra step was taken to make a firm confirmation of the reduced ion by adopting the e.s.r. method. E.s.r. gives an indication of the presence, and valence state of a paramagnetic species. The unreduced ion cores  $V^{5+}$  are diamagnetic and hence can not be detected by e.s.r., while the reduced ions  $V^{4+}$  have spin  $S = 1/2$  leading to a single resonance line influenced by nuclear hyperfine interaction. All e.s.r spectra exhibit a somewhat rather resolved hyperfine structure. The spectrum of  $V^{4+}$  ions become deformed as a result of introducing the third oxide into the binary glass system. It is clear from the spectrum in Figure 4.6 that with increase of  $V^{4+}$  concentration the width of the hyperfine structure component increases. It may be suggested that the broadening effect as a result of the higher spin concentration effect, could be due to an increase in the covalent bonding between the central V ion and the surrounding ligands. This increase in covalency is also supported by Muncaster et al<sup>68</sup>, and it has been revealed that the contribution of the 3d electron to the hyperfine splitting decreases with increasing  $V_2O_5$  content. This arises because the 3d orbital is increasingly screened from its nucleus through overlap of the electron orbits of the surrounding ligands. This produces an expansion of the 3d orbital resulting in a decreased interaction with the vanadium nucleus.

Table 4.3 and 4.4 give the e.s.r parameters and also

include the result of chemical analysis. The effect of temperature variation on the e.s.r spectrum was investigated over temperature range down to 77K. No change was observed in the spectra for all the glasses when the temperature was reduced from 300 to 77K. This indicates that the paramagnetic spin concentration is independent of temperature and therefore the temperature dependence of the conductivity arises from a change in effective carrier mobility. Figure 4.7 shows the effect of increasing  $\text{BaCl}_2$  content which controls the electrical conductivity as a result of modification of the reduced vanadium valence ratio and a change in concentration of the paramagnetic ions.

## CHAPTER 5.

### OPTICAL PROPERTIES.

#### 5.1 INFRARED SPECTROSCOPY.

##### **5.1.1 Basic Principle:**

Infrared spectroscopy is a well known acceptable technique for structural studies. It promotes transitions in a molecule between rotational and vibrational energy levels of the ground (lowest) energy states. Molecules are made up of atoms linked by chemical bonds. The movement of the atoms and the bonds may be illustrated mechanically by balls and springs in motion respectively. The movement as a result of vibration may be divided into two components, namely the stretching and the bending of the bonds joining the atoms. Bending of bonds gives rise to deformation due to the change of the bond angle between the atoms of a molecule. These deformations occur at frequencies lower than those of the stretching vibrations. The frequencies of vibration of the atoms are dependent on the masses involved and the nature of the bonds, in a way related to the structure of the entire molecules and its environment. This is why each component has a unique infrared spectrum and taking the infrared spectrum of a compound helps in its identification. Certain atomic movements give rise to bands which occur in approximately the same position in a large variety of compounds and are only slightly affected by the rest of the molecule. The vibrations may therefore be assigned to certain groups of atoms which

are termed functional groups. These functional groups of atoms have distinguished characteristics, e.g. multiple bonds,  $C=O$ ,  $C\equiv N$ ,  $C=C$  etc or single bonds between dissimilar atoms e.g.  $C-H$ ,  $C-O$ ,  $O-H$  etc. Where the vibrations of the group do not affect the other groups in the molecule. If the molecule contains two functional groups which are the same and which are adjacent or nearly adjacent, certain vibrations can and do couple together so moving the absorption band of the single group to either a new, characteristic, position or the coupling can be such that the vibration is no longer easily recognised. For a molecule composed of  $n$  atoms there are  $3n$  degrees of freedom associated with the momentum coordinates. Of these, three will be rotational modes (only two rotational modes in a linear molecule). This means that there will be  $3n-6$  or  $3n-5$  degrees of freedom of the molecule, each of which gives rise to a vibration of the molecule. Certain vibrations may occur for a molecule which do not necessarily result in an infrared absorption being observed. Some sets of vibrations are degenerate i.e. they are identical but in perpendicular directions and these multiple vibrations only result in one infrared absorption band being seen in the spectrum. The prime necessity for an infrared absorption to occur is that there must be a change in dipole moment in the molecule when the vibration occurs. The greater the change in dipole moment the stronger is the infrared absorption. This explains why the absorption bands of hydrocarbons are much weaker than the absorption of groups whose components differ in their electronegativities e.g.  $C=O$ ,  $C-O$ ,  $O-H$ . There are

no rigid rules for interpreting an infrared spectrum but certain requirements are necessary for a satisfactory result to be obtained:

- a) The spectrometer should be accurately calibrated.
- b) The resolving power of the spectrometer must be tested.
- c) The sample should be reasonably pure or its chemical history known so that the impurities may be recognised.

A precise assignment of all the absorption occurring in the spectrum is not feasible and should not be attempted, when only a qualitative identification is to be investigated, instead, information as to the presence or absence of specific functional groups should be sought. Although the utility of infrared spectroscopy to the organic chemist has been thoroughly studied and reported, but the application of this technique to the inorganic compounds has been somewhat less successful. Many simple inorganic compounds such as the borides, nitrides, and oxides do not absorb radiation in the region between 4000 and 800  $\text{cm}^{-1}$  which, for many years, was the extent of the infrared region covered by most commercial spectrometers. Only within the last few decades have instruments become available which include the region below 800  $\text{cm}^{-1}$ .

The infrared spectra of phosphates, in particular binary phosphate glasses, have been reported by a number of authors. One common feature of these investigations is the quantitative nature of the interpretation of the spectral results. Corbridge and Lowe<sup>69</sup> have studied the infrared spectra of various inorganic phosphorus compounds including



the crystalline and glassy metaphosphates and their work has been used as the basis of interpretation of succeeding workers. The influence of the cations on the bonding in the phosphate skeleton in binary glasses containing  $\text{Na}_2\text{O}$ ,  $\text{MgO}$ ,  $\text{SrO}$ ,  $\text{BaO}$ ,  $\text{CaO}$ , and  $\text{ZnO}$  has been studied by Bohovich<sup>71</sup> using Raman spectroscopy. These spectra are characterized by a series of low-frequency bands, including a band at about  $700\text{ cm}^{-1}$  which was assigned to the symmetrical vibration of the  $-\text{P}-\text{O}-\text{P}-$  group and the bands at  $1155 - 1230\text{ cm}^{-1}$  arising from symmetrical and antisymmetrical vibrations of the  $\text{PO}_2$  group. A study of spectral vibrations as a function of composition in the system  $\text{CaO}-\text{P}_2\text{O}_5$  led to the conclusion that the introduction of oxide modifiers into glassy  $\text{P}_2\text{O}_5$  causes depolymerization of its three-dimensional structural network. In another development, the group frequencies in the range less than  $600\text{ cm}^{-1}$ ,  $600 - 1200\text{ cm}^{-1}$  and  $1200 - 1300\text{ cm}^{-1}$  are known to be associated with the stretching vibration of the bond bending of the  $\text{O}-\text{P}-\text{O}$  unit,  $\text{P}-\text{O}$  bond and  $\text{P}=\text{O}$  bond respectively<sup>71,72</sup>. Sayer et al<sup>73</sup> have studied the infrared absorption spectrum of a number of transition metal phosphate glasses in particular vanadium phosphate glasses. The spectra show an absorption band at  $1015\text{ cm}^{-1}$ , which is attributed to the  $\text{V}-\text{O}$  stretching frequency of the  $\text{VO}_5$  structural unit. The intensity of the absorption increases as the  $\text{V}_2\text{O}_5$  content is raised above 70 mole per cent, the conclusion drawn was that the  $\text{VO}_5$  structural unit is retained in the high vanadium content glasses indicating that they retain the short range order of crystalline  $\text{V}_2\text{O}_5$  but as the  $\text{V}_2\text{O}_5$  content decreases other

structures are also formed. Anderson and Compton<sup>74</sup> interpret the broad absorption band that occurs between 1085-1100  $\text{cm}^{-1}$  as being caused by a phosphorus-oxygen vibration. This is at a somewhat lower energy than predicted simply by scaling the masses of vanadium and phosphorus ions and it is suggested that the force constants are different for the different ions.

In this work, we use infrared absorption spectroscopy as a complimentary tool to x-ray diffraction and the other methods of studying the structure of glass in the region of 4000-200  $\text{cm}^{-1}$ . The attempt was to study the infrared spectra of different glasses to ascertain whether any kind of local order characteristic of the constituent oxides is maintained in the final glass and to relate the observed absorption maxima to atomic groups of known structure, in order to resolve some structural problems, arising from the complex nature of the glassy materials.

#### 5.1.2 Experimental methods.

Infrared spectral measurements were carried out by using a Pye Unicam spectrophotometer (model SP 2000) in the frequency range 200  $\text{cm}^{-1}$  (0.024 eV) - 4000  $\text{cm}^{-1}$  (0.496 eV). Transmission spectra were obtained using KBr-pellet samples. Selected glass samples were ground into fine powder and then a small amount of the glass powder was mixed and ground with KBr with a ratio of about 1/15 respectively. The KBr-glass pellets were made by introducing a certain amount of the mixture between two smooth cylindrical steel casts under a

force of 15 tons in a vacuum for 3-5 minutes.

### 5.1.3 Results and Discussions.

The infrared absorption spectra of the series of  $\text{TeO}_2$ - $\text{BaO}$ - $\text{BaCl}_2$ ,  $\text{V}_2\text{O}_5$ - $\text{BaO}$ - $\text{BaCl}_2$  and  $\text{TeO}_2$ - $\text{BaO}$ - $\text{V}_2\text{O}_5$  glasses are shown in figures 5.1, 5.2 and 5.3 respectively and the spectra of crystalline  $\text{TeO}_2$ ,  $\text{V}_2\text{O}_5$ ,  $\text{BaO}$ ,  $\text{BaCl}_2$ ,  $\text{BaTeO}_3$  and  $\text{BaV}_2\text{O}_7$  have also been recorded for comparison with vitreous states. A KBr-glass pellet was kept in the open air for a few hours and the spectra obtained for this specimen exhibited strong bands at  $3200$  and  $3700\text{ cm}^{-1}$ , which is associated with OH stretching vibrations of the water and hydroxyl groups respectively. A medium band was also noted in the region  $1600$ - $1650\text{ cm}^{-1}$  which is assigned to the H-O-H bending motion. For many inorganic compounds infrared absorption occur in the region below  $1200\text{ cm}^{-1}$ , and for this reason the remaining spectra were recorded below this wavelength. The IR spectra of the tellurite phases in both crystalline and vitreous states are shown in Figure 5.6. The main absorption frequencies in the  $800$  to  $400\text{ cm}^{-1}$  range are assigned to stretching vibrations of the Te-O bonds. The typical broadening of the bands is observed in the spectra of the glasses.

The spectra of pure  $\text{TeO}_2$  and  $\text{BaTeO}_3$  in crystalline states showed very close similarity, which is direct proof for the similarities of the structural units and of the short range order. For this reason, interpretation of tellurite glass spectra can be based on conclusions, drawn for their

crystalline phases. As mentioned earlier, the vibrations of a specific group of atoms in a lattice may be regarded as relatively independent from motions of the rest of the atoms. The Te-O vibrations of crystalline tellurites, built up by  $\text{TeO}_3$  groups may be examined on the basis of  $C_{3r}$  point symmetry and for crystalline built of  $\text{TeO}_4$  groups may be examined from a viewpoint of  $C_{2r}$  point symmetry<sup>75</sup>. The IR spectrum of crystalline  $\text{TeO}_2$  are assigned the stretching frequencies of 780, 714, 675 and  $635\text{ cm}^{-1}$ .

Figure 5.6 illustrates the IR spectra of pure  $\text{TeO}_2$  glass. The band at  $635\text{ cm}^{-1}$  increases markedly and becomes a determining one. The rise in intensity is probably due to higher degree of the dipole moment involved in the vibration as a result of reduction in symmetry. Figure 5.8 shows the spectrum of a binary glass system of (75) $\text{TeO}_2$ -(25) $\text{BaO}$  which can be characterised by an intensive absorption maximum at  $675\text{ cm}^{-1}$  and the comparison with the spectra of crystalline  $\text{TeO}_2$ - $\text{BaO}$  indicates that some similarity exists between these two states. Figure 5.1 shows the spectrum of the ternary glass system of (75)  $\text{TeO}_2$ -(25-x) $\text{BaO}$ -x $\text{BaCl}_2$ , with the incorporation of  $\text{BaCl}_2$  two new absorption bands appear at 250 and  $260\text{ cm}^{-1}$ , and can be assigned to the naturally occurring chlorine species. It also indicates that introduction of  $\text{BaCl}_2$  shifts the absorption maximum from 675 to  $655\text{ cm}^{-1}$  but the increasing chloride content does not affect the overall shape of the spectra in any significant manner.

Figures 5.2 refer to the spectra of (65) $\text{V}_2\text{O}_5$ -(35-x) $\text{BaO}$ -x $\text{BaCl}_2$ . In contrast to tellurite glasses the spectra of the

binary system of  $V_2O_5$ -BaO differ from that of the crystalline phase. In the ternary system it may be noticed that basically there are five absorption bands appearing at positions 250, 260, 620-650, 890 and  $980\text{ cm}^{-1}$ . The maximum absorption is recorded at  $625\text{ cm}^{-1}$ . A weak band at  $980\text{ cm}^{-1}$  could indicate a shift from  $1010\text{ cm}^{-1}$  which is believed to be the normal vibrational frequency of the vanadium-oxygen bond and is also observed in  $V_2O_5$ - $B_2O_3$ . The absorption band at  $890\text{ cm}^{-1}$  is a spectral sign of a linear structure of the  $VO_2$  group observed previously<sup>76</sup>. The broad band at 620-650  $\text{cm}^{-1}$  could be due to the combined effects of V-O-Ba vibrations as observed by Moridi<sup>44</sup> and then by Anvary<sup>77</sup>. A band at 250-255  $\text{cm}^{-1}$  is also noted and which may be assigned to chlorine atoms which tends to form a bridge between two metal atoms. In general the stretching frequencies of a bridging atom are much lower than terminal frequencies.

Figure 5.3 represents the infrared spectra of  $(75)TeO_2-(25-x)BaO-(x)V_2O_5$  system with increasing  $V_2O_5$  content up to 25% by keeping the  $TeO_2$  content constant. There is a rise in the band intensity at  $680\text{ cm}^{-1}$  at the expense of the band at  $780\text{ cm}^{-1}$ . This shift may be related to a quantitative effect of  $TeO_3$  groups accumulation and a decrease in the number of  $TeO_4$  group in the glass. The spectra of the binary glass system of  $(75)TeO_2-(25)V_2O_5$  has a spectrum different from that of the crystalline phase.

## 5.2 ULTRA-VIOLET AND VISIBLE SPECTROSCOPY.

### 5.2.1 Introduction:

The optical absorption of a substance such as glass in the ultra-violet and visible regions depends strongly on the electronic structures and involves the interaction between the incoming radiations and the electronic states of the glasses under consideration. The electronic states depend on the glass composition; each one has its own microstructure governed by the ions and ionic groups. The absorption depends on how tightly the electrons are bound in the microstructure. Photon-induced electronic transitions can occur between different bands and observation of changes in optical absorption coefficient can lead to the determination of the energy band gap. Such electronic transitions between the valence and conduction bands start at the absorption edge which in a crystalline material corresponds to the minimum energy difference between the lowest minimum of the conduction band and the highest maximum of the valence band. If these extrema lie at the same point in  $k$ -space, the transition are called direct. If this is not the case, the transitions are possible only when phonon-assisted and are called non-direct. In transition metal oxide glasses, in general, a photon with a certain range of energy could be absorbed by transition metal ions present in the glass, by two different processes.

i) The absorption may be due to internal transitions between the  $d$ -orbital electrons.

ii) The absorption may be due to transfer of an electron from a neighbouring atom to the transition metal ion and vice

versa. The absorption in the vanadium glasses is thought to arise from direct forbidden transition between the oxygen 2p bands and the vanadium 3d bands of the  $V_2O_5$  in the glass.

The fundamental absorption edge in most amorphous semiconductors in the lower energy and absorption ranges usually follows the Urbach rule<sup>23</sup>.

$$\text{i.e. } \alpha(\omega) = \text{constant} \exp(\hbar\omega/E_e).$$

where  $\alpha(\omega)$  is the absorption coefficient at angular frequency  $\omega$ , ( $\omega=2\pi\nu$ ) and  $E_e$  is the width of the tail of localised state in the band gap.  $E_e$  is typically in the range of (0.006-0.14) eV (18) for many amorphous materials below and at room temperature but for some ionically-bonded oxide glasses the values may be as high as 0.6 eV and above room temperature this value tends to increase with increasing temperature. According to Davis and Mott<sup>16</sup> the value of  $E_e$  is very much the same in a variety of materials. Dow and Redfield<sup>79</sup> proposed that the special Urbach rule arises from a random internal electric field broadening of an exciton line, while in explaining the nature of exponential absorption edges in non-crystalline materials Tauc<sup>24</sup> believes that such edges can arise from the interband transitions involving the tails of localised states where the density of states falls exponentially. The absorption in many amorphous materials is believed to be associated with indirect transitions and is observed to obey the following relation above the exponential tail;

$$\alpha(\omega)\hbar\omega = \text{constant}(\hbar\omega - E_{\text{opt}})^2 \quad \dots\dots(5.1)$$

This equation is widely used<sup>(20 - 34 - 80 - 82)</sup> for various

oxide glasses including the transition metal oxide glasses and the same quadratic equation is being used to investigate the  $V_2O_5$ -BaO-BaCl<sub>2</sub> and TeO<sub>2</sub>-BaO-BaCl<sub>2</sub> in this work.

### 5.2.2 Experimental methods.

All of the glasses investigated were effectively opaque, even in quite thin sections. In order to increase the region of transmission, much thinner specimens were required. It was found that suitable specimens could be obtained by blowing large bubbles of molten glass. The glasses were heated in a silica crucible to their melting temperature and a small amount of glass was collected on the end of a hollow silica rod, If the glass was of correct viscosity, a large sausage-shaped bubble could be blown. When it had solidified, the bubble was broken and the pieces collected and stored in a desiccator. A piece of the bubble was held in the beam of the spectrometer by attaching it to a plastic frame. It was possible to estimate the film thickness by using a sigma comparator. The film thickness were generally found to be around 2 $\mu$ m.

The absorption coefficients of these specimens were measured at room temperature in the wavelength range of 200 - 700 nm, using a Perkin - Elmer model 137 UV spectrometer. The optical absorption coefficient  $\alpha(\omega)$  were calculated by using the formula;

$$\alpha(\omega) = 1/d \log(I_0 / I_t) \quad \dots\dots(5.2)$$

Where  $I_0$  and  $I_t$  are the intensities of the incident and



transmitted beam respectively, and  $d$  is the thickness of the specimen.

### 5.2.3 Results and Discussion:

The optical absorption spectra for two series of  $V_2O_5$ -BaO-BaCl<sub>2</sub> and TeO<sub>2</sub>-BaO-BaCl<sub>2</sub> glasses having different BaCl<sub>2</sub> contents are shown in figures 5.9 and 5.10 respectively as a function of wavelength. It is clear that unlike those of crystalline semiconductors there is no sharp absorption band since the energies in the various bands are distributed around an average. It is noted however, that the absorption as a function of wavelength shows a steady decline, which is the characteristic of glassy materials. The values of the optical edge are obtained by extrapolating from the linear region of the plots of the quantity  $(\alpha h\nu)^{1/2}$  against the photon energy  $h\nu$  as suggested by Tauc<sup>24</sup>.

The  $E_{opt}$  value is a minimum in the absence of the halogen ion, this is because the concentration of non-bridging oxygen ions associated with vanadium ion is rather small. By partial substitution of BaO with BaCl<sub>2</sub> the values of  $E_{opt}$  increase continuously up to 7 mole% BaCl<sub>2</sub> and thereafter decrease. The graphs of  $(\alpha h\nu)^{1/2}$  versus  $h\nu$  show straight lines with some deviations at lower photon energies which following Redfield<sup>83</sup> may be due to imperfections in the materials.

In TeO<sub>2</sub>-BaO-BaCl<sub>2</sub> glasses, the value of  $E_{opt}$  is a minimum for zero BaCl<sub>2</sub> content. The introduction of BaCl<sub>2</sub> causes a shift in absorption edge towards higher energies. The values of  $E_{opt}$  lie in the range of 2.04 - 2.23 eV and 3.71

-3.89 for vanadate and tellurite glasses respectively. Figures 5.11 and 5.12 show the dependence of  $(\alpha\hbar\omega)^{1/2}$  on photon energy for both glass systems. From the results obtained quite a number of facts may be concluded. At low concentration of  $\text{BaCl}_2$ , the chloride ions act as bridging ions and provide connectivity for the vitreous network. It is generally accepted that absorption is caused by the transition of an electron from the state where it is bonded to an excited state. By introducing  $\text{BaCl}_2$  in the glass system, the electron bonded to a negative halogen ion requires additional energy to make such a transition. This energy which is a combined effect of the electron affinity of the chloride ion and the work done against the Coulomb attraction causes the value of  $E_{\text{opt}}$  to be increased up to 7 mole% of  $\text{BaCl}_2$ , but for a higher percentage of  $\text{BaCl}_2$  (>7%) it is possible that the chloride ions are loosened and act as non-bridging ions, resulting in a reduction of  $E_{\text{opt}}$ .

## CHAPTER 6.

### ELECTRICAL PROPERTIES.

#### .1 D.C. CONDUCTIVITY.

The electrical properties of oxide glasses have been extensively studied by many workers in the past. The conductivity of a material depends on the number of mobile electrons or ions present and also on the ease with which they can jump from one hole in the network to the next. Metals are essentially electronic conductors whereas traditional glasses are usually ionic. The ionic conductivity of virtually all oxide glasses results from the transport of monovalent cations such as  $\text{Na}^+$  in sodium silicate glass. Some of the early experiments which indicated that the electric current in soda-silica glass was due to the movement of sodium ions through the glass were carried out by Burt in 1925 using ordinary electric light bulbs. In 1954 certain special glasses containing multivalent oxides such as transition metal oxide glasses were found to have electrons available for carrying a current because they contain cations of reduced valency. This type of semi-conducting glasses was studied in the early days by Baynton, Rawson and Stanworth<sup>57</sup>. Most chalcogenide glasses, i.e. those containing pure or combined sulphur, selenium or tellurium are also electronic conductor. It is their semiconducting and switching properties that have excited interest in these glasses.

The conduction in transition metal oxide glasses is believed to involve the motion of small polarons. The conduction theory for small polarons was developed by Holstein<sup>26</sup> and Friedman<sup>84</sup>. Since that time many papers have been published {Monakata<sup>58</sup>, (1960), MacKenzie<sup>85</sup> (1964), Nester<sup>61</sup> (1965), Schmidt<sup>86</sup> (1968), Mott<sup>1</sup> (1968), Drake<sup>87</sup> (1969), Mott and Austin<sup>28</sup> (1969), Linsley et al<sup>88</sup> (1970), Sayer and Manning<sup>39</sup> (1972), Bandyopahyay et al<sup>89</sup> (1977), Khan et al<sup>90</sup> (1985), and Ravishankar Harani et al<sup>91</sup> (1986)} on electronic conduction of T.M. oxide glasses. Conductivity in these glasses arises through electron transfer from a lower valence state to a higher valence state e.g. ( $V^{4+} \leftrightarrow V^{5+}$ ), and it has been established that in vanadate glasses, the valency states lower than  $V^{4+}$  are unlikely and that  $V^{4+}$  ions probably share five-fold co-ordination with the surrounding oxygen ions, similar to the vanadium ions in crystalline  $V_2O_5$ . The transport mechanism is therefore seen as taking place in a single band composed of 3d levels, and the carriers as electrons localised on  $V^{4+}$  ions. Schmid<sup>86</sup> has predicted from theoretical considerations that if the interaction between any excess electrons and ionic lattice is strong, a small polaron will move by hopping process. The polaron consists of an electron which moves through the lattice, carrying with it a distortion of the lattice near the ion that it occupies. Conduction in the small polaron system has been reviewed by Austin and Mott<sup>28</sup> who suggested that the conductivity  $\sigma$  in these glasses can be expressed by the relation :

$$\sigma = \{ \nu_{ph} \cdot (Ne^2 R^2) / kT \} C(1-C) \exp.(-2aR) \exp.(-W/kT) \dots (6.1)$$

where  $\nu_{ph}$  is the phonon frequency,  $N$  is the concentration of the charged species per unit volume,  $e$  is the electronic charge,  $R$  is the average distance between the T.M. ion centres,  $C$  is the fraction of sites occupied by an electron.

e.g.  $(V^{4+} / V^{5+})$  etc.  $\alpha$  is the decay component of the wave function with distance  $R$ . The tunnelling term  $\exp(-2\alpha R)$  can be set approximately equal to unity if:

$$J > \hbar\omega_0.$$

where  $J$  is the polaron bandwidth and  $\omega_0$  is the dominant angular phonon frequency. This represents an adiabatic case. If  $J < \hbar\omega_0$  then the term  $\exp(-2\alpha R)$  remains in the expression for conductivity and the non-adiabatic regime is involved. Austin and Mott expressed the activation energy in the following fashion.

$$W = W_H + (1/2)W_D \quad \text{for} \quad T > \theta_D/4 \quad \dots\dots(6.2)$$

$$= W_D \quad \text{for} \quad T < \theta_D/4 \quad \dots\dots(6.3)$$

where the Debye temperature  $\theta_D$  is defined by:

$$\hbar\omega_0 = k\theta_D.$$

$W_D$  is the disorder energy and  $W_H$  is the hopping energy which is equal to  $(1/2)W_p$ . The polaron binding energy  $W_p$  is defined to be the total potential energy of the electron and that of its attendant lattice distortion. The binding energy is given by:

$$W_p = 1/2 \left( \frac{e^2}{\epsilon_p r_p} \right) \quad \dots\dots(6.5)$$

$\epsilon_p$  is the effective dielectric constant and is defined by

$$1/\epsilon_p = 1/\epsilon_\infty - 1/\epsilon_s \quad \dots\dots(6.6)$$

$\epsilon_s$  and  $\epsilon_\infty$  are the static and high frequency dielectric constants of the material.

Logomolov et al<sup>92</sup> found that the value of the polaron radius for crystalline solids is given by the equation

$$r_p = (1/2)(\pi/6N)^{1/3} \quad \dots\dots(6.7)$$

where  $N$  is the number of sites per unit volume. Hence the polaron should decrease in size as the number of sites increases.

## 3.2 PREPARATION OF SPECIMENS.

A number of bulk glass samples was prepared from the  $V_2O_5$ -BaO-BaCl<sub>2</sub>,  $TeO_2$ -BaO-BaCl<sub>2</sub> and  $V_2O_5$ - $TeO_2$ -BaO systems as described in chapter 4. A special sample holder Fig. 6.1 was designed for grinding in order to obtain parallel-faced surfaces. The annealed glasses were ground mechanically with a flexibox grinding machine using different grades of SiC powder. On achieving a thickness of about 2mm the samples were then cleaned with acetone and polished mechanically using diamond paste of grade 6 $\mu$ m. A light mobile oil and white spirit were used as lubricants during the process of grinding and polishing respectively. After polishing, the specimens were dried and annealed in the furnace at about 150<sup>0</sup>C for half an hour to relieve surface stress and to

remove volatile contaminants. Gold electrodes were evaporated in a guard ring configuration.

The prepared samples were kept at 200°C for two hours and then gradually cooled to room temperature. This process of heat treatment produces a good ohmic contact up to field as high as  $10^4$  V/cm.

### 3. ELECTRICAL CIRCUIT AND MEASURING METHODS.

The d.c. electric conductivity values of all specimens were measured by using the circuit as shown in Fig. 6.2. The current was measured by a Keithley 610C electrometer capable of measuring currents down to  $10^{-14}$  A. The power supply used as a Keithley 240A high voltage supply unit which could be used as a stabilized d.c. voltage source up to 1210V. The conductivity of a glass at a given temperature could be calculated from the applied voltage and current as follows:

$$R = V/I = \rho d/s = 1/\sigma \cdot d/s \quad \text{or} \quad \sigma = dI/sV \dots\dots(6.8)$$

here V is the applied voltage, d is the sample thickness, measured by using a micrometer screw gauge, s is the guarded electrode area and I is the electric current. Figure 6.3 represents the special sample holder that was made for room and high temperature measurements. The sample was kept in position with a pressure contact maintained by a spring. The heater was in the form of a cylindrical wire-round furnace. The temperature of each side of the sample was separately measured with Cu-constantan and chromel alumel thermocouples.

temperature was controlled by a Eurotherm temperature controller and operated by setting the pointer to the required temperature. When the heater reaches its equilibrium condition the temperature was steady to within  $\pm 3^{\circ}\text{C}$  before measurements were made. To eliminate the possibility of surface leakage during the current measurement, a guard ring configuration, as shown in Figure 6.3 was used. All measurements were carried out under a vacuum of about  $10^{-5}$  torr, in order to prevent any effects of the ambient atmosphere on the conduction.

#### 4 RESULTS.

The d.c. electrical conductivity values of all glasses under consideration were measured over the temperature range 293 to 453K. The variation of conductivity with temperature for all glasses are shown in Figures 6.5, 6.6, and 6.7. The d.c. conductivity increases with temperature and is a negative exponential function of inverse temperature. It can be expressed by the common Arrhenius equation.

$$\sigma = \sigma_0 \cdot \exp.(-W/kT) \quad \dots\dots(6.9)$$

where  $\sigma_0$  is a pre-exponential constant and W is an activation energy. The activation energies were calculated from the slopes of the log-conductivity versus the reciprocal temperature variation from the relation

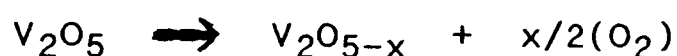
$$W = 0.198 \delta(\log \sigma) / \delta(1/T) \quad \dots\dots(6.10)$$



Experimental data show that  $\log \sigma$  varies linearly with the reciprocal of the absolute temperature. Tables 6.1 and 6.2 show that sodium tellurite glasses have relatively high conductivities as compared with barium vanadate glasses. Figures 6.8 and 6.9 show the variation of thermal activation energy  $W$  versus concentration. It is clear that by increasing the  $V_2O_5$  content in  $V_2O_5$ - $TeO_2$ - $BaO$  glasses, the activation energy decreases, whereas the addition of  $BaCl_2$  in  $TeO_2$ - $BaO$ - $Cl_2$  glasses causes the activation energy to increase and the conductivity to decrease. In the  $V_2O_5$ - $BaO$ - $BaCl_2$  glass system, by keeping a fixed proportion of vanadium in the system, the experimental data reveals that beyond 7% addition of  $BaCl_2$  there is a systematic change in the behaviour of the glass system. With the addition of chlorine up to 7% the conductivity decreases but beyond this value it increases, indicating structural changes. The logarithm of conductivity versus activation energy gives a straight line which implies that the pre-exponential term ( $\sigma_0$ ) is constant for all samples.

In order to check the type of conduction, a fixed voltage of 200 volts was applied over an extended period of time and the current was measured thereby giving a value of resistance. Apart from a short-term initial variation in current with time, the current is essentially constant over an extended period. This can be taken as evidence that a significant polarization effect in these glasses is absent and the electrical conductivity would in this case be due to transport of electrons rather than ions.

Figures 6.10 and 6.11 represent the effect of annealing on the electrical conductivity of  $V_2O_5$ -BaO-BaCl<sub>2</sub> glasses. As the annealing temperature is increased the electrical conductivity rises. It has been suggested by Khawaja that upon annealing, the oxygen deficiency is compensated by reduction of some vanadium ions to a lower oxidation state.



Here  $x$  increases with increasing temperature. The increase in the conductivity of the annealed sample could be due to the fact that upon annealing at 250°C for 2 hours, significant quantities of both  $V^{3+}$  and  $V^{4+}$  could easily co-exist. The change in colour of the sample from reddish-brown before annealing to dark-brown after annealing could be due to a change in oxidation state of the vanadium ion. The increase in conductivity on annealing was attributed by Khan et al.<sup>93</sup> to the change in microstructure of the glass. Nester and Ungery<sup>94</sup> used the following formula to determine the concentration of vanadium ions in the vanadate glasses.

$$N = \rho_G (W\%) N_0 / A.W. \times 100 \quad \dots\dots(6.11)$$

Using the same formula we calculated the concentration of vanadium ions in  $V_2O_5$ -BaO-BaCl<sub>2</sub> and  $V_2O_5$ -TeO<sub>2</sub>-BaO glasses in each composition range. Results are given in tables 6.1 and 2. In the above equation,  $N$  is the total ion concentration,  $\rho_G$  is the density of glass (in gr/cm<sup>3</sup>),  $W\%$  is the weight percent of vanadium(gr),  $N_0$  is the Avogadro number ( $6.023 \times 10^{23}$ ) and  $(A.W)$  is the atomic weight. The average V-V

spacing in these glasses were determined by using the total ion concentration in the relation

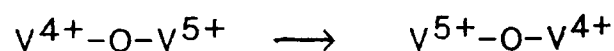
$$R = (1/N)^{1/3} \quad \dots\dots(6.12)$$

Figure 6.10 represents the activation energy as a function of  $r_0$ -V spacing for  $V_2O_5$ - $TeO_2$ -BaO glasses.

The variations of ion spacing versus concentration are shown in Figure 6.11.

### 6.5DISCUSSION.

The d.c. electrical conductivity of the glasses under consideration was found to be mainly dependent on the transition metal oxide and its valence states. It is generally recognized that the T.m. oxide glasses exhibit semiconductivity and the conduction in such glasses is due to a hopping process, that is the transfer of an electron and/ or a hole between the ions of the same transition metal in the different valence state, i.e.



The experimental data in most publication are discussed in terms of the Mott theory. Equation (6.1) is usually applied for the analysis of d.c. conductivity and can be compared with equation (6.9). In many ways equation (6.1) is similar to equation (6.9) for the hopping of polarons. The pre-exponential term in the present glasses was found to be almost constant while on the other hand the conductivity was

function of T.M. oxide content and oxidizing agent i.e.  $\text{BaCl}_2$ . The addition of  $\text{BaCl}_2$  alters the valence state and hence controls the conductivity of the glass. It may be suggested that as the chlorine replaces the oxygen ions, it may be possible that at low chlorine content, the chloride ions act as bridging bonds and the new bridge bonds provide connectivity for the vitreous network. These bridging chlorine ions are difficult to free from sites, since a pair of bonds must be broken and consequently, as expected reduce the conductivity. The conductivity decrease was also associated with an increase in activation energy. At a high admixture of  $\text{BaCl}_2$  (>7%) it is possible that the chlorine ions act as non-bridging ions, consequently they become liberated from the glass network as they become more loosely bonded to the network.

The change in composition mainly affects the activation energy (Fig. 6.8). In fact an increase in T.M. oxide content results in a decrease in T.M.-ion spacing (Fig. 6.11) which accordingly leads to a decrease in the activation energy  $W$  (Fig. 6.8). Such a variation of activation energy  $W$  with ion spacing has been observed for many T.M. oxide glasses. Different investigators (28-39-92-95) calculated the small polaron radius  $r_p$  from the relation

$$r_p = 1/2 (\pi/6N)^{1/3} \quad \dots\dots(6.13)$$

postulated by Bogomolov et al<sup>93</sup>. The theory of small polaron states that the polaron radius  $r_p$  should be smaller than the site separation and greater than the radius of the ion on

high the electron is localized. The  $r_p$  values obtained here are recorded in Table 6.1 and 6.2. The polaron radius is a function of the T.M. oxide concentration in these glasses and decreases as the T.M. oxide content increases. It is clear from Table 6.1 and 6.2 that  $r_p$  for each composition is less than the site spacing. Generally the conduction mechanism in the glasses under investigation could be summarized as follows:

- i) Conduction in these glasses is ohmic.
- ii) The log conductivity versus reciprocal temperature plot displays linear behaviour which is typical of the small polaron hopping mechanism.
- iii) The pre-exponential factor is almost constant.
- iv) The T.M. oxides and oxidizing agent could be dominant actors in these glasses. Upon oxidation the 3d shell gains an electron from the 4s shell by an amount determined by the degree of oxidation.
- v) Activation energy decreases and conductivity increases with increasing T.M. oxide concentration.
- vi) The activation energy  $W$  for conduction is proportional to the vanadium ion separation.
- vii) The conduction behaviour of the glasses displays features which can be determined and are characterised by the classical Mott formalism.
- viii) The conduction mechanism in vanadate glasses in the glass composition range is certainly electronic.
- ix) The electrical conductivity depends on the thermal history of the glass.

## CHAPTER 7

### 7.1. SUMMARY AND CONCLUSION

In this chapter we shall attempt to summarise the main features of the experimental results and to point out similarities or anomalies where apparent.

#### **(i) $V_2O_5$ -BaO-BaCl<sub>2</sub> series.**

The d.c. electrical conductivity varies by the introduction of BaCl<sub>2</sub> into the glass system as chlorine ions replace some of the oxygen ions. The conductivity measured at room temperature continuously decreases up to 7 mole% BaCl<sub>2</sub>, but beyond about 7 mole% the conductivity increases.

The activation energy varies with the composition from 0.43 to 0.51 eV up to 7 mole% BaCl<sub>2</sub> and then beyond this it decreases gradually from 0.51 to 0.39 eV.

Measurements of density and  $V^{4+}$  ion concentration determined by e.s.r. spectroscopy indicate that at 7mole% BaCl<sub>2</sub> a systematic change is occurring in the structure of the glass as the incorporation of halogen(chlorine)alters the ratio of the normal and reduced valencies of the vanadium ions.

The absorption spectrum as a function of wavelength shows that, in contrast to crystalline  $V_2O_5$ , there is no sharp absorption edge(which is characteristic of the glassy state)and it also illustrates the variation of position of the absorption edge as the content of BaCl<sub>2</sub> is increased. The values of  $E_{opt}$  increase continuously up to 7 mole%BaCl<sub>2</sub> and thereafter decrease. The values lies in the range of 2.04-2.23 eV.

It is generally accepted that optical absorption is caused by transition of an electron from its bound state to a state of higher energy. By the inclusion of BaCl<sub>2</sub> in the glass system, the electron associated with a negatively charged halogen ion requires additional energy to make such a transition. This energy which is related to the combined effects of the electron affinity of the chlorine ion and the work done against the Coulomb attraction causes the value of  $E_{opt}$  to be increased at low concentration of BaCl<sub>2</sub>(7mole%). With further inclusion of chlorine however the values of  $E_{opt}$  reduce as the higher concentration leads to a disruption of the network and some of the chlorine ions break away from their bridging role, leading to a rise in disorder in the structure of the glass. There is a change in optical absorption coefficient when

$\hbar\omega$  for the incident photon exceeds  $(E_C - E_V)$  and an electron can travel only by hopping from one site to another in the state for which  $E_V < E < E_C$  is localized.

The infra-red absorption spectra show five absorption bands at 250, 260, 620-650, 890 and 980  $\text{cm}^{-1}$ . The maximum absorption is recorded at 625  $\text{cm}^{-1}$ . A band at 980  $\text{cm}^{-1}$  could indicate a shift from 1010  $\text{cm}^{-1}$  which is believed to be the normal vibration frequency of the vanadium-oxygen bond. The broad band at 620-650  $\text{cm}^{-1}$  could be due to the combined effect of V-O-Ba vibrations. The band at 250-255  $\text{cm}^{-1}$  may be assigned to chlorine atoms and involves a change in the behaviour of bridging chlorine ions as the stretching frequencies which for a bridging atom are normally somewhat lower than the terminal frequencies.

## (ii) $\text{TeO}_2$ -BaO-BaCl<sub>2</sub> series

The main results are as follows:

The dc electrical conductivity decreases by the addition of BaCl<sub>2</sub> up to 7mole% BaCl<sub>2</sub> by keeping the content of glass former ( $\text{TeO}_2$ ) constant. It shows very close similarities with the barium-vanadate glasses, although it was not found possible to make a glass with the composition of BaCl<sub>2</sub> greater than 7mole%, but below this composition conductivity follows the same trend as for the first series.

The plot of  $\text{Log } \sigma$  (electrical conductivity) with inverse temperature showed a linear relation within the temperature range from room temperature to 180°C. The addition of the halogen to the glass causes the activation energy to increase as the conductivity decreases. The linearity of the  $\text{log } \sigma$  versus  $1/T$  curves show that the pre-exponential term ( $\sigma_0$ ) is constant for all samples. Further investigations on the electrical conductivity confirm that no significant polarization effect in these glasses is observed and the conductivity is due to the transport of electrons rather than ions.

The incorporation of halogen into this series of glasses increases the value  $E_{\text{opt}}$  from 3.71eV to 3.89eV, which probably due also to the combined effect of electron affinity and Coulomb attraction as discussed for the first series of the glasses.

Infra-red spectral measurements were recorded for both crystalline BaO,  $\text{TeO}_2$  and BaCl<sub>2</sub> and glassy samples for comparison. A typical broadening of the bands is observed in the spectra of the glasses, which indicates the similarities of the

structural units and of the short range order. With the incorporation of  $\text{BaCl}_2$  two new absorption bands appears at about 250 and 260  $\text{cm}^{-1}$  and can be assigned to the naturally occurring chlorine species. It also indicates that the introduction of the chlorine shifts the absorption maximum from 675 to 655  $\text{cm}^{-1}$  but the overall shape of the spectra do not change in any significant manner.

### (iii) $\text{TeO}_2$ - $\text{BaO-V}_2\text{O}_5$ series.

The third system was made as an attempt to establish how features typical of the two glass forming oxides  $\text{TeO}_2$  and  $\text{V}_2\text{O}_5$  are retained in the glassy state.

The dc electrical conductivity was found to be higher than for barium vanadate glasses. Increasing the content of TM oxide leads to a decrease in V-V ion spacing, which accordingly leads to a decrease in activation energy from 0.38 to 0.31 eV and the polaron radius is also found to decrease as the TM oxide content is increased.

In general the conductivity and carrier concentrations are largely controlled by  $W/kT$ , the ratio of the activation energy to the thermal energy.

The e.s.r. investigation revealed that the vanadium ion exists in more than one valency states and the e.s.r. spectrum exhibits a rather resolved hyperfine structure due to interaction of the unpaired electron with the vanadium nucleus. It is found that the width of the hyperfine structure component increases as the concentration of ( $\text{V}^{4+}$ ) ions increases. This arises because the contribution of the 3d electrons to hyperfine splitting decreases with  $\text{V}_2\text{O}_5$  content and the 3d orbital is increasingly screened from its nucleus through overlap of the electron orbits of the surrounding ligand. This produces an expansion of the 3d orbital resulting in a decreased interaction with the vanadium nucleus.

The thermal history of the samples affects their conductivity. As the annealing temperature rises the conductivity increases. It has been suggested that the deficiency of the oxygen is compensated by reduction of some vanadium ions to a lower oxidation state and that the change in the appearance of the sample after the annealing, is direct proof of a change in oxidation state of the vanadium ion.

### (iv) General.

The experimental data for all of these glasses seem to have some similarities, particularly those of barium-vanadate and barium-tellurite doped with barium



chloride. For these glasses all parameters measured decrease with increase in the concentration of  $\text{BaCl}_2$  in the range 0 to 7 mole% , but increase again for further additions of  $\text{BaCl}_2$ . The effect of halogen on copper phosphate glasses investigated by Hogarth and Popov shows such behaviour, but the critical value for copper chloride in those glasses is in the range of 3 to 5 mole% of  $\text{CuCl}_2$  and the general picture is much the same.

Infra-red spectroscopy revealed some similarities in the band position for example a broad band at  $620\text{-}650\text{ cm}^{-1}$  in glasses having vanadium and barium components in their composition and may well be the combined effect of V-O-Ba vibrations and a weak band at  $980\text{ cm}^{-1}$  could indicate a shift from  $1010\text{ cm}^{-1}$  which is believed to be the normal vibration frequency of the V-O bond. A band at  $250\text{-}260\text{ cm}^{-1}$  is also noted for those glasses containing halogen atoms and the introduction of chlorine certainly shifts the absorption maximum from  $675$  to  $655\text{ cm}^{-1}$  but the overall shape of the spectrum does not change in any significant manner. In contrast to tellurite glasses, the spectra of glasses containing TMI differ from that of the crystalline phase, which is probably due to a more dominant effect of the dipole moment involved in the vibration as a result of the reduction in the symmetry. All glasses show that thermal and optical excitation processes are two important ways of inducing semiconducting behaviour. Their properties are strongly affected by the presence of the third oxide and this can make their initial study confusing, but it is on this account that technologically important materials and devices can be made, since there is a significant effect on the overall electronic structure as well as on the resultant physical properties of the glasses, when a third component (which may include a halogen) is incorporated in the glasses.

## REFERENCES.

1. Mott, N.F., J. Non-Cryst. Solids, 1, 1(1968).
2. Zachariasen, W.H., J. Am. Chem. Soc., 54, 3841 (1932).
3. Rawson, H., "Inorganic Glass Forming Systems" (Academic Press), (1967).
4. Sargeant, P.T., and Roy, R., Mat. Res. Bulletin, 3, 265 (1968).
5. Mott, N.F., and Davis, E.A., "Electronic Processes in Non-Crystalline Materials", Clarendon Press, Oxford, (1971).
6. Van Wazer, J.R., J.Am. Ceram. Soc., 72, 639(1950).
7. Stevels, J.M., J.Soc. Glass Tech.,35, 284(1951).
8. Anderson, P.W., Phys.Rev., 109, 1492 (1958).
9. Kolomiets, V.T, Lebedev, E.A. and Takasami, I.A., Sov. Phys. Semiconductors, 3, 621(1969).
10. Ioffe, A.F. and Regel, A.R., Prog. Semicond., 4, 237 (1960).
11. Gubanov, A.I., "Quantum Electron Theory of Amorphous Conductors Consultants Bureau", N.Y., (1965).
12. Anderson, P.W., Phys. Rev., 109 1492 (1958).
13. Ovshinsky, S.R., Phys. Rev. Letters, 21, 1450 (1968).
14. Cohen, M.H., Fritzsche, H. and Ovshinsky, S.R., Phys. Rev. 22, 1065 (1969).
15. Fritzsche, H., "Amorphous and Liquid Semiconductors" Chap. 5, pp.221, Ed. J. Tauc (Plenum), (1974).
16. Davis, E.A. and Mott, N.F. Phil Mag., 22, 903 (1970).
17. Mott, N.F. Phil. Mag., 24, 911 (1971).
18. Marshall, J.M. and Owen, A.E., 24, 1281 (1971).
19. Mott, N.F. and Twose, W.D., Adv. in Phys., 10, 107 (1961).

20. Mott, N.F. and Davis, E.A., "Electronic Processes in Non-Crystalline Materials", Clarendon Press, Oxford (1971).
21. Miller, A., Abraham, S.E., Phys. Rev., 120, 745 (1970).
22. Grant, A.J. and Davis, E.A., Solid State Communication, 15, 563 (1974).
23. Urbach, F., Phys. Rev., 92, 1324 (1953).
24. Tauc, J., "The Optical Properties of Solids", ed. Abels, F. (North-Holland, Amsterdam), 277 (1970).
25. Emin, D. and Holstein, T., Ann. Phys. (N.Y.) 53, 621 (1969).
26. Holstein, T., Ann. Phys. 8, 343 (1959).
27. Mott, N.F. and Gurney, R.W., "Electronic Processes in Ionic Crystals", Oxford, London (1950).
28. Austin, I.G. and Mott, N.F., Adv. in Phys., 18, 41 (1969).
29. Bosman, A.J. and Van Daal, H.J., Adv. in Phys., 19, 1 (1970).
30. Van Daal, H.J., Proc. 2nd Int. Conf. on Conduction in low-mobility materials, Taylor and Francis, London, 17 (1971).
31. Kennedy, T.N., Hakim, R and Mackenzie, J.D., Mat. Res. Bull, 2, 193 (1967).
32. Roscoe, H.E., Phil. Trans. Roy. Soc., 158, 1 (1958).
33. Denton, E.P., Rawson, H., and Stanworth, J.E., Nature, 173, 1030 (1954).
34. Malik, M.S., PhD. Thesis, Brunel University (1989).
35. Hajian, M., MPhil. Dissertation, Brunel University, (1982).
36. Hansen, K.W., J. Electro. Chem. Soc., 112, 994 (1965).
37. Hansen, K.W. and Splann, M.T., *ibid*, 113, 895 (1966).
38. Kinser, D.L., *ibid*, 117, 546 (1970).
39. Sayer, M. and Mansingh, A., Phys. Rev. Bul., 6, 1629 (1972).

40. Ahmed, M.M., PhD. Thesis, Brunel University (1982).
41. Moridi, G.R., PhD. Thesis, Brunel University(1975).
42. Mohammed Elahi, S., PhD. Thesis, Brunel University (1979).
43. Moridi, G.R. and Hogarth, C.A., Int. J. Electronics 37, 141 (1974).
44. Hogarth, C.A., and Hosseini, A.A., J. Mater. Sci., 18, 2697 (1983).
45. Malik, M.S., and Hogarth, C.A., J. Mater. Sci., 8, 655 (1989).
46. Khan, M.N., J. Mater. Sci., 20, 2207 (1985).
47. Dimitriev, Y., Marinov, M., Ivanova, Y. and Popov, M.C.R, Acad. Bulg. Sci., 23, 507 (1970).
48. Dimitriev, Y., Mariniva, M. and Ivanova, Y., ibid, 24, 319 (1971).
49. Grechanik, L.A., Petrovykh, N.V., and Karpechenko, V.G., Sov. Phys. Sol. State, 2, 1908 (1961).
50. Lynch, G.F., Sayer,M., Segel, S.L., and Rosenblatt, G., J. App. Phys., 42, 2587 (1971).
51. Linsley, G.S., PhD. Thesis, University of Sheffield (1968).
52. Kinser, D.L., and Wilson, L.K., Proc. 2nd. Solid State. Conf, Cairo (1973).
53. Bogomalova, L.D., Dolgolenko, T.F., Lazukin, V.N., and Filatova, I.V., Sov. Phys. Sol. State, 16, 5 (1974).
54. Morin, F.J., Bell. Syst. Tech. J, 37, 1047 (1958).
55. de Boer, J.H., and Verwey, E.J.W., Proc. Phys. Soc. (London), 49, 66 (1937).
56. Mott, N.F., Proc. Phys. Soc. (London), 62A, 416 (1949).
57. Baynton, P.L., Rawson, H. and Stanworth, J.E., J. Electrochem. Soc., 104, 237 (1957).
58. Munakata, M., Sol. State Electronics, 1, 159 (1960)
59. Ioffe, V.A., Patrina, J.B. and Poberovshaya, I.S., Sov. Phys. Sol. State, 2, 609 (1960).

60. Hamblen, D.P., Weidel, R.A., and Blair, G.E., J. Amer. Ceram. Soc., 46, 499 (1963).
61. Nester, N.H. and Kingery, W.D., Proc. 7th. Int. Cong. on Glass, Brussels, 106 (1965).
62. Hosseini, A.A., PhD. Thesis, Brunel Univ. (1982).
63. Anderson, G.W. and Luehrs, W.D., J. Appl. Phys., 39, 1634 (1968).
64. Sears, F.W., Zemansky, M.W., and Ypung, H.D., "College Physics", Fourth ed., Addition- Wesley Publishing Company, Chapt. 12, 201 (1974).
65. Gossing, R.G. and Stevels, J.M., J. Non-Cryst. Sol., 5, 217 (1970).
66. Jonscher, A.K., Thin Solid Films, 1, 213 (1967).
67. Landsberger, F.R., and Bray, P.J., J. Chem. Phys., 53, 2757 (1970).
68. Muncaster, M., J. Non-Cryst. Solids, 24, 399 (1977)
69. Corbridge, D.E.C., Lowe, E.J., J. Chem. Soc. 493 (1954).
70. Bohovich, Y.S., Opt. Spectry., (USSR), (English Transl.), 12, 269 (1962).
71. Shih, C.K. and Su, G.J., Proc. 7th Inter. Congr. Glass. Brussels, 8, (1965).
72. Wong, J., J. Non-Cryst. Solids, 20, 83 (1976).
73. Sayer, M., Mansingh, A., Reyes, J.M., and Lynch, G.F., Proc. 2nd. Int. Conf. on Conduction in Low-Mobility Materials, Taylor and Francis, London, 115 (1971).
74. Anderson, G.W., and Compton, W.D., J. Chem. Phys., 52, 6166 (1970).
75. Herzberg, G. "Molecular Spectra and Molecular Structure" Part 11. Van Nostrand-Reinhold, Princeton, New Jersey (1945).
76. Hogarth, C.A., and Hosseini, A.A., J. Mater. Sci. Letter, 359 (1984).
77. Anvary, S.F., PhD. Thesis, Brunel University (1976)
78. Chopra, K.R. and Bahi, S.K., Thin Solid Film, 11, 377 (1972).

79. Dow, J.D. and Redfield, D., Phys. Rev. B5, 594 (1972).
80. Koffyberg, F.P. and Kazio1, N.J., J. Appl. Phys. 47, 4701 (1976).
81. Koffyberg, F.P., Phys. Status Solidi B, 80, 669 (1977).
82. Nouruzi-Khorassani, A., PhD Thesis, Brunel Univ. (1978).
83. Redfield, D. and Afromowitz, A., Appl. Phys. Lett. 11, 138 (1967).
84. Friedman, L., Phys. Rev., A133, 1668 (1964).  
Friedman, L. and Holstein, T., Ann. Phys. 21, 294 (1963).
85. Mackenzie, J.D., "Modern Aspects of the Vitreous State", 3rd Ed. Butterworths (1964).
86. Schmid, A.P., J. Appl. Phys., 39, 3140 (1968).
87. Drake, C.F., Scanlan, I.F. and Engel, A., Phys. Status Solidi, 32, 193 (1969).
88. Linsley, G., Owen, A.E. and Hayattee, F.M., J. Non. Cryst. Solids, 4, 208 (1970).
89. Bandyopadhyay, A.K. and Isard, J.O., J. Phys. D., Appl. Phys. 10, 199 (1977).
90. Khan, M.N., J. Mater. Sci. Lett., 5, 685 (1986).
91. Ravishankar, H. and Hogarth, C.A., J. Mater. Sci. Lett. 5, 492 (1986).
92. Bogomolov, V.N., Kudimov, E.K. and Firsov, A., Sov. Phys. Solid State, 9, 2502 (1968).
93. Khan, M.N., Hassan, M.A. and Hogarth, C.A., Phys. Stat. Sol. (a) 106, 191 (1988).
94. Nèster, H.H. and Kingery, W.D., VII Internat. Congress on Glass, Brussels, 106 (1965).
95. Greaves, G.N., J. Non-Cryst. Solids, 11, 427 (1973)

Glass system -	Approximate range of $V_2O_5$ content forming glass
$V_2O_5 - P_2O_5$	<95%
$V_2O_5 - GeO_2$	10%-75%
$V_2O_5 - TeO_2$	10%-60%
$V_2O_5 - As_2O_3$	<50%
$V_2O_5 - BaO$	63%-73%
$V_2O_5 - PbO$	46%-62%

**Table(3.1)- Composition range for glass formation of various vanadate glasses as a determined by Denton et. al.**

Batch composition (mole%)			Weight loss (%)
$V_2O_5$	BaO	$BaCl_2$	
65	35	0	0.00
65	32	3	0.00
65	30	5	0.10
65	28	7	0.15
65	25	10	0.20
65	22.5	12.5	0.15
65	20	15	0.30

Table(4.1)-The effect of melting on composition of glasses.



Glass sample notation	V <sub>2</sub> O <sub>5</sub> mole%	BaO mole%	BaCl <sub>2</sub> mole%	TeO <sub>2</sub> mole%	Relative density	Molar volume Cm <sup>3</sup>
A	65	35	0	-	3.75	45.96
B	65	32	3	-	3.63	47.81
C	65	30	5	-	3.51	49.75
D	65	28	7	-	3.50	50.21
E	65	25	10	-	3.51	50.53
F	65	20	15		3.64	49.48
G	25	0	-	75	4.65	35.52
H	20	5	-	75	4.945	33.08
I	15	10	-	75	5.05	32.14
J	10	15	-	75	5.19	31.00
K	-	25	0	75	5.36	29.48
L	-	22	3	75	5.22	30.59
M	-	20	5	75	5.17	31.10
N	-	19	6	75	5.10	31.63
O	-	18	7	75	5.05	32.05

Table(4.2)- Composition, Density and molar volume values for different glasses.

mole%)	Weight of sample (g)	total (g)	Spin concentration		V <sup>4+</sup> content in 100g of glass	$\frac{[V]}{[V]_{total}}$
			Spin/g	Spin/cm <sup>-3</sup> x(10 <sup>20</sup> )		
0	0.1504	38.1	9.15x10 <sup>19</sup>	2.06	0.774	0.020
3	0.1277	38.1	1.05x10 <sup>20</sup>	1.89	0.762	0.020
5	0.1210	38.1	1.10x10 <sup>20</sup>	1.88	0.749	0.019
7	0.1503	38.1	8.48x10 <sup>19</sup>	1.79	0.717	0.018
10	0.1447	38.1	1.69x10 <sup>20</sup>	3.15	1.430	0.037
12.5	0.1466	38.1	1.52x10 <sup>20</sup>	3.28	1.286	0.034
15	0.1200	38.1	1.79x10 <sup>20</sup>	3.45	2.116	0.055
standard	0.0172					

Table(4.3)-Parameters of e.s.r. spectra of glasses in the system V<sub>2</sub>O<sub>5</sub>-BaO-BaCl<sub>2</sub>.

Sample designation	Weight of sample (g)	V <sub>total</sub> (g)	Spin concentration		V <sup>4+</sup> content in 100g of glass	$\frac{V^{4+}}{V_{total}}$
			Spin/ g x10 <sup>19</sup>	Spin/Cm <sup>-3</sup> x10 <sup>20</sup>		
3	0.2002	14.54	16.00	4.50	1.350	0.093
1	0.2038	10.77	6.27	1.80	0.530	0.049
	0.2109	7.44	4.68	1.39	0.396	0.053
	0.2109	4.94	2.94	0.87	0.250	0.051

Table(4.4)-Parameters of e.s.r. spectra of glasses in the system TeO<sub>2</sub>-BaO-V<sub>2</sub>O<sub>5</sub>

Sample	Conductivity at 373 K ( $\Omega \text{ cm}$ ) <sup>-1</sup> $\times 10^{-6}$	Activation energy W(eV)	Number of sites $N \times 10^{22}$ ( $\text{cm}^{-3}$ )	V-V spacing (nm)	Polaron radius $r_p$ (nm)	TMI content (%)
a	2.5	0.43	1.68	0.390	0.157	38.1
b	1.40	0.47	1.63	0.394	0.158	38.1
c	1.20	0.51	1.58	0.398	0.160	38.1
d	0.74	0.49	1.57	0.399	0.161	38.1
e	4.80	0.38	1.58	0.398	0.160	38.1
f	6.50	0.39	1.64	0.393	0.158	38.1

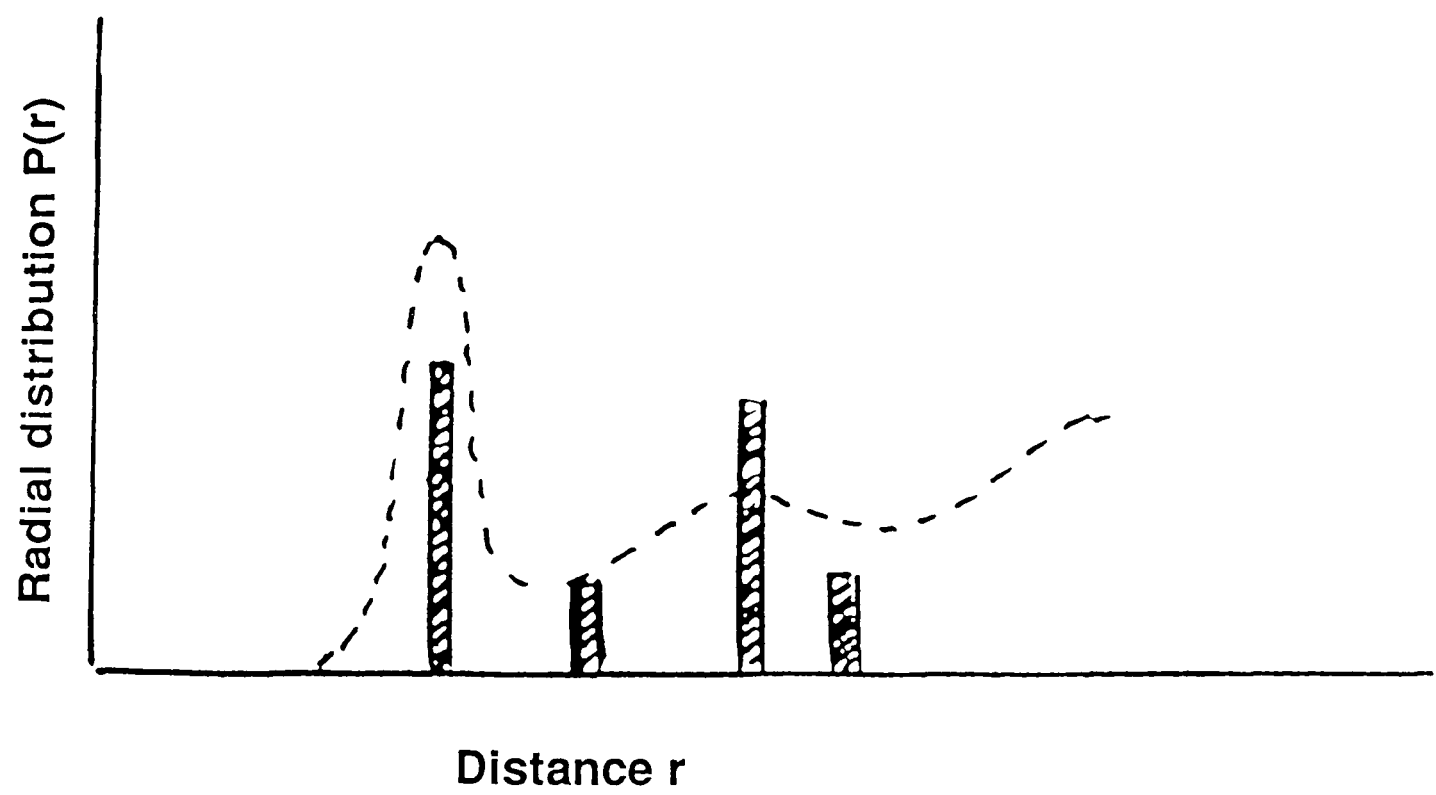
**Table (6.1)-Physical parameters of some barium vanadate glasses doped with barium chloride.**

Sample	Conductivity at 373 K ( $\Omega \text{ cm}$ ) <sup>-1</sup> $\times 10^{-4}$	Activation energy W(eV)	Number of sites $N \times 10^{22}$ ( $\text{cm}^{-3}$ )	V-V spacing (nm)	Polaron radius $r_p$ (nm)	TMI content (%)
g	21	0.31	7.98	0.508	0.205	14.54
h	13	0.33	6.29	0.542	0.218	10.77
i	8.4	0.36	4.43	0.609	0.245	7.44
j	5.8	0.38	3.02	0.692	0.283	4.94

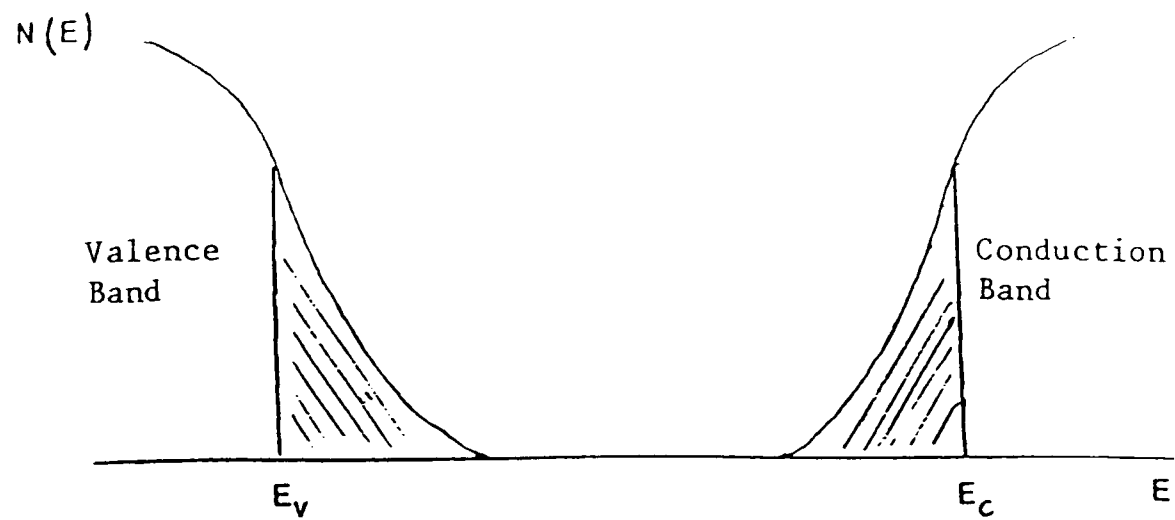
**Table (6.2)-Physical parameters of vanadium tellurite glasses containing barium oxide.**

BaCl <sub>2</sub> content (%)	0	3	5	7	10	12.5	15
E <sub>opt</sub> (eV)	2.04	2.16	2.18	2.23	2.16		2.05
W (eV)	0.43	0.47	0.51	0.49	0.38	0.38	0.39

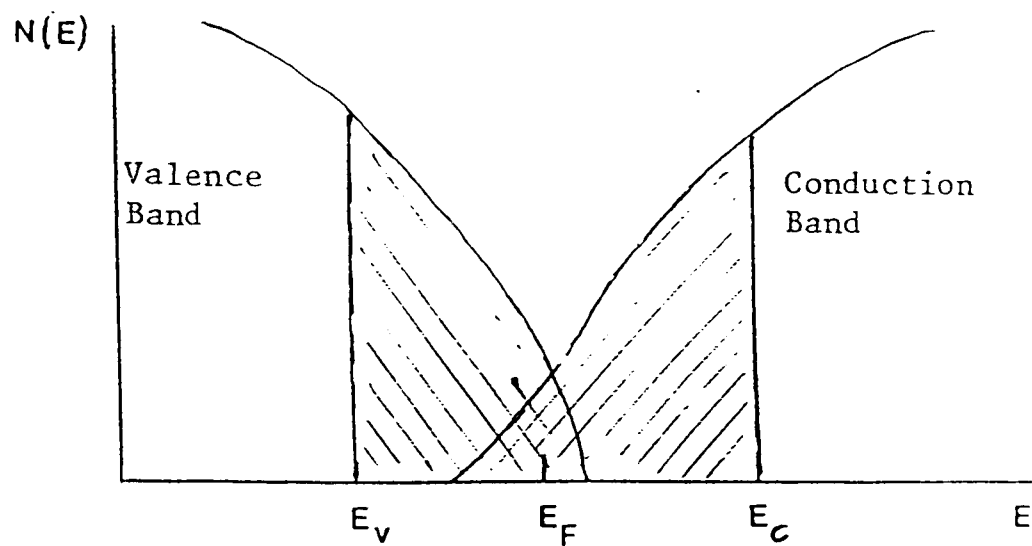
**Table(6.3)-The effect of composition on E<sub>opt</sub> and activation energy(W).**



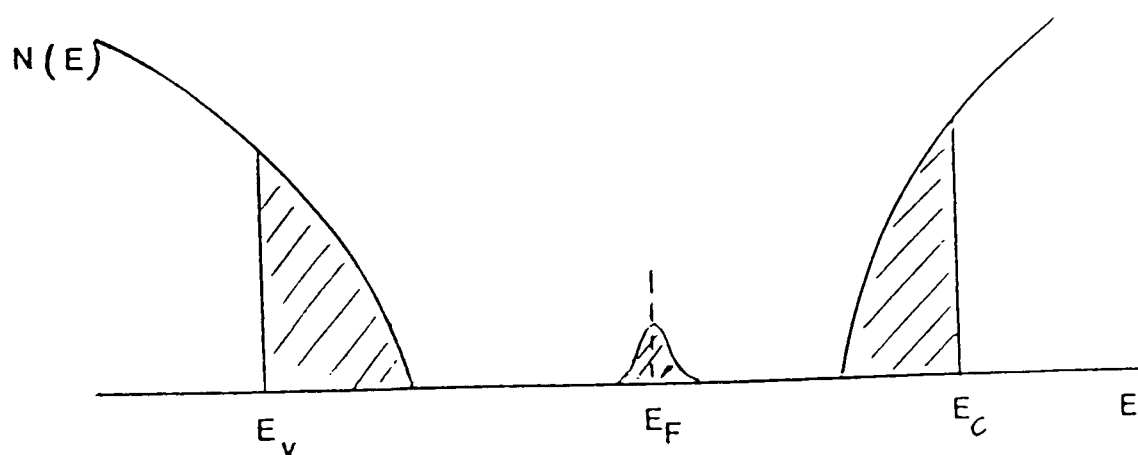
Figure(2.1)- Radial distribution  $P(r)$  versus distance  $r$  .



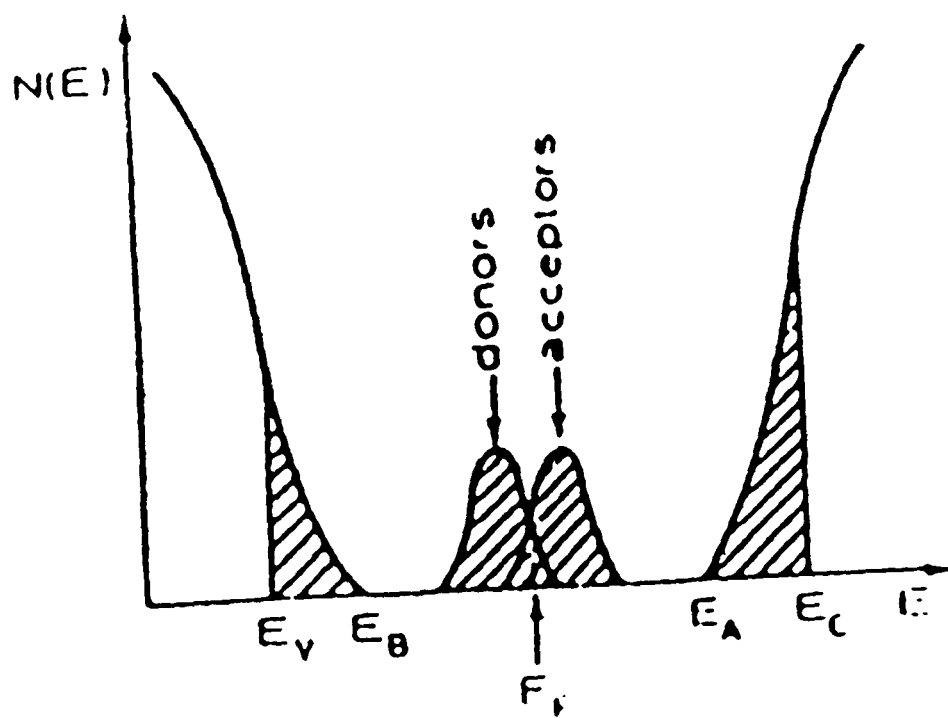
Figure(2.3)- Basic band model for amorphous semiconductors.



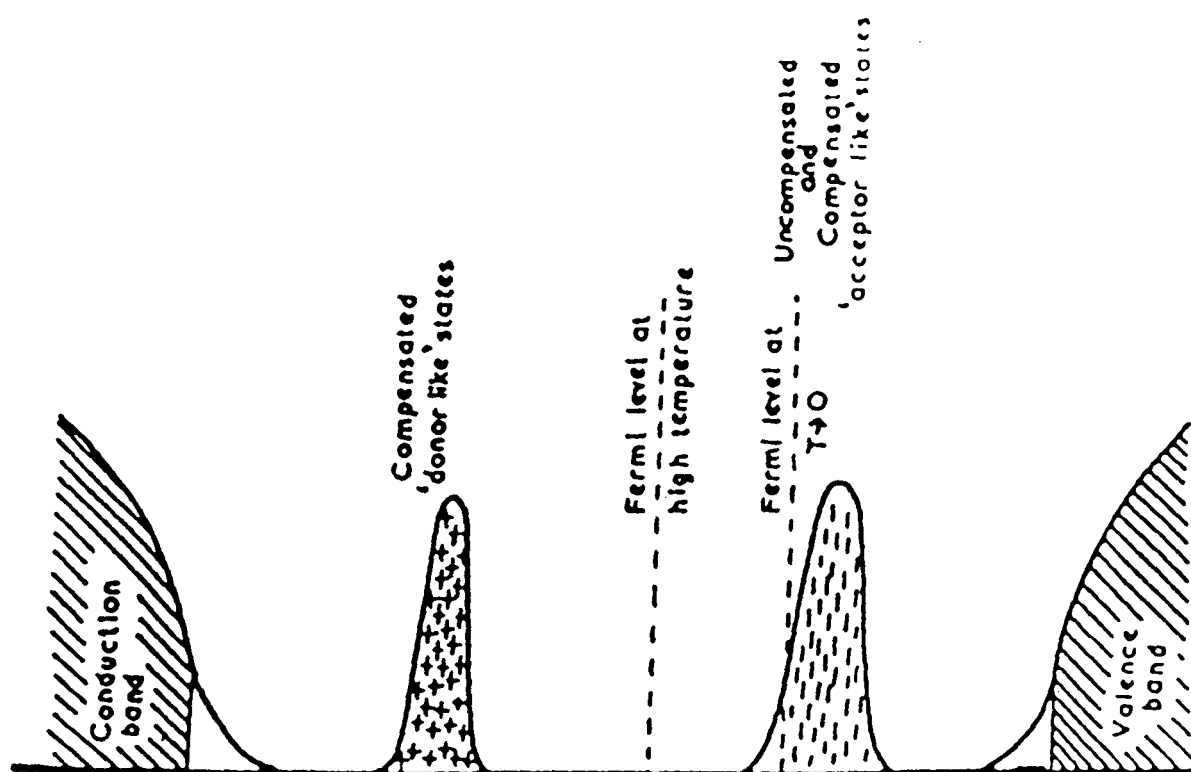
Figure(2.4)-Band model for amorphous semiconductors in CFO model.



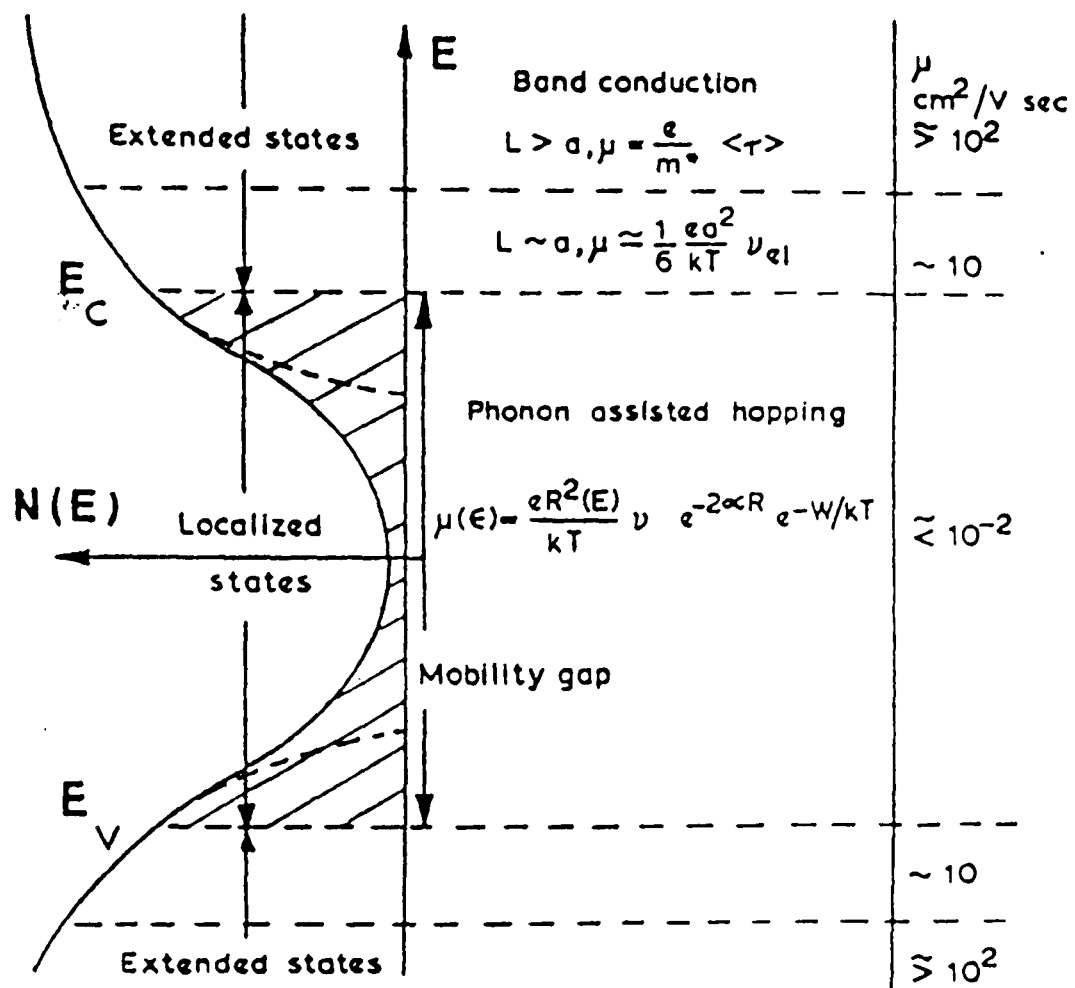
Figure(2.5)-Density of states according to Davis and Mott model.



Figure(2.6)-Density of states, Mott's model.

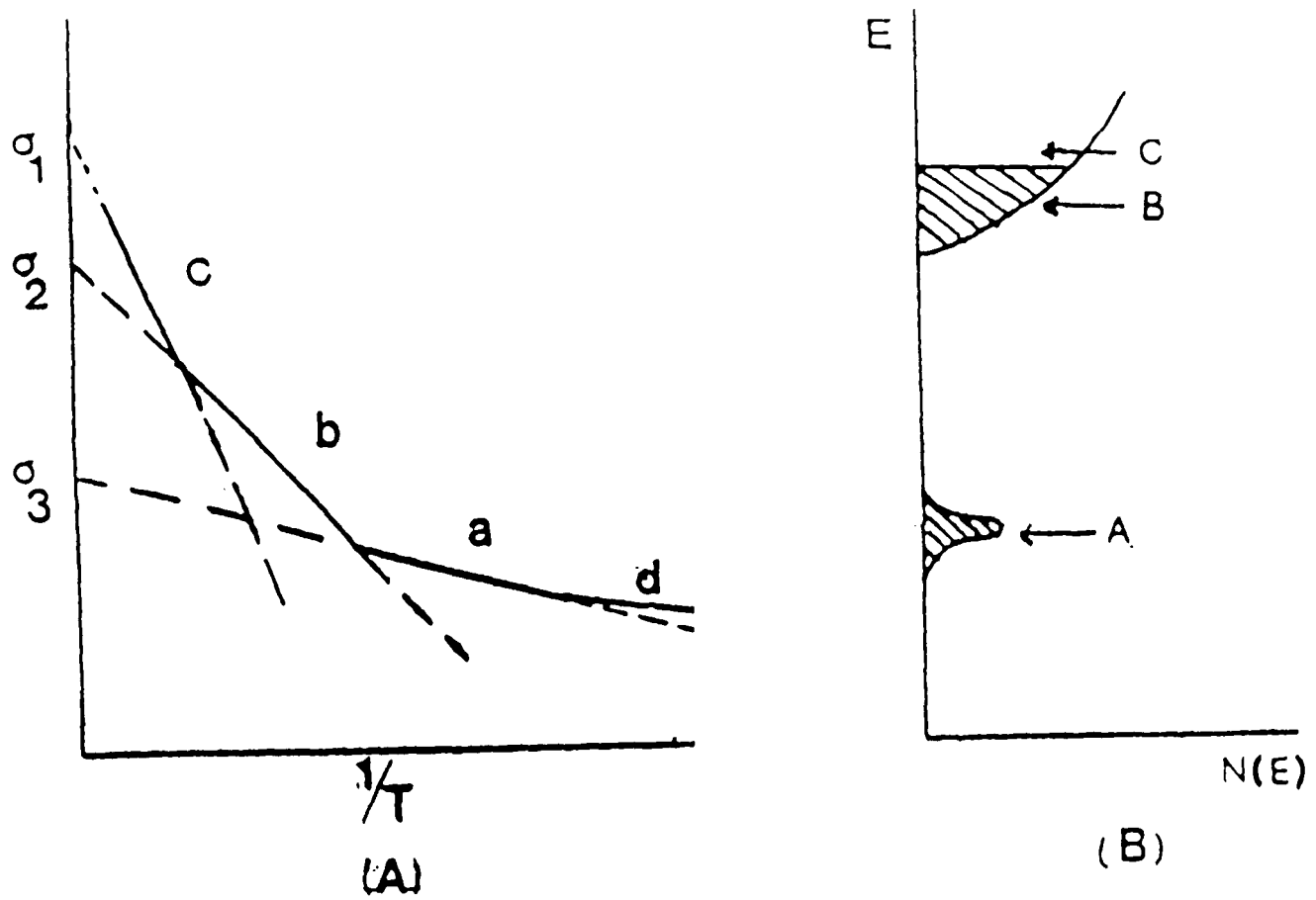


Figure(2.7)-Marshall and Owen model.

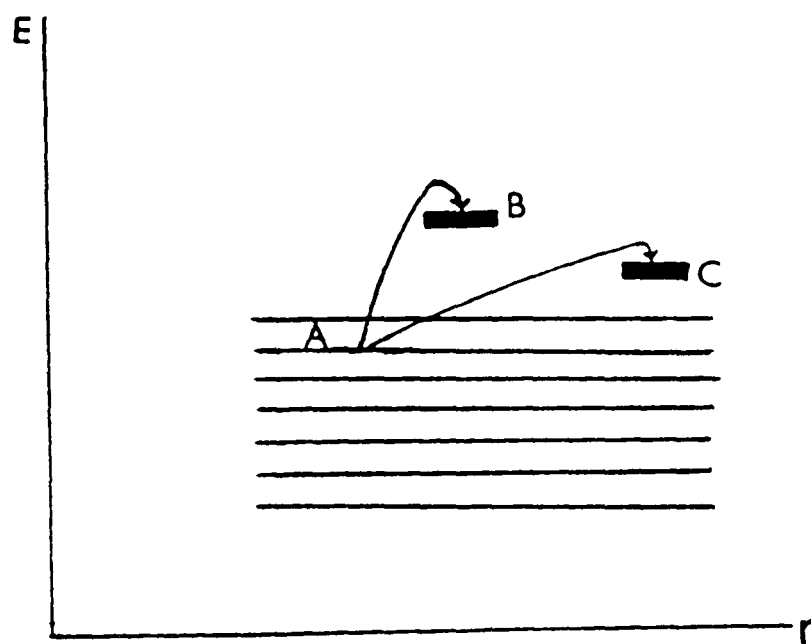


Figure(2.8)-Schematic representation of the density of states in an amorphous semiconductor showing the various conduction mechanism(after Spear).

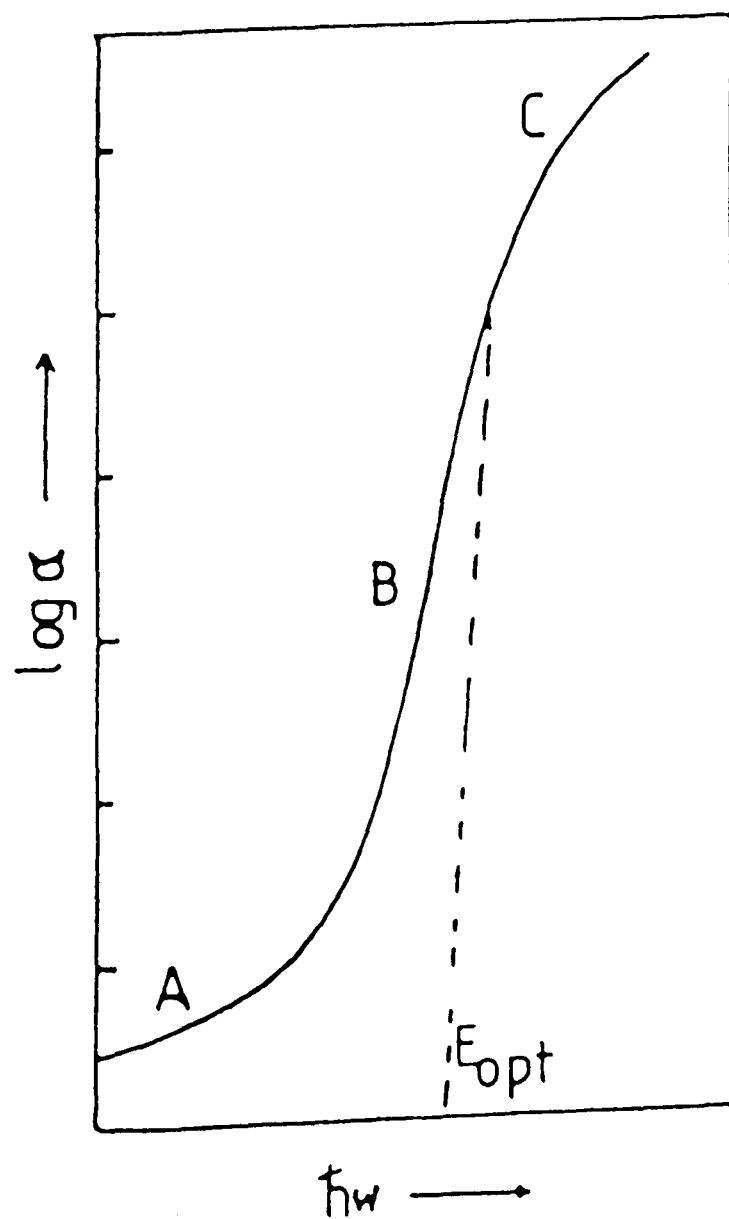




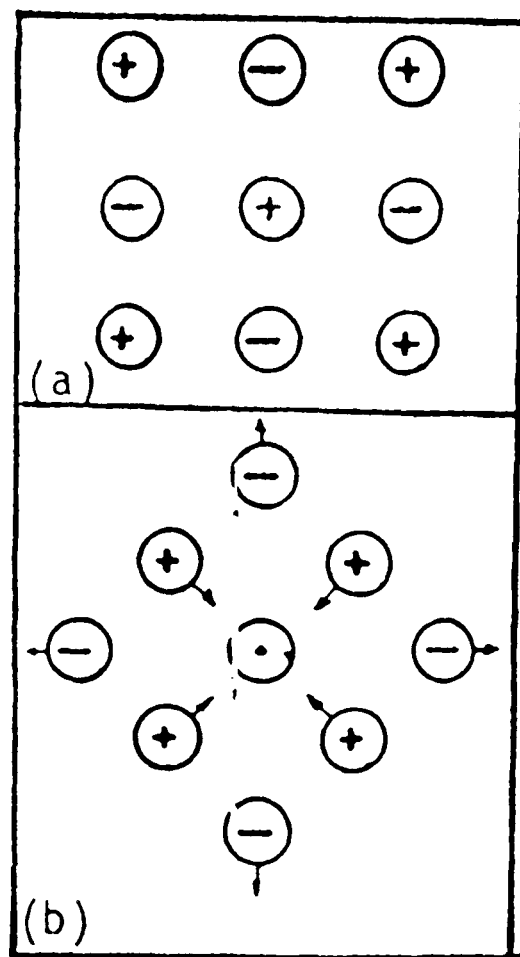
Figure(2.9)-Schematic representation of the temperature dependence of conductivity in amorphous semiconductor.



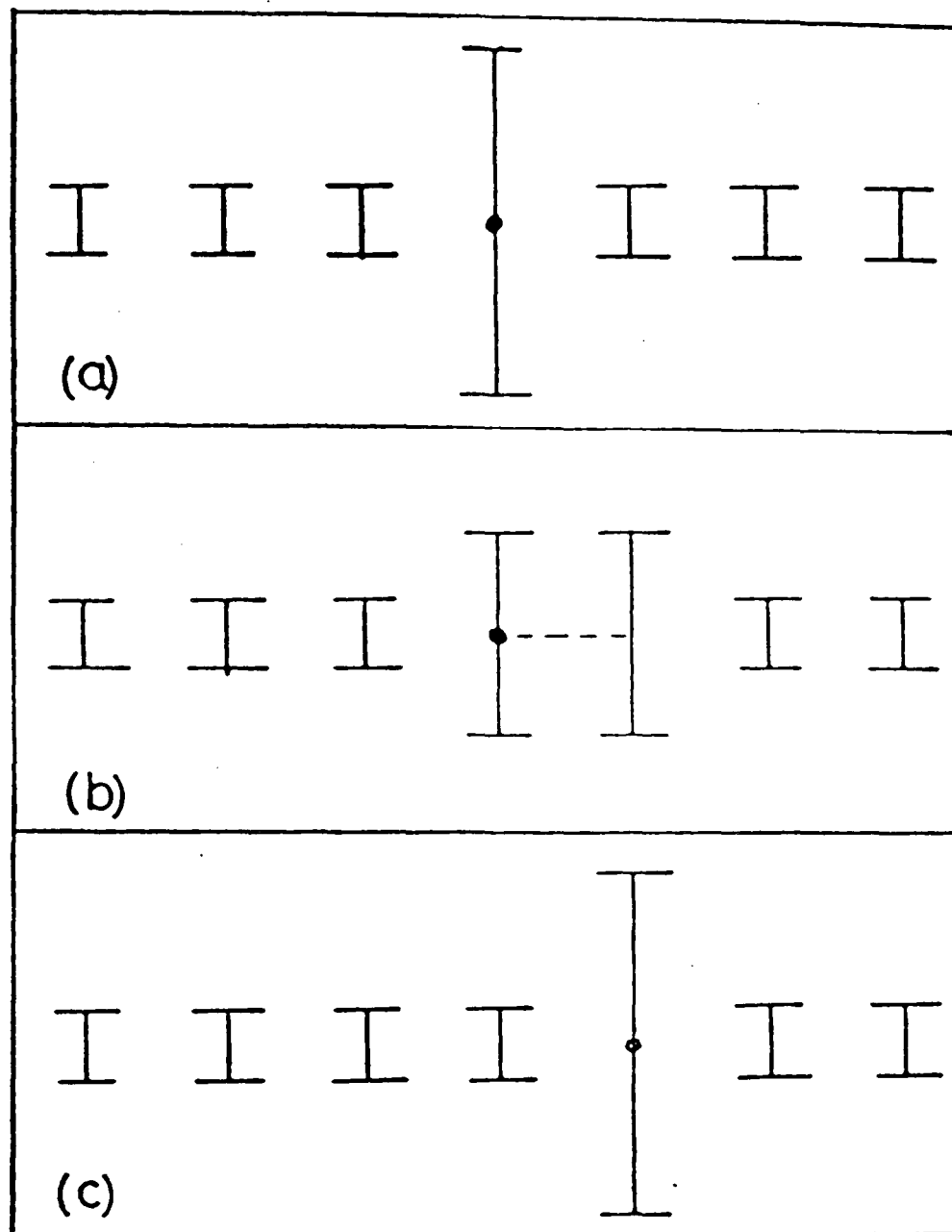
Figure(2.10)-The mechanism of hopping conduction.



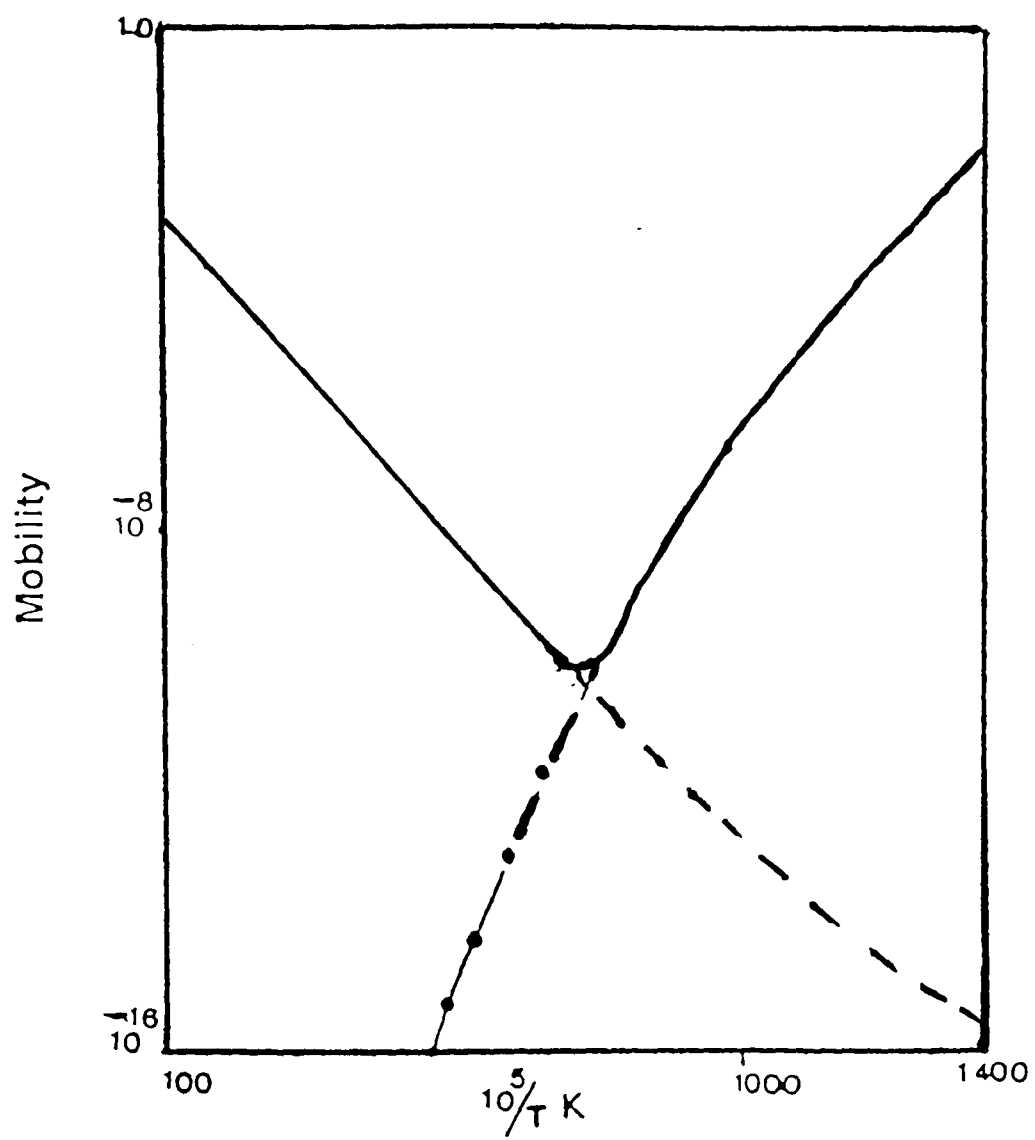
**Figure(2.11)- The general shape of absorption edge of the amorphous semiconductors.**



**Figure(2.12)-(a)Shows asection of an ionic lattice while(b)shows the adjustment of the positions of ions in response to an excess electron present on the central positive ion.**

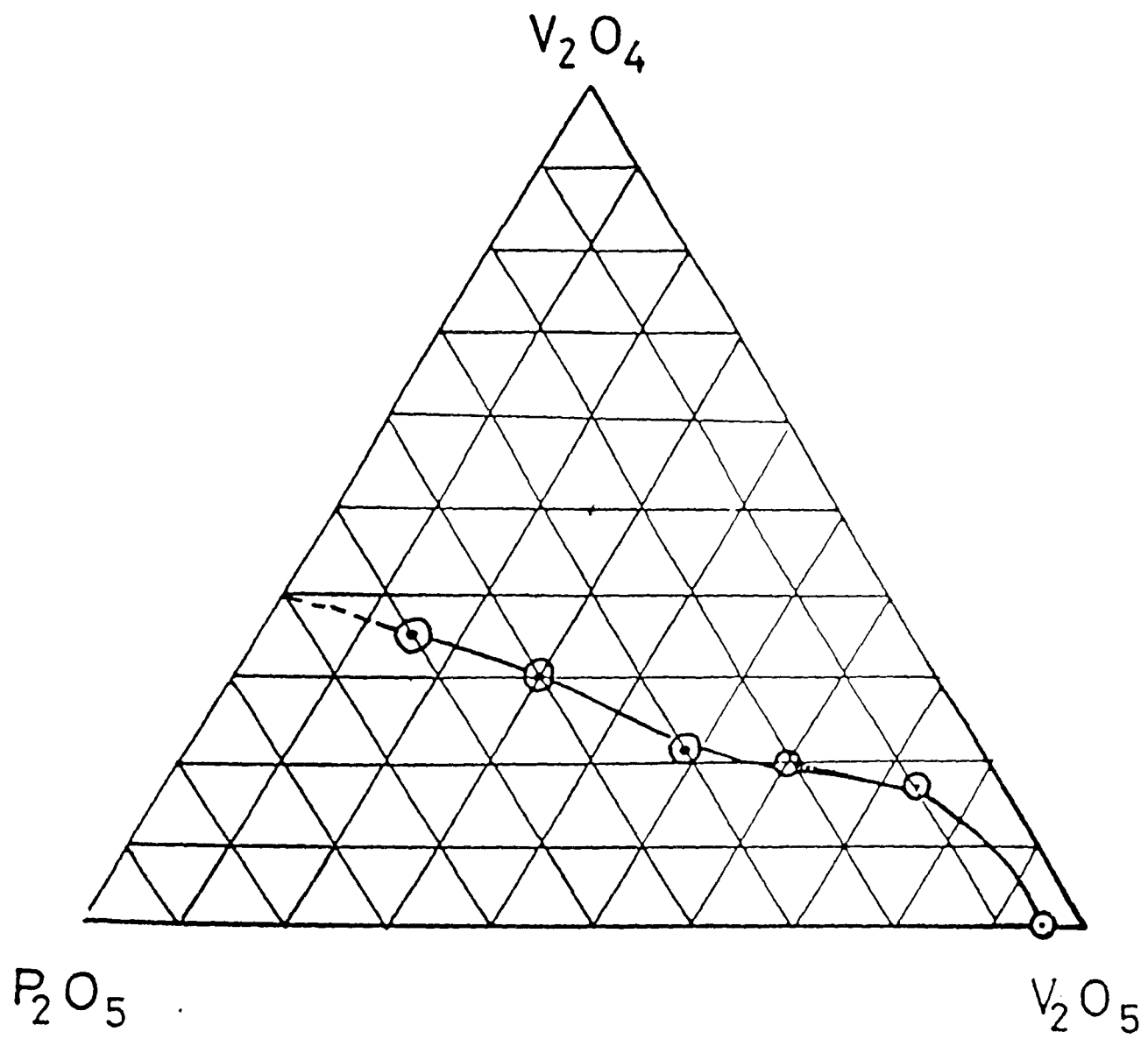


Figure(2.13)-The small-Polaron jump process.

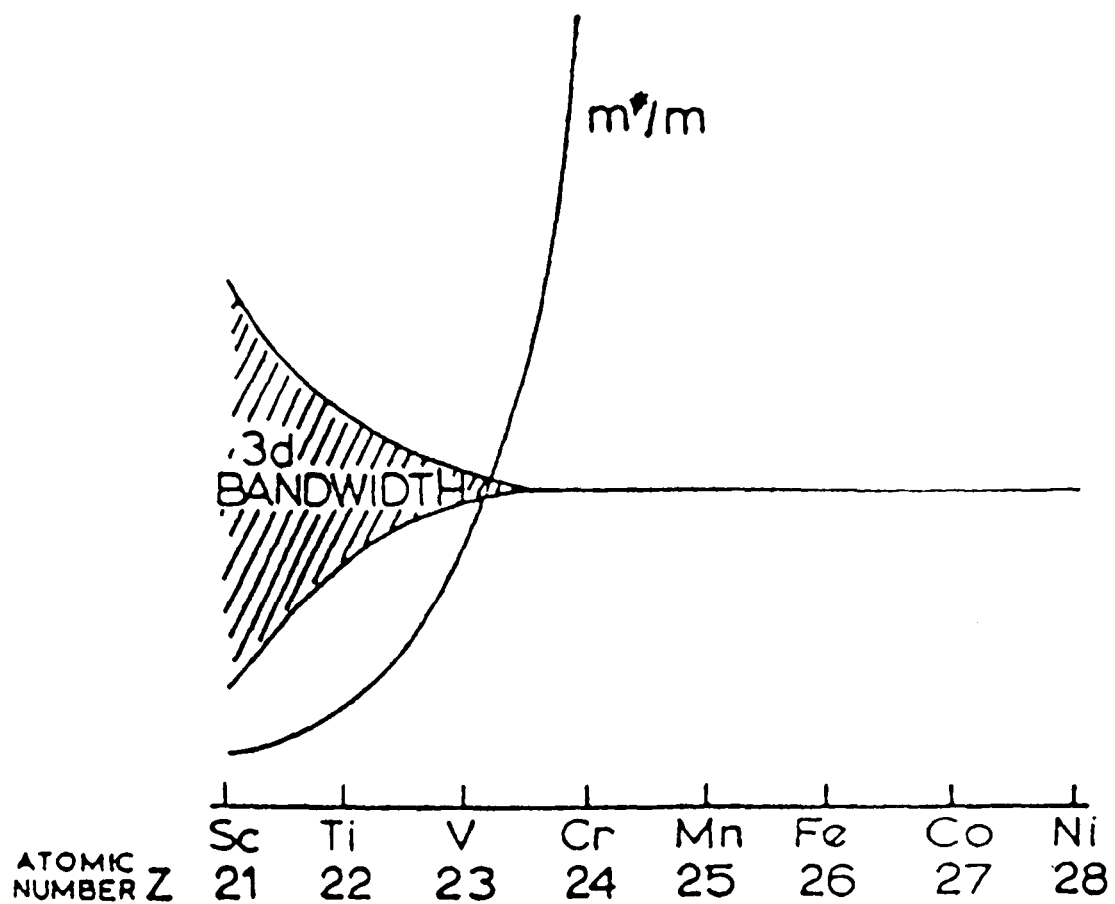


**Figure(2.14)- Behaviour of mobility as a function of temperature for a small polaron (after Holstein).**

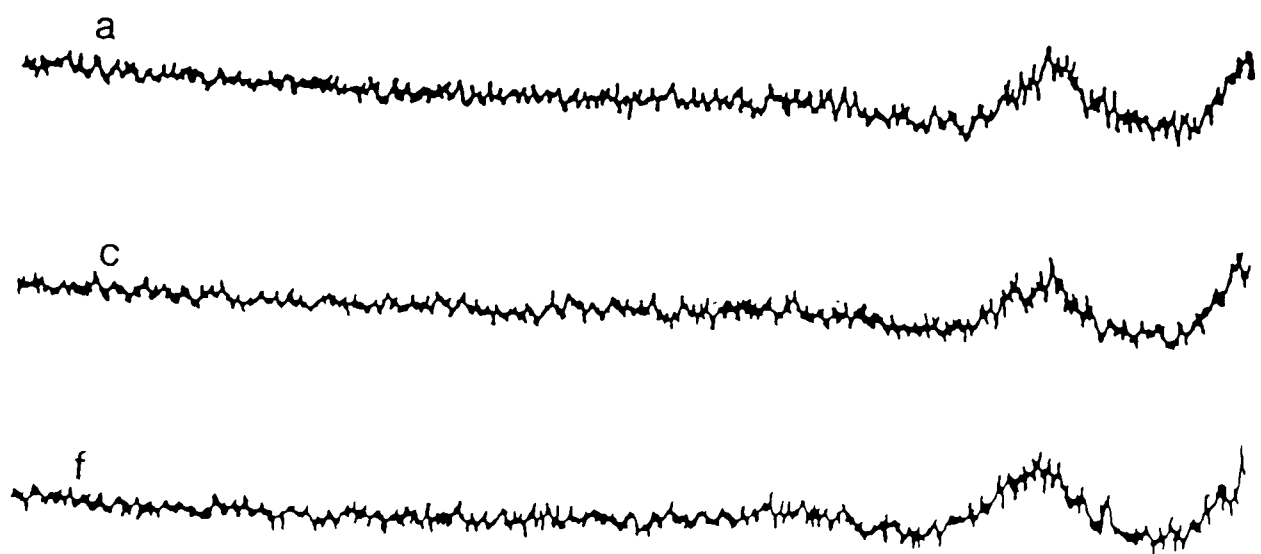
- Band mobility
- Hopping mobility
- Combined mobility



Figure(3.1)-Ternary phase diagram showing glass formation in the  $V_2O_5$ - $V_2O_4$ - $P_2O_5$  system using data given by Linsley.



Figure(3.2)- Schematic representation of the decrease in 3d bandwidth and increase in effective mass( $m^*$ ) with increasing atomic number (after Morin).

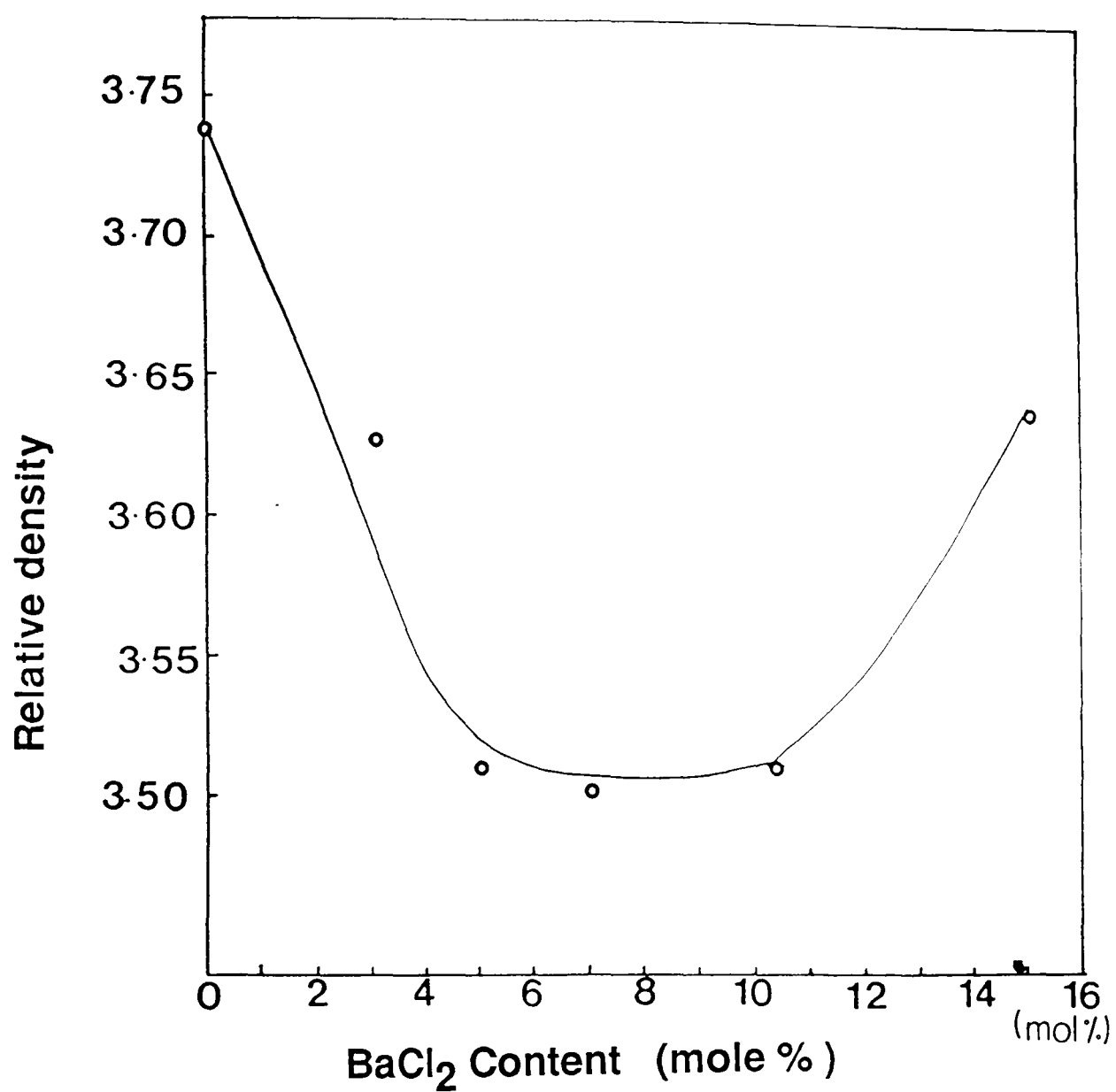


**Figure(4.1)- Typical x-ray powdered diffraction patterns for different glasses.**

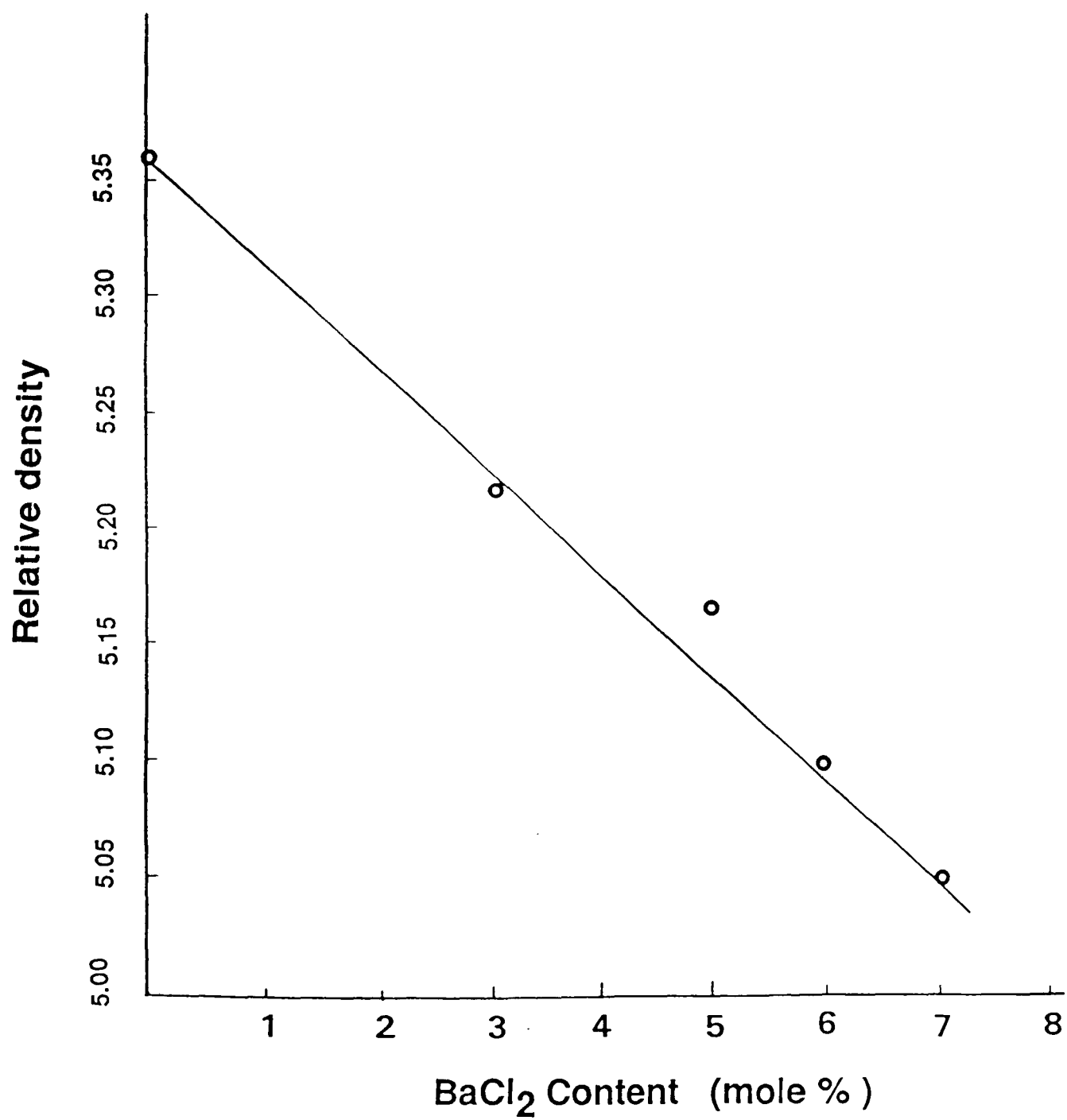
**(a)-65%V<sub>2</sub>O<sub>5</sub>-35%BaO,(c)-65%V<sub>2</sub>O<sub>5</sub>-30%Bao-5%BaCl<sub>2</sub>**

**(f)-65%V<sub>2</sub>O<sub>5</sub>-20%BaO-15%BaCl<sub>2</sub>**

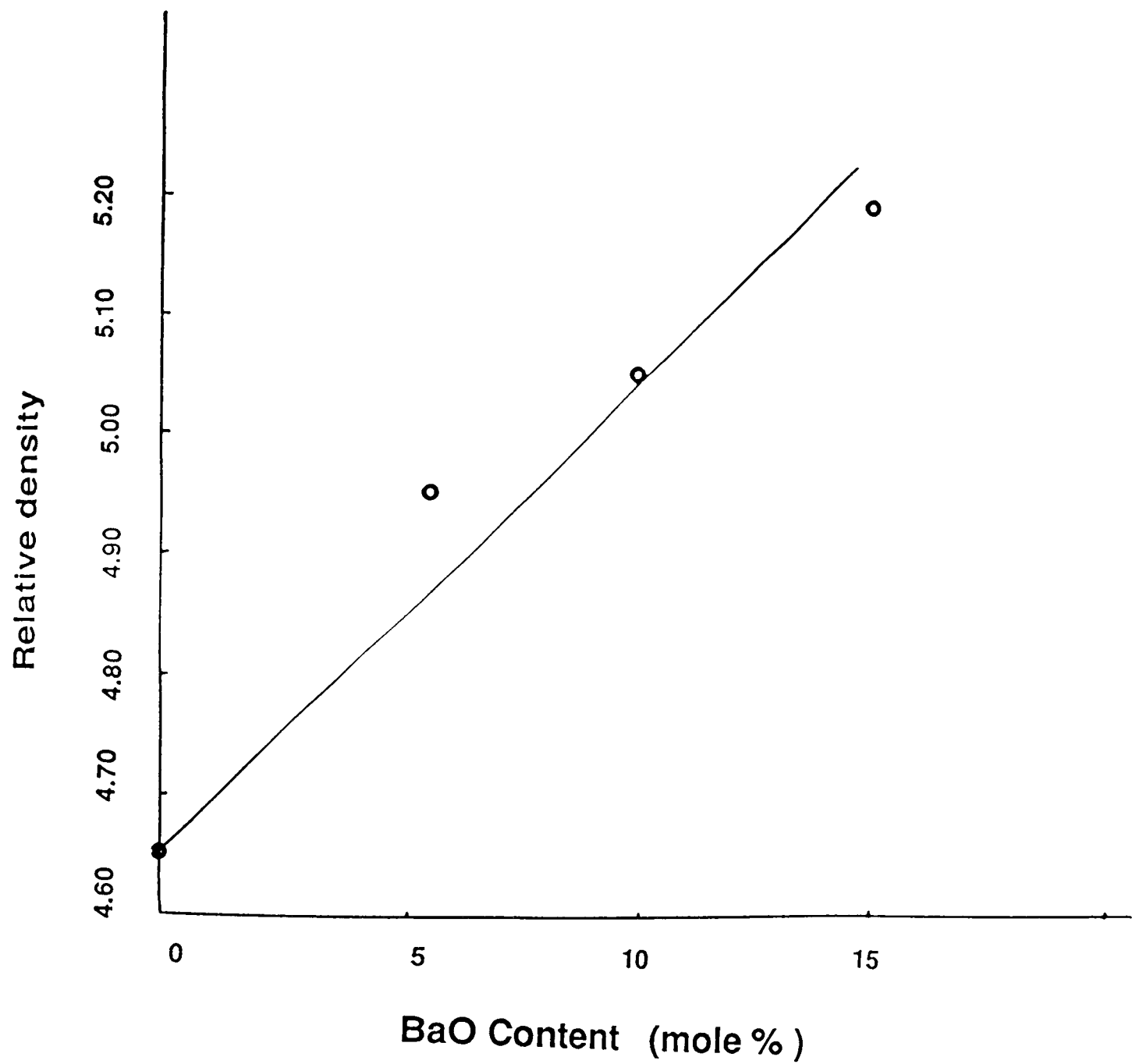




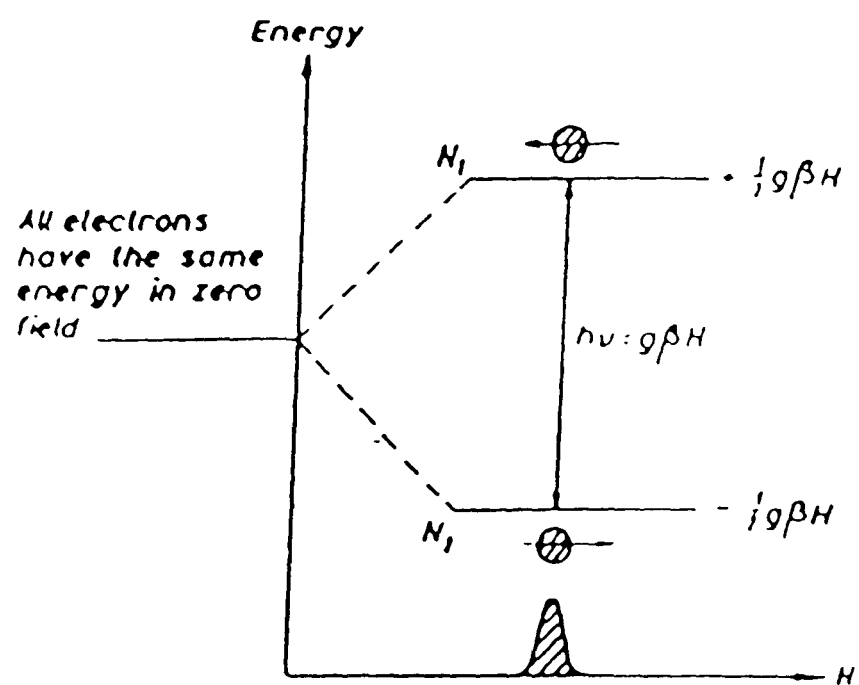
Figure(4.2)-The variation of relative density with BaCl<sub>2</sub> content for V<sub>2</sub>O<sub>5</sub>-BaO-BaCl<sub>2</sub> glass system, annealed at 200°C for 2 hours.



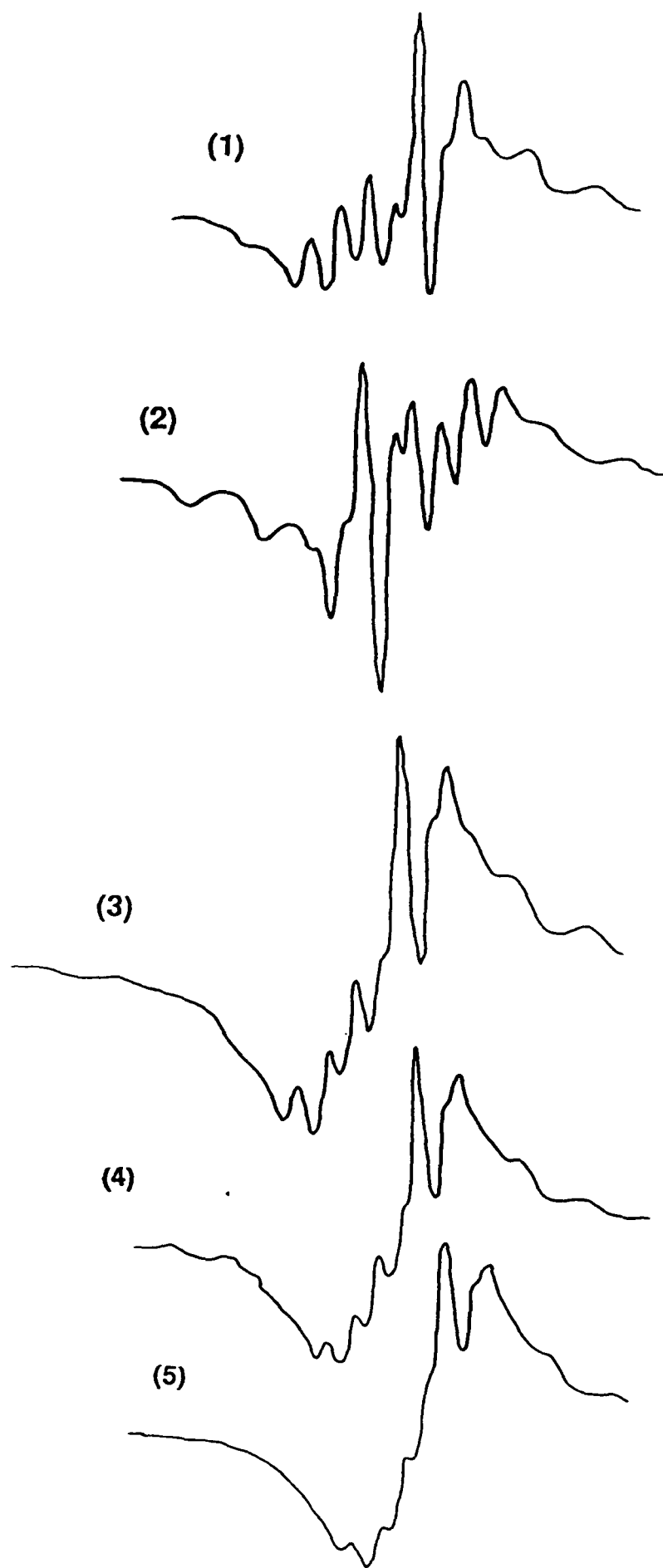
Figure(4.3)-The variation of relative density with BaCl<sub>2</sub> content for TeO<sub>2</sub>-BaO-BaCl<sub>2</sub> glass system,annealed at 200C for 2 hours.



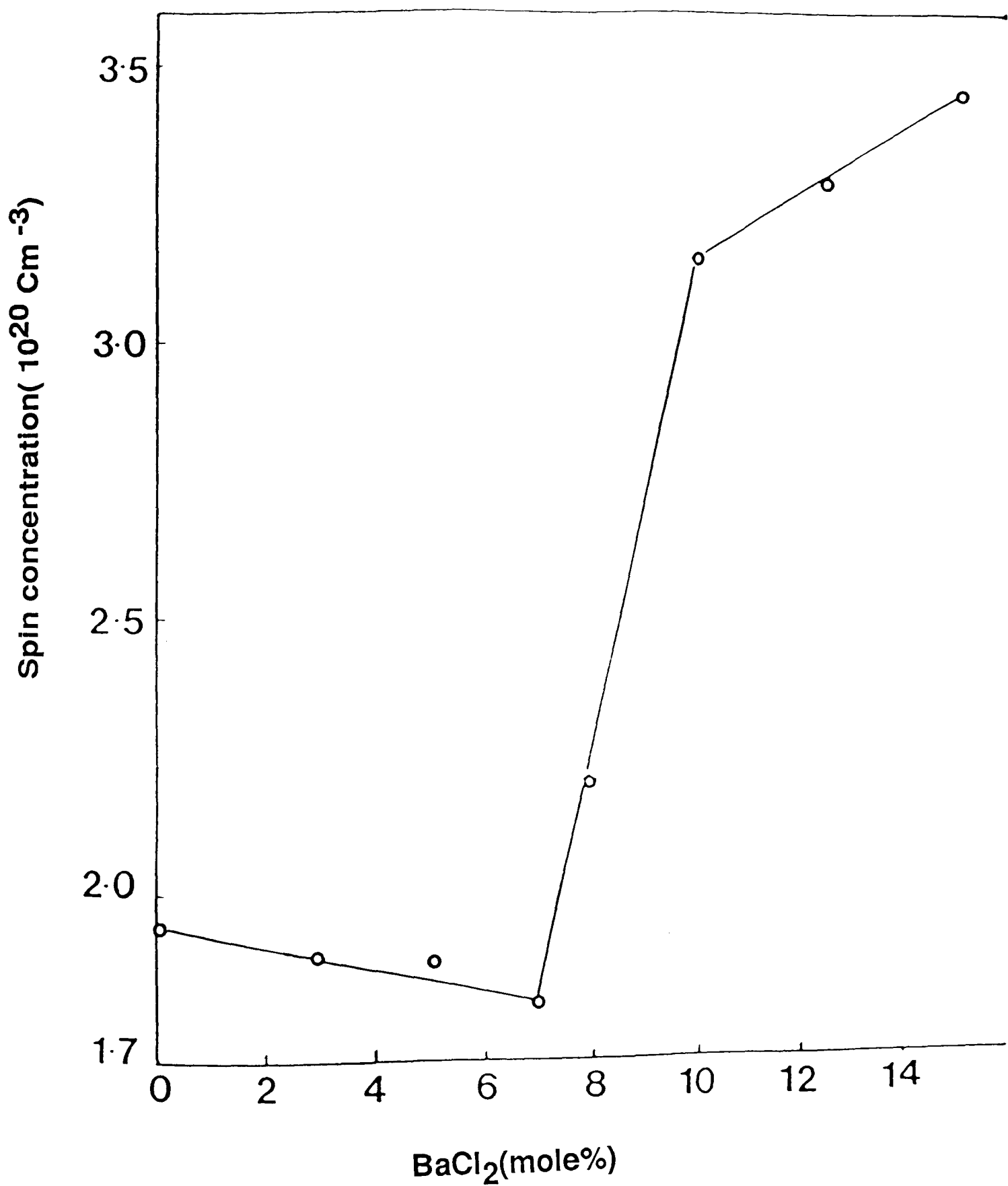
Figure(4.4)-The variation of relative density with Bao content for  $\text{TeO}_2$ -  $\text{V}_2\text{O}_5$ - BaO Glass system.



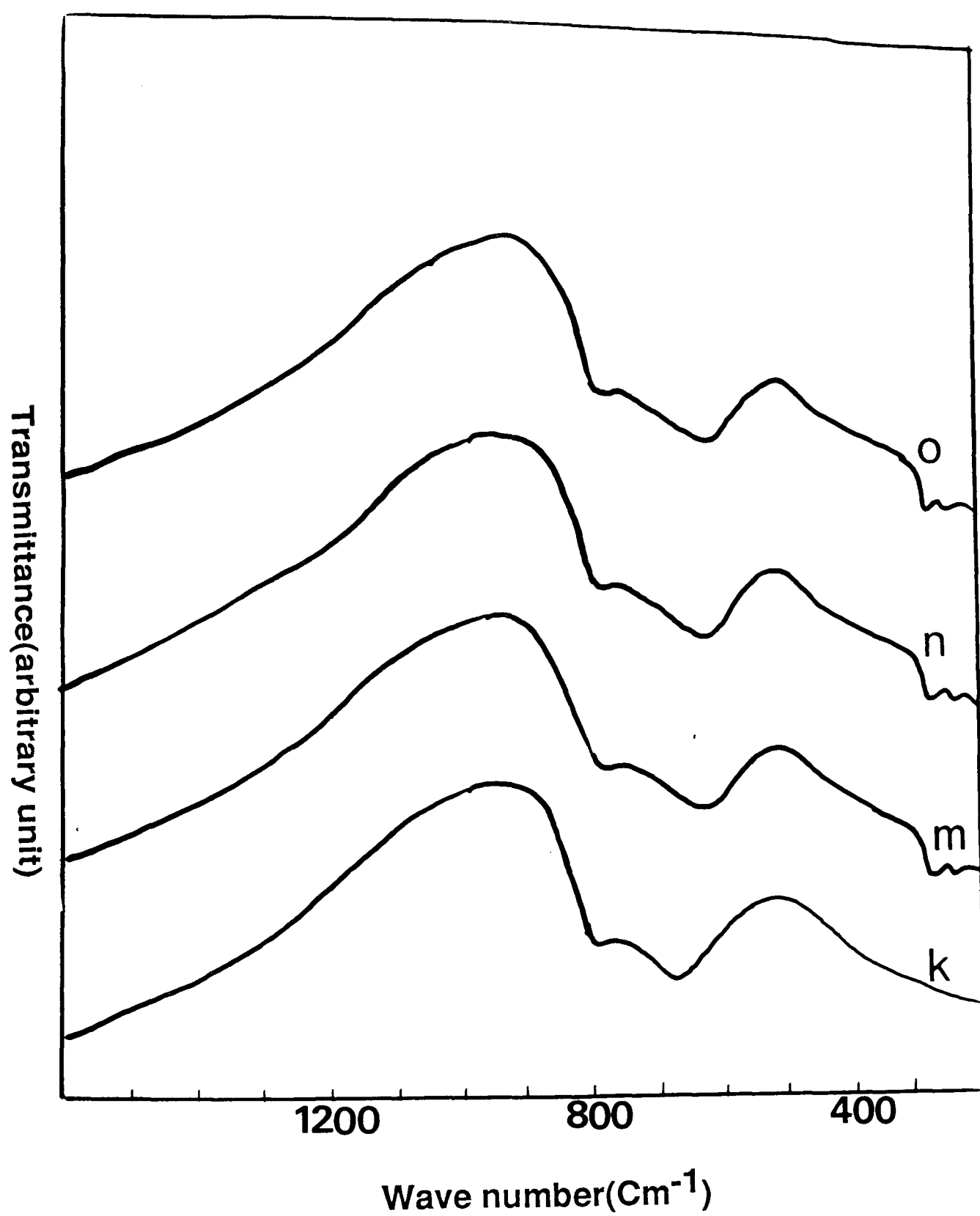
Figure(4.5)-Splitting of the energy levels of a single unpaired electron under the influence of an applied magnetic field H.



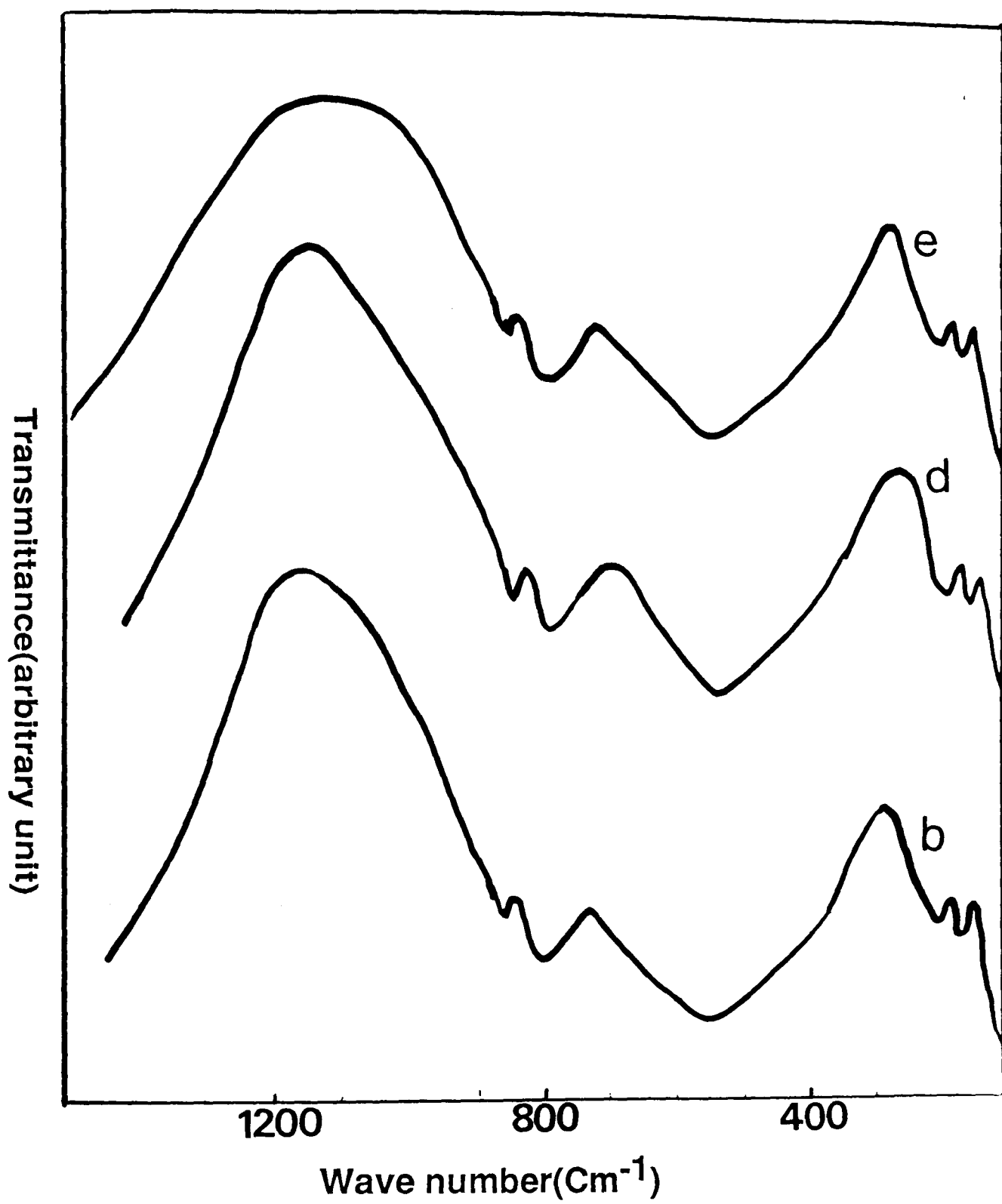
**Figure(4.6)-Electron spin spectra of varying compositions (in mole%)  $V_2O_5$ - BaO-  $BaCl_2$ . (1)0 mole% ,(2)3 mole%,(3)7mole%, (4)10mole%,(5)15mole%.**



Figure(4.7)-The dependence of the total spin concentration on BaCl<sub>2</sub> content for glasses of the V<sub>2</sub>O<sub>5</sub>- BaO- BaCl<sub>2</sub> system.

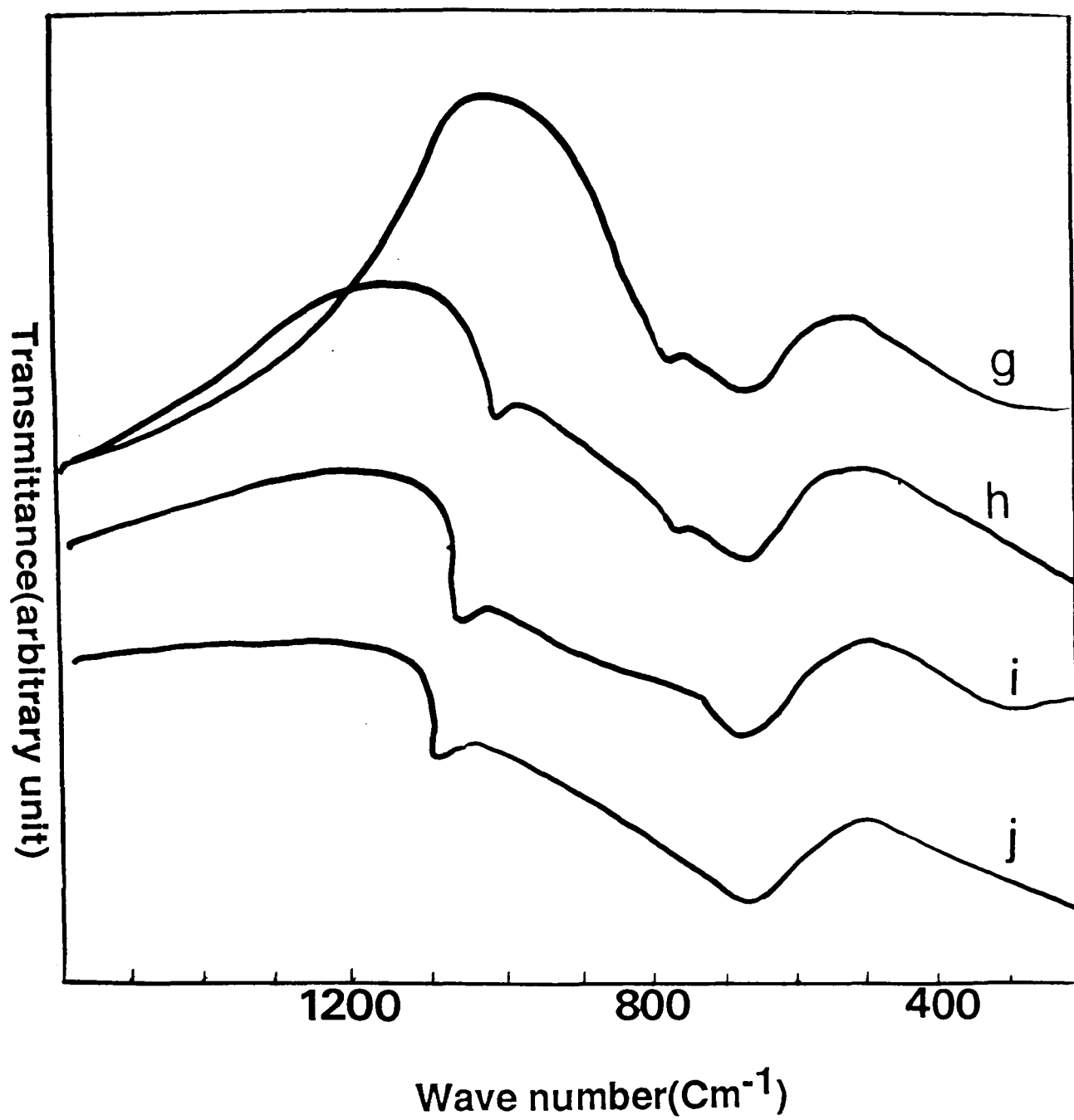


Figure(5.1)-Infra-red absorption spectra for a series of  $\text{TeO}_2\text{-BaO-BaCl}_2$  glasses.

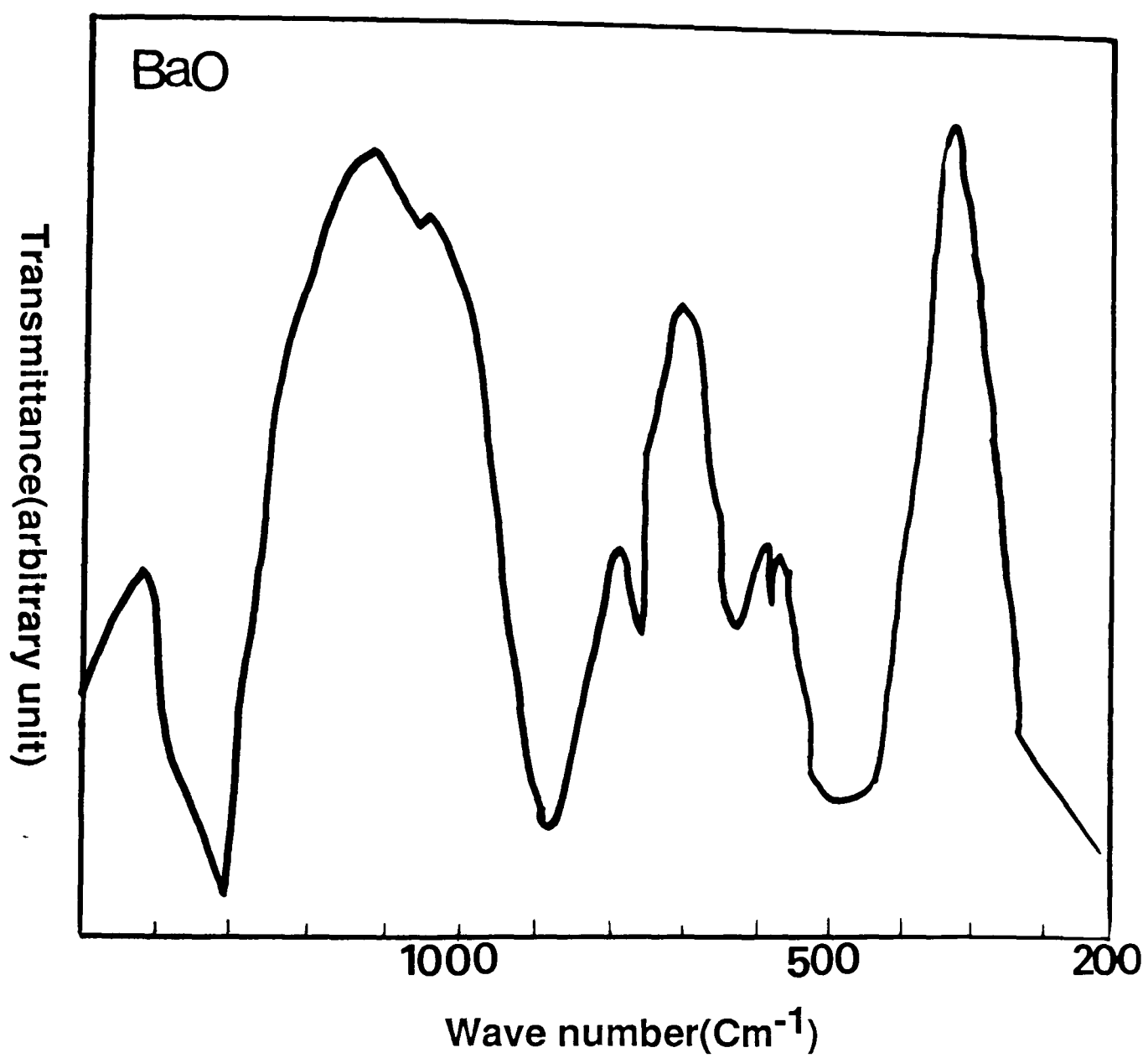


Figure(5.2)-Infrared absorption spectra for a series of  $\text{V}_2\text{O}_5$ -  $\text{BaO}$ -  $\text{BaCl}_2$  system.

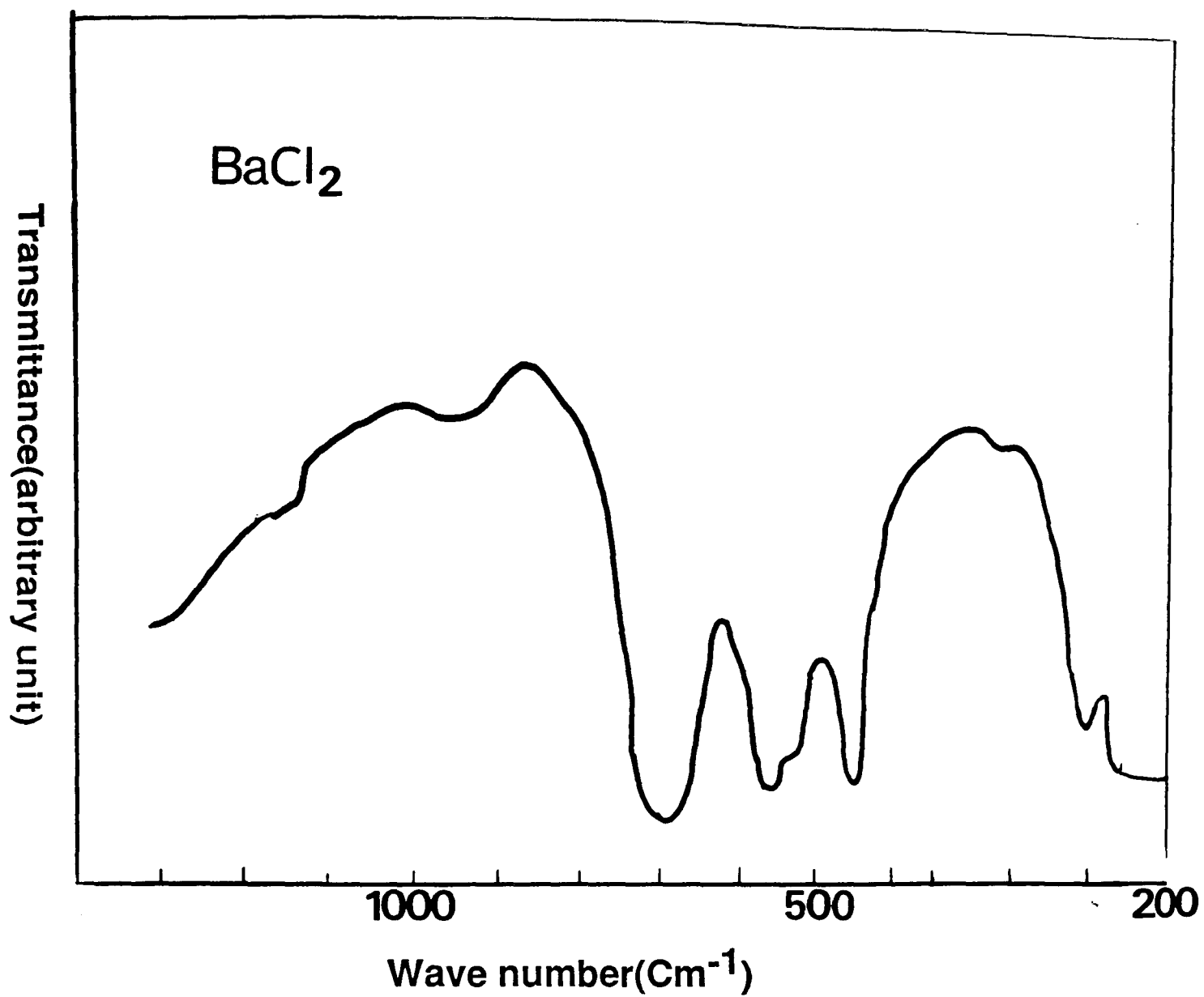




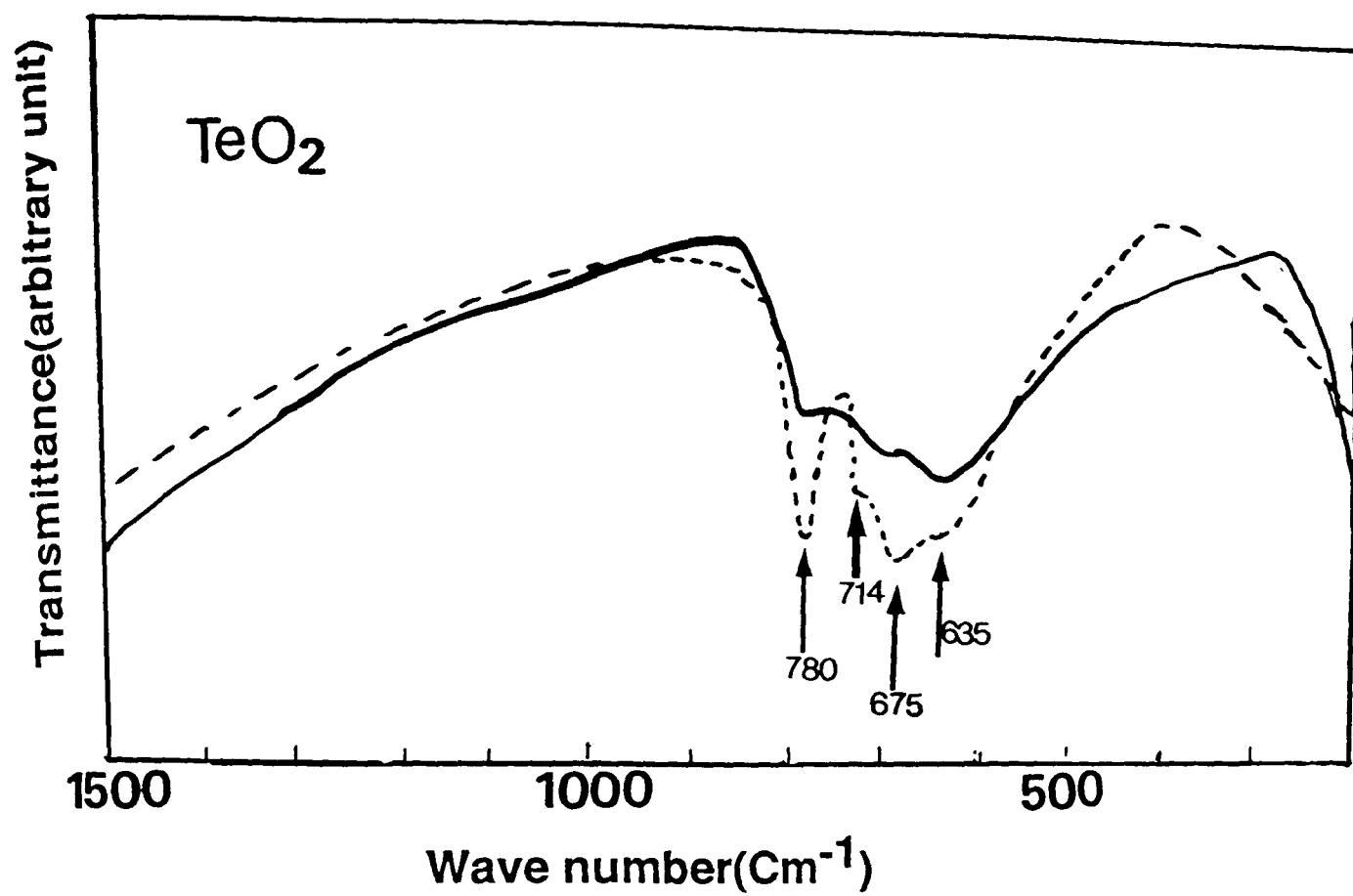
Figure(5.3)-Infra-red absorption spectra for a series of  $\text{TeO}_2\text{-BaO-V}_2\text{O}_5$  glasses.



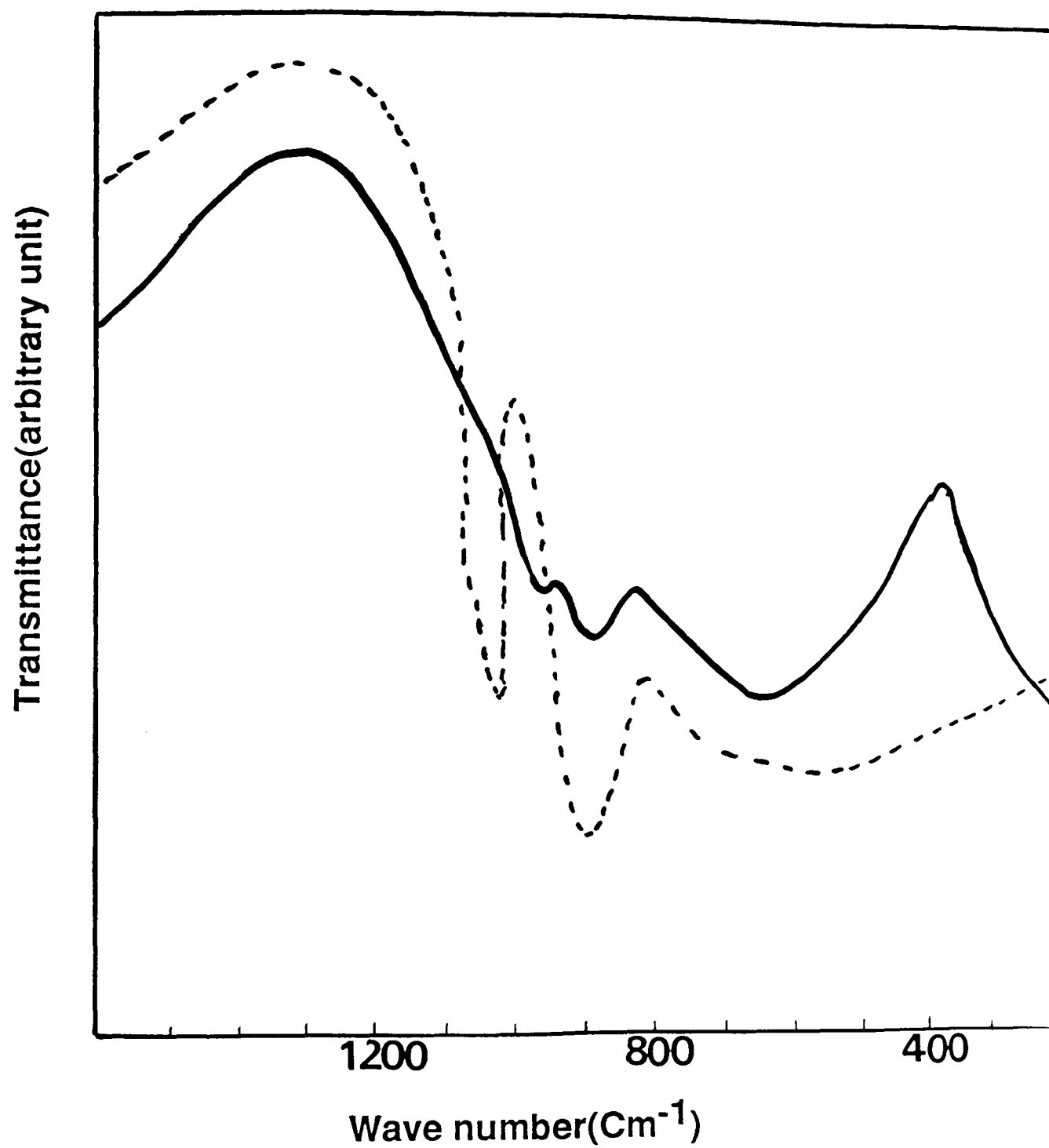
Figure(5.4)-Infra-red spectra of pure BaO in crystalline state.



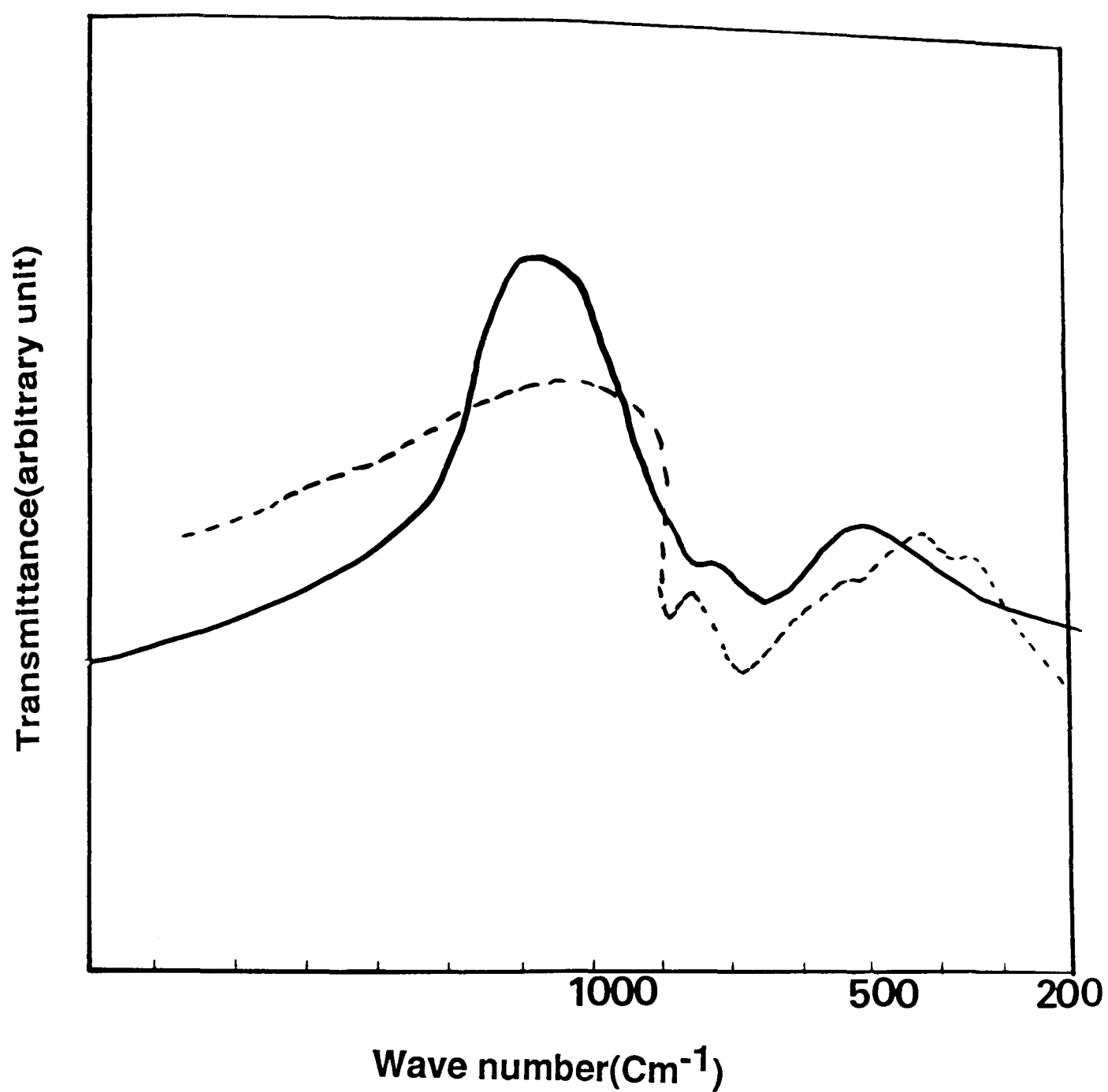
Figure(5.5)-Infra-red spectra of pure  $\text{BaCl}_2$  in crystalline state.



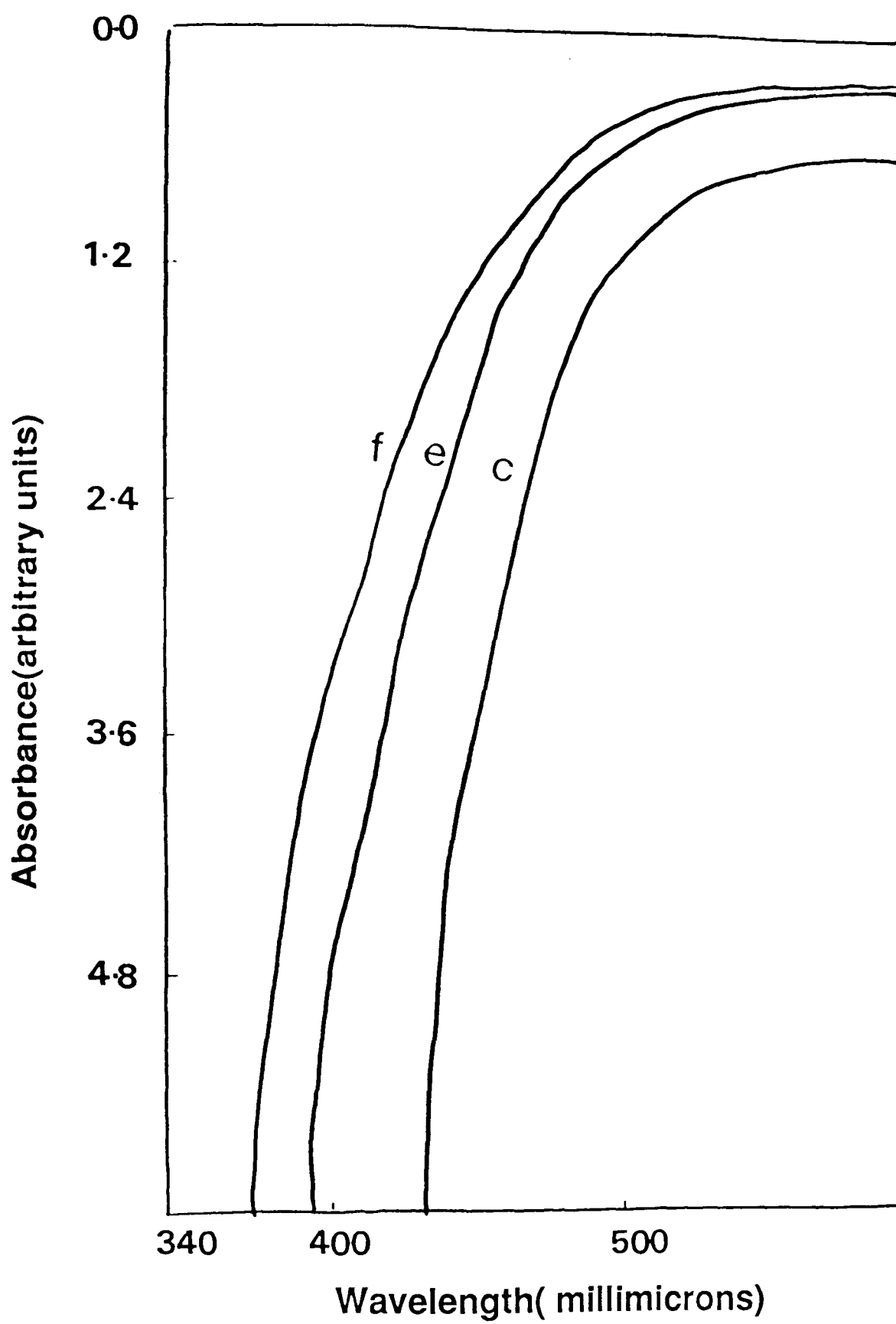
Figure(5.6)-The Infra-red spectra of tellurite phases in both crystalline(---) and glassy(—) states.



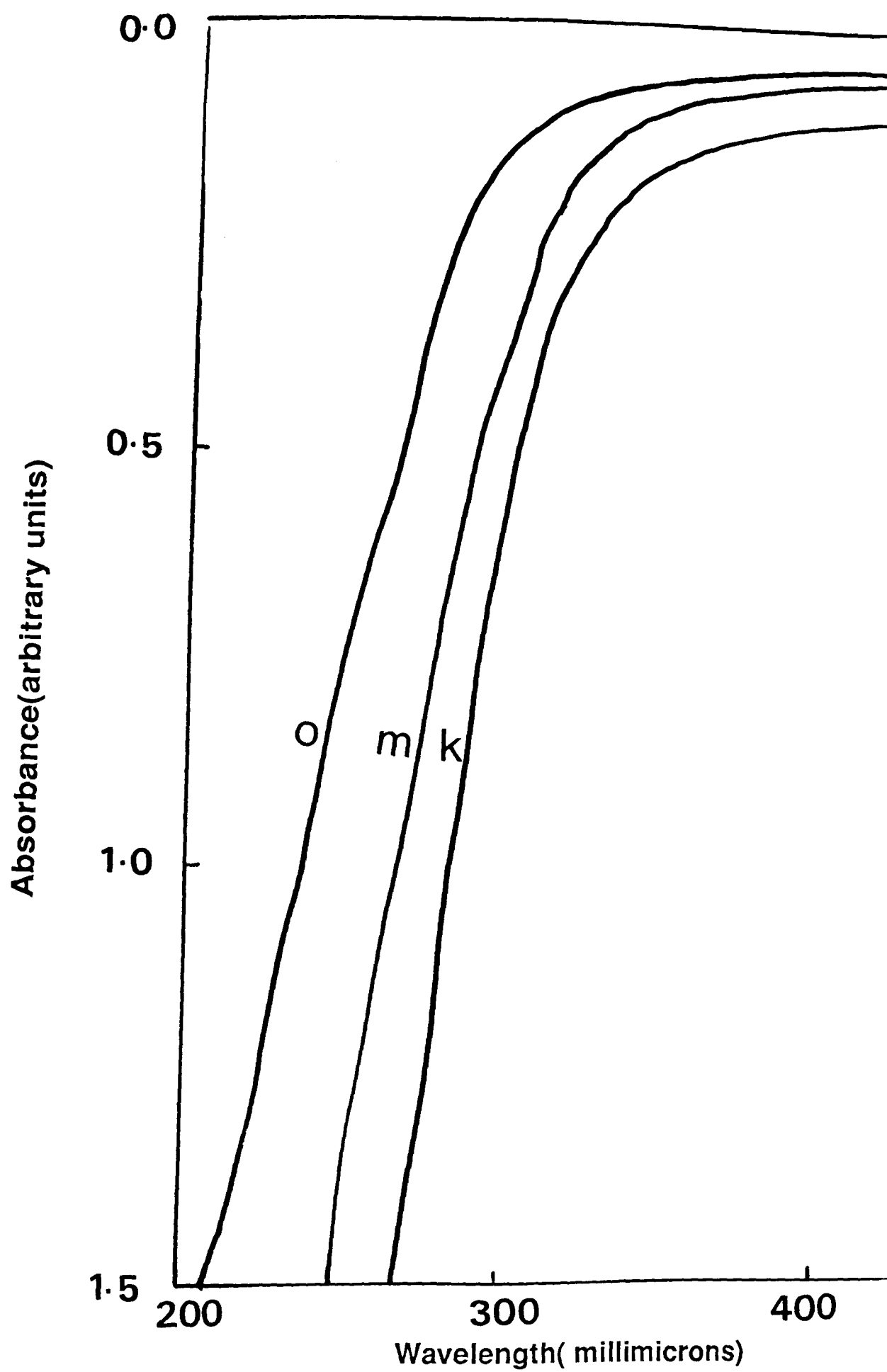
Figure(5.7)-The infra- red spectra of the binary system of  $V_2O_5$ -BaO in both crystalline (---)and glassy(—)states.



Figure(5.8)- The infra-red spectra of  $\text{TeO}_2\text{-BaO}$  in both crystalline(---) and glassy (—) states.

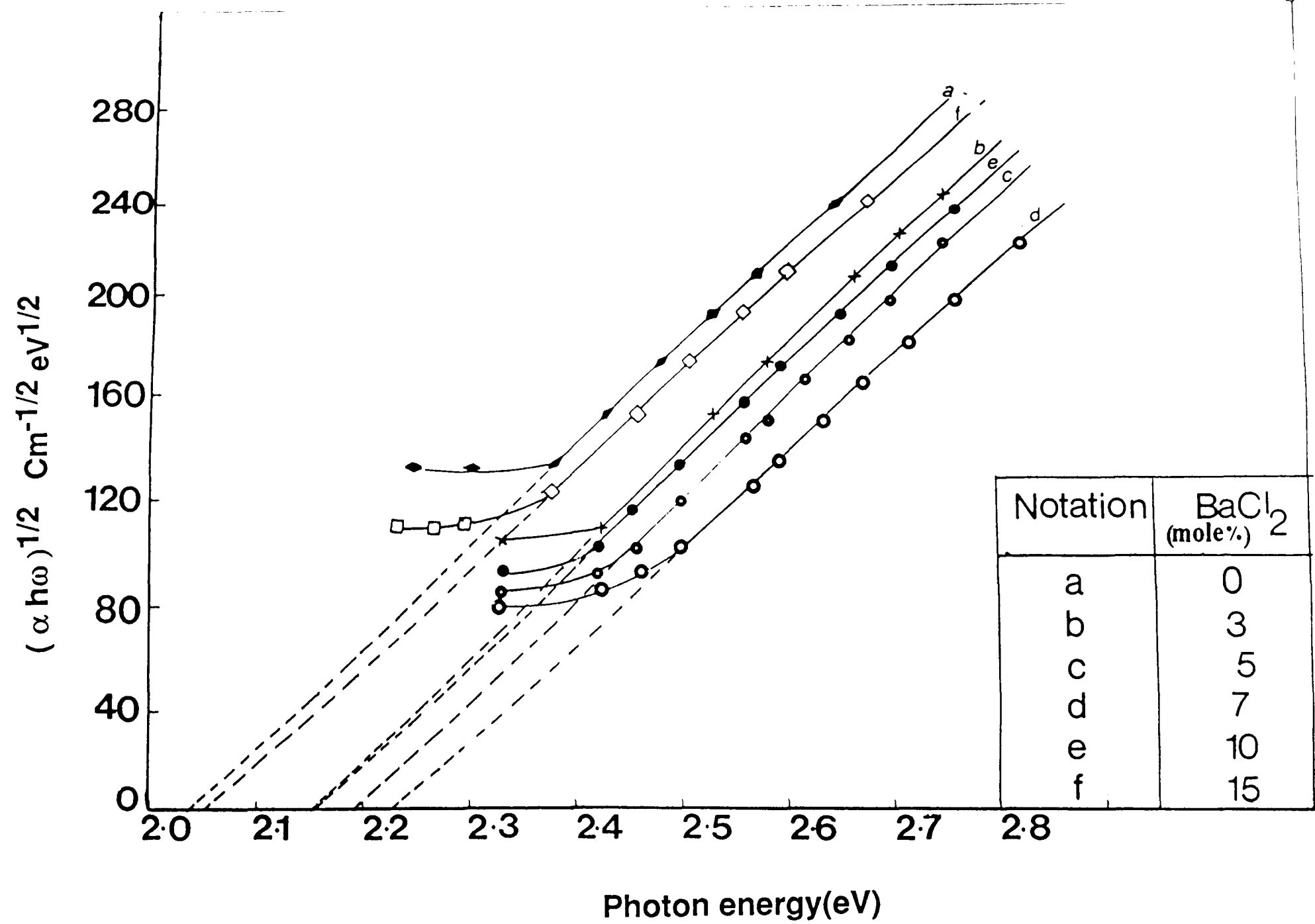


Figure(5.9)-Optical absorption as a function of wavelength in UV region for a series of  $V_2O_5$ - BaO-  $BaCl_2$  glasses.

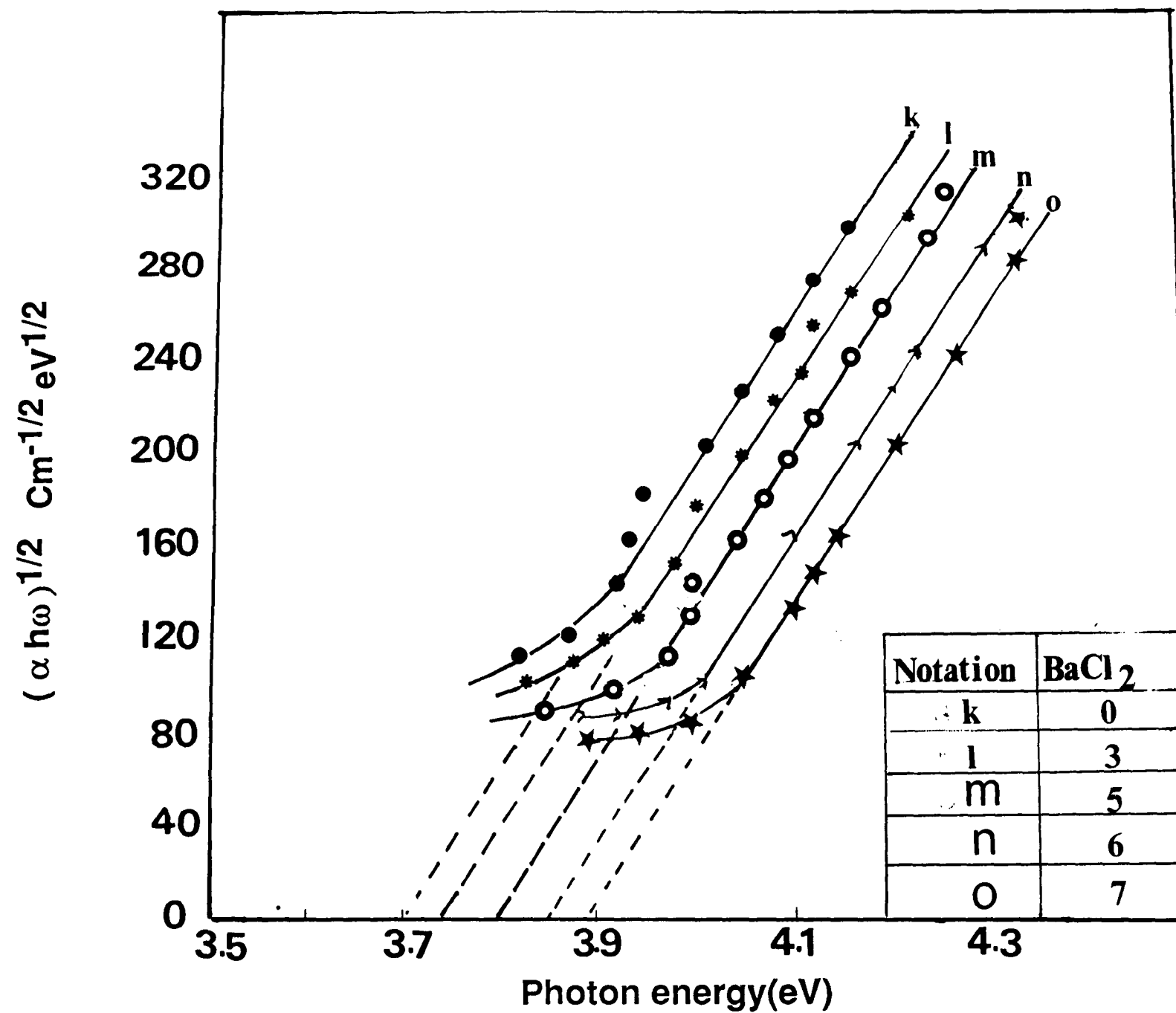


Figure(5.10)-Optical absorption as a function of wavelength in UV region for a series of  $\text{TeO}_2\text{-BaO-BaCl}_2$  glasses.

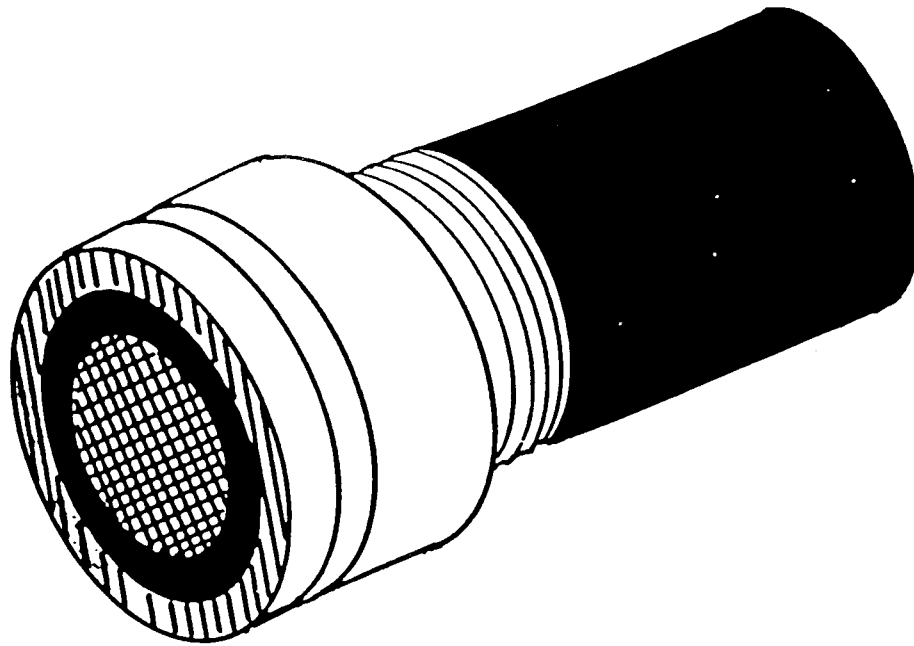




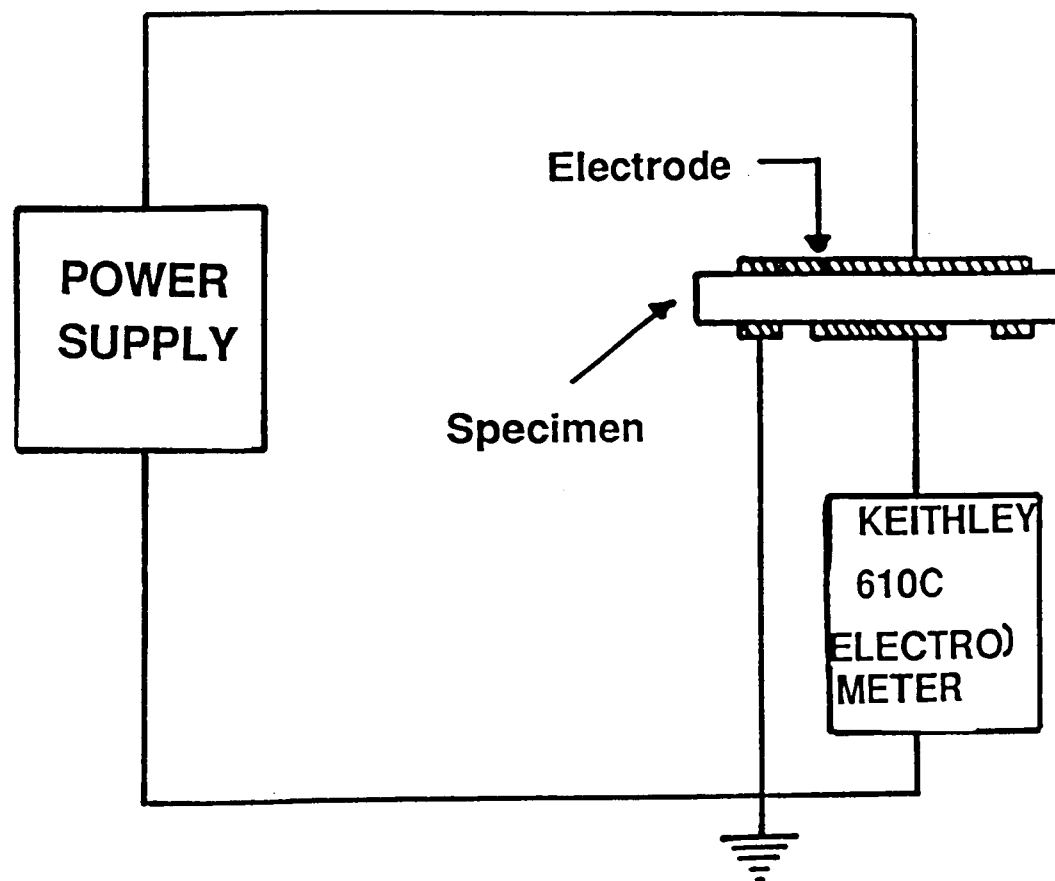
Figure(5.11)- $(\alpha h\omega)^{1/2}$  as function of energy for glass system of  $V_2O_5$ - BaO- BaCl<sub>2</sub>.



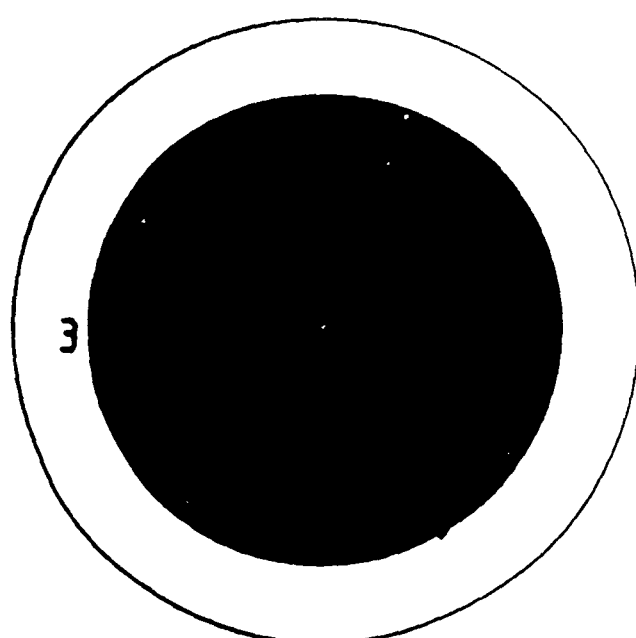
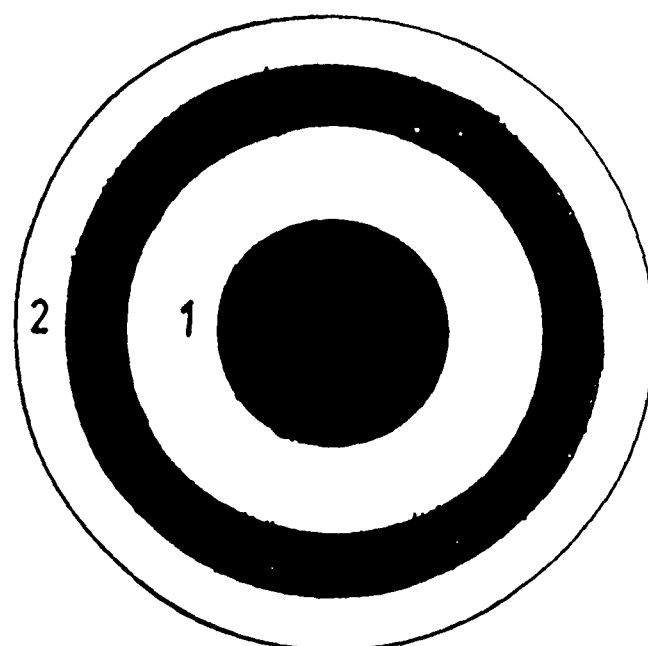
Figure(5.12)- $(\alpha h\omega)^{1/2}$  as function of energy for glass system of  $\text{TeO}_2\text{-BaO-BaCl}_2$



Figure(6.1)-Specimen holder for grinding .

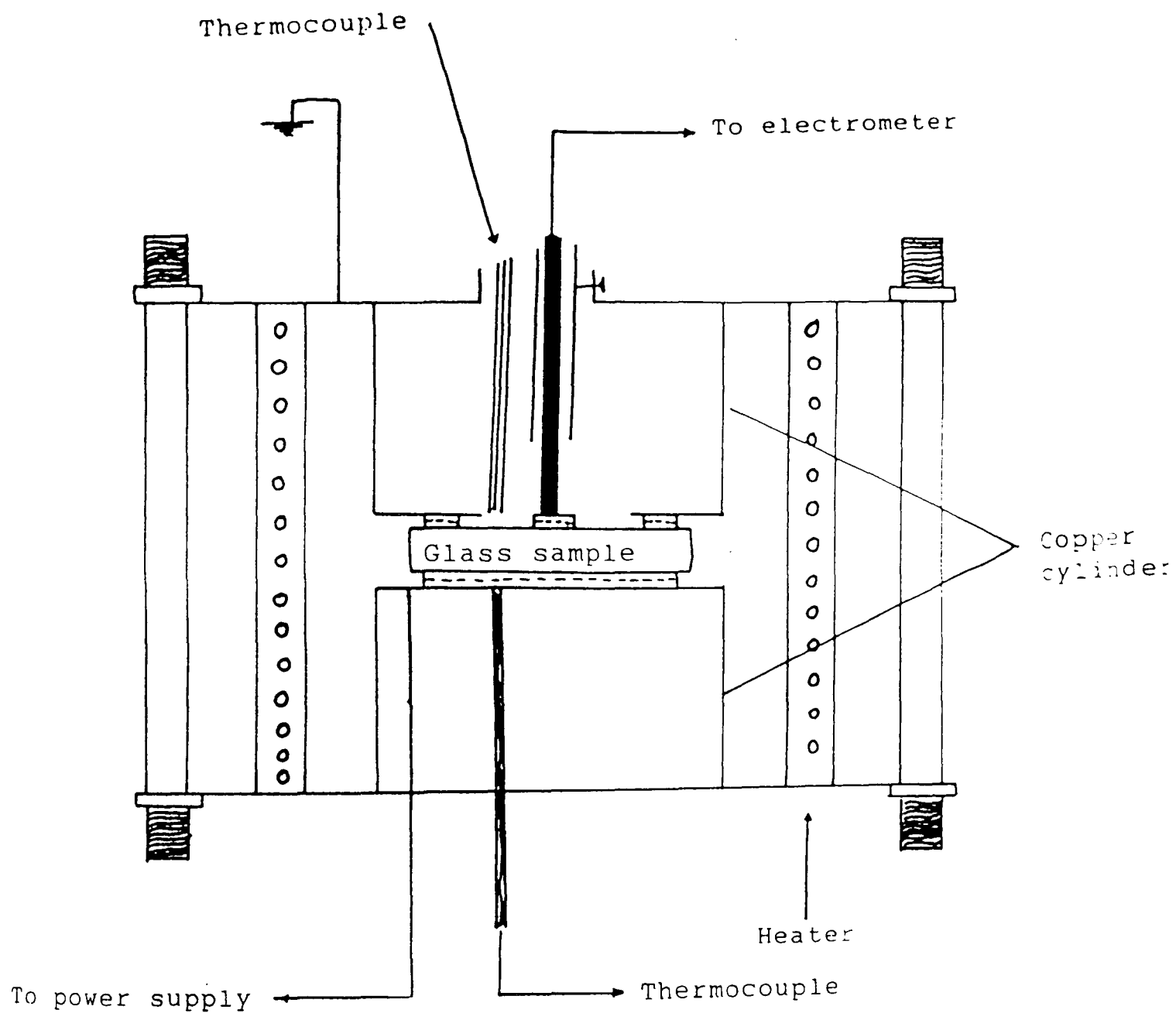


Figure(6.2)-Electrical circuit for conductivity measurements.

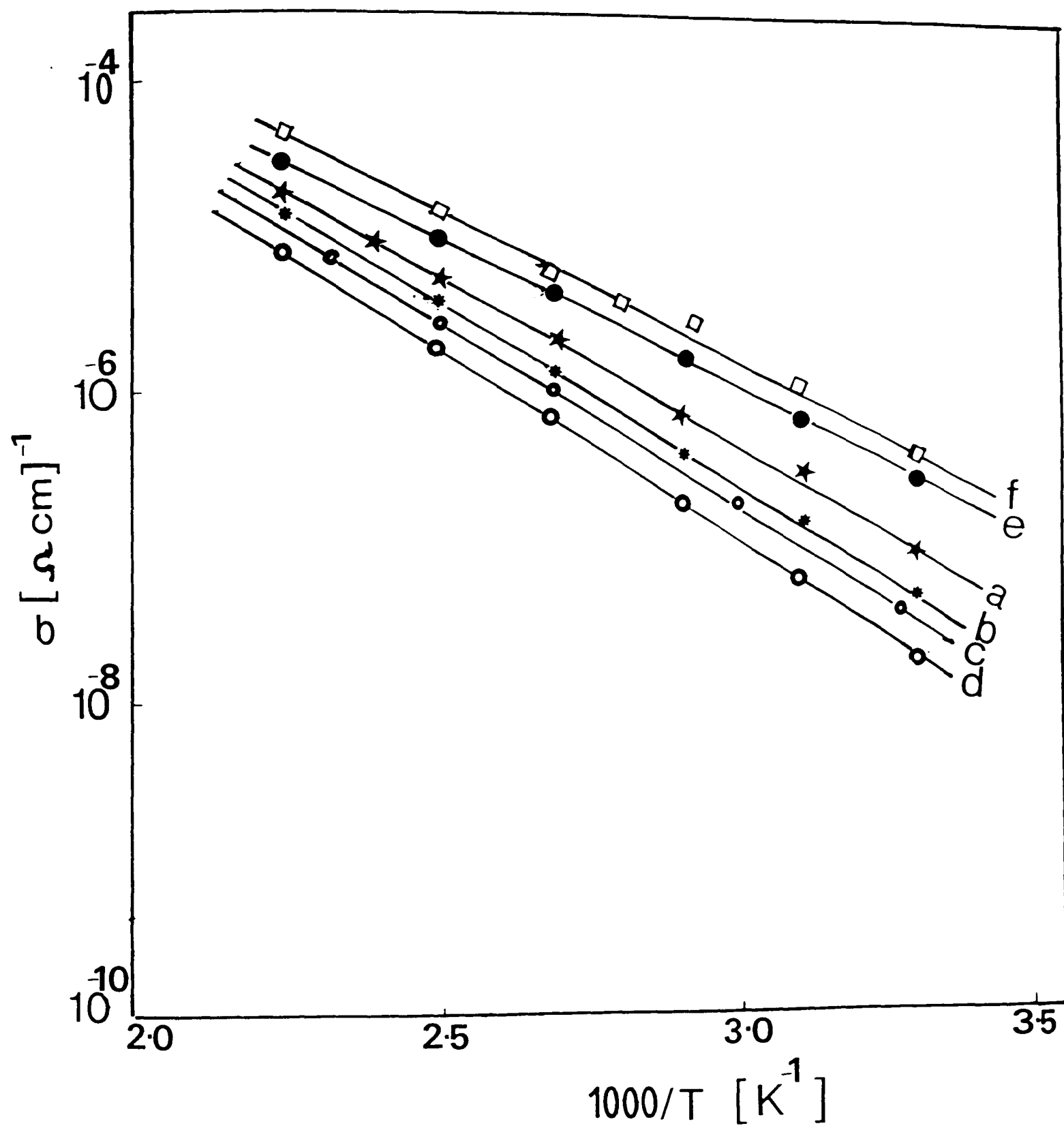


**Figure(6.3)-Schematic representation of electrode configuration on the glass disc.**

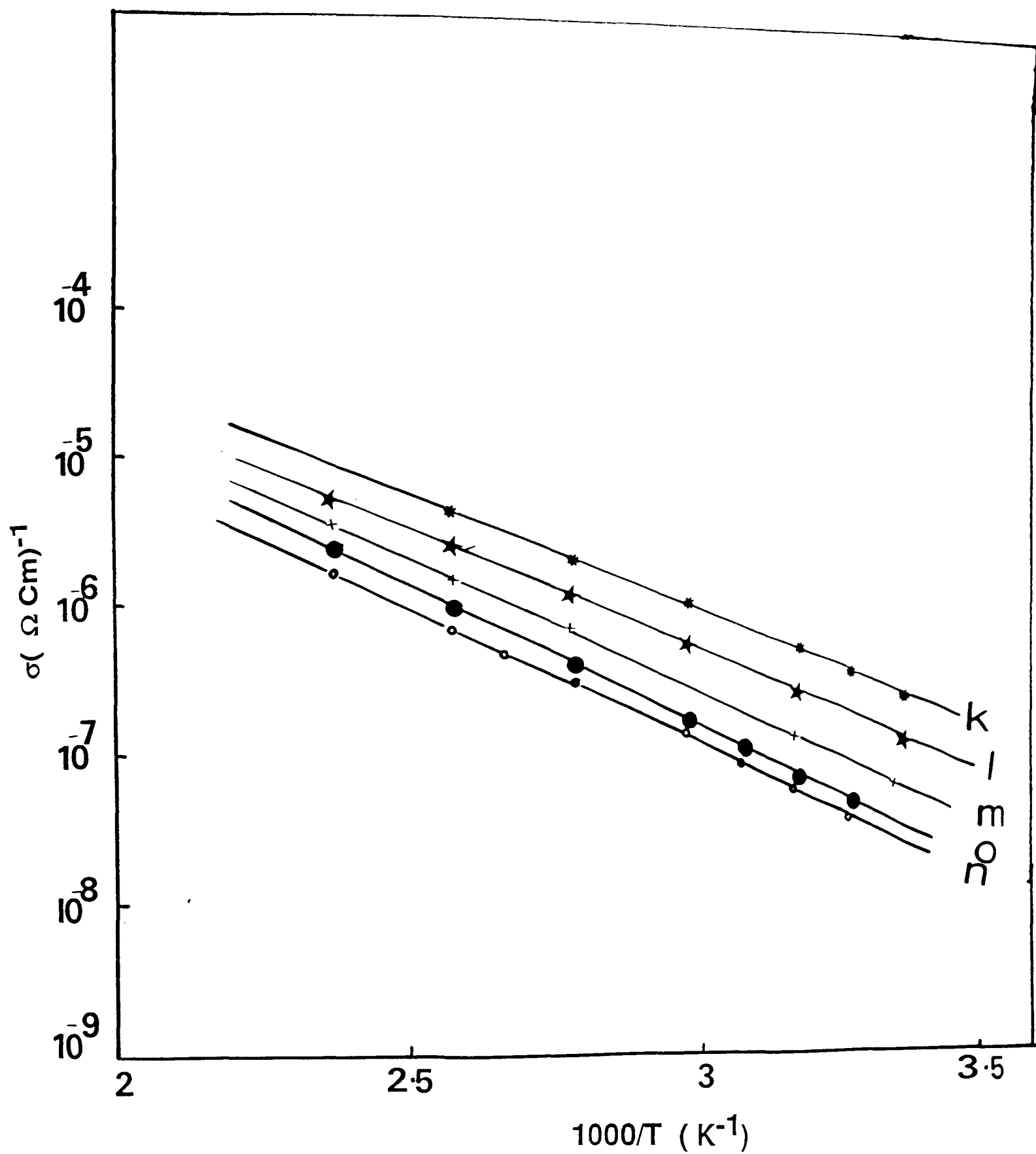
- 1-Centre electrode**
- 2-Guard ring**
- 3-Bottom electrode**



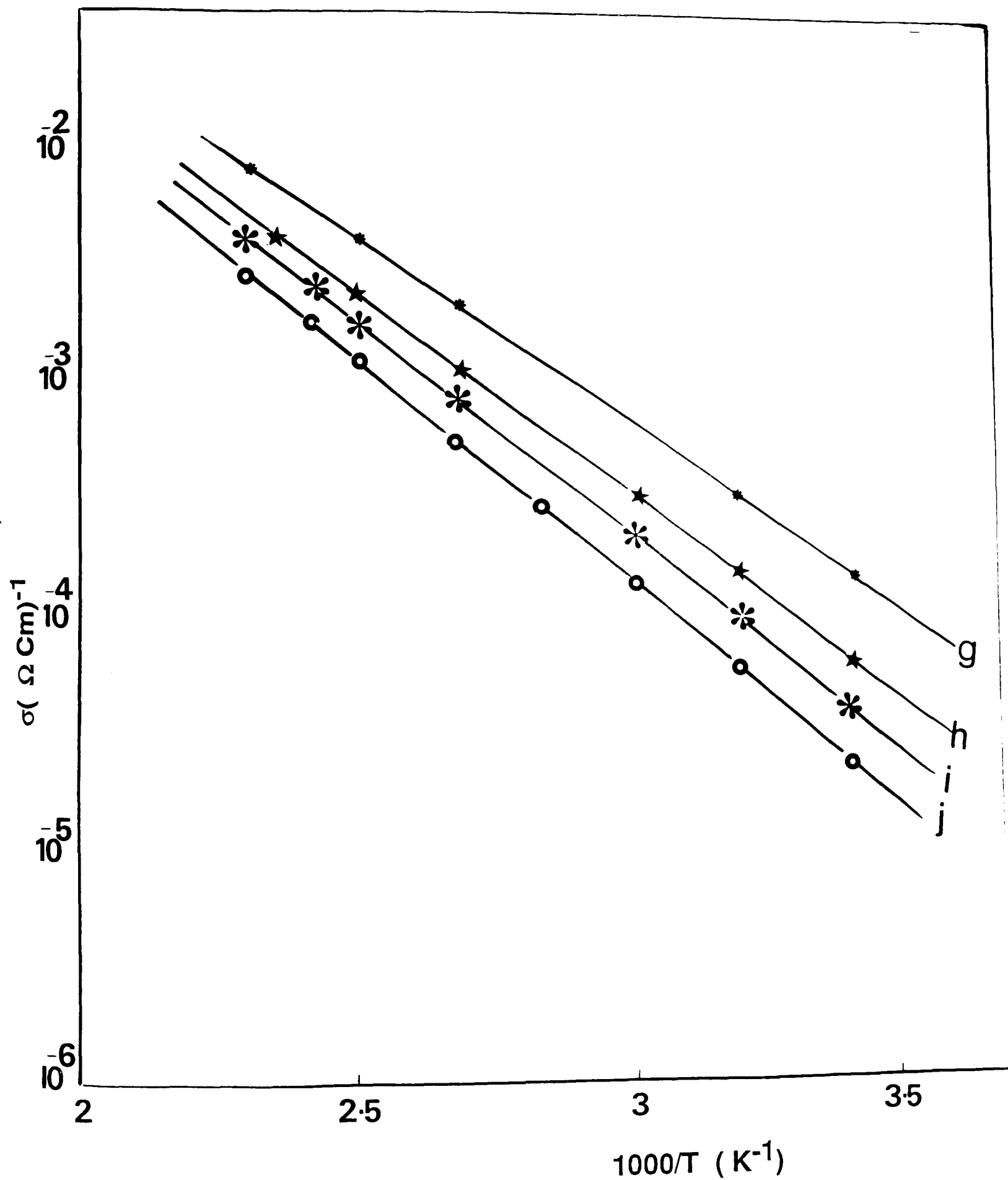
Figure(6.4)-Sample holder used for electrical conductivity at high temperature.



Figure(6.5)- Electrical conductivity as a function of reciprocal temperature for  $\text{V}_2\text{O}_5$ - BaO-  $\text{BaCl}_2$  glasses.

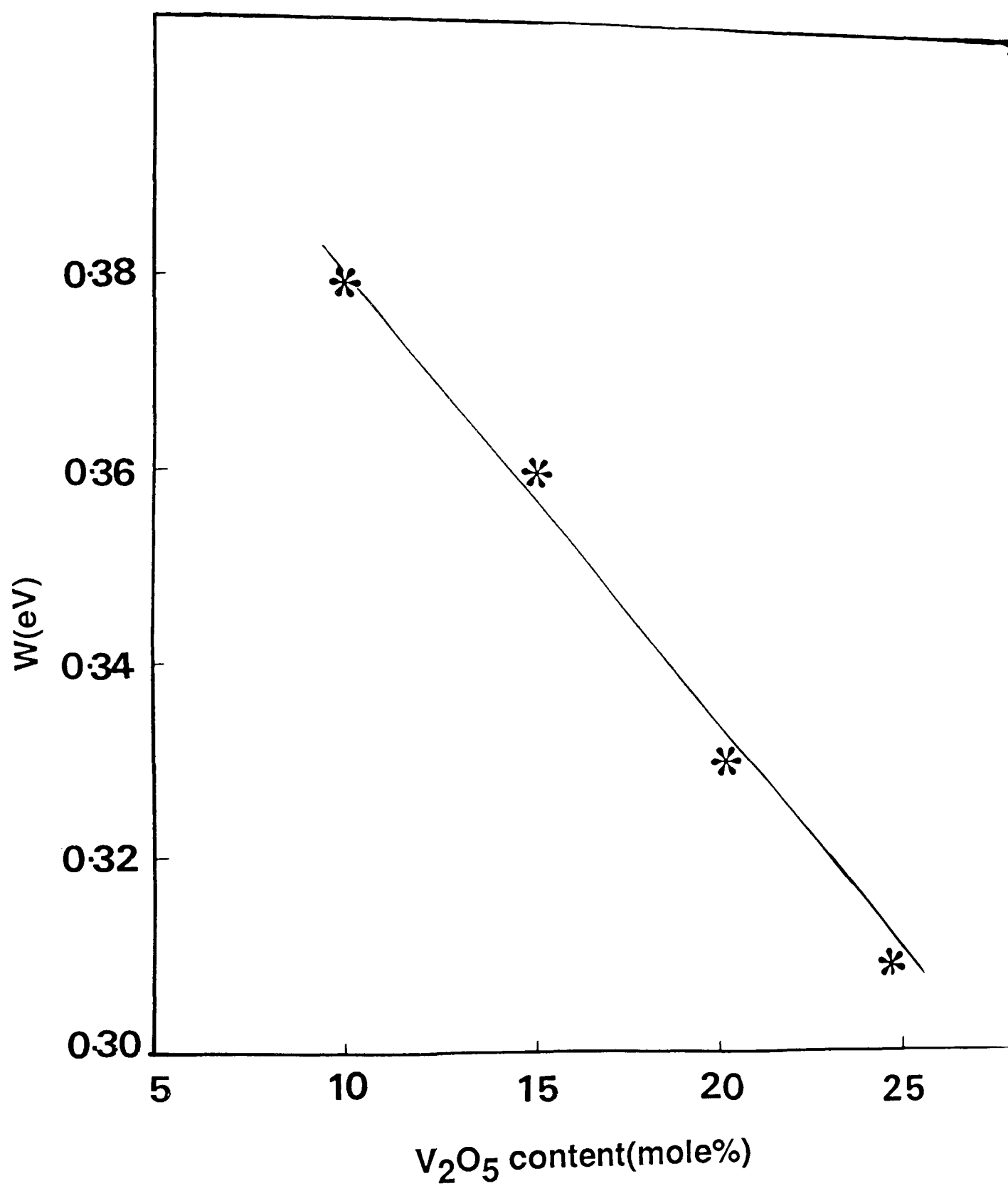


Figure(6.6)- Electrical conductivity as a function of reciprocal temperature for  $\text{TeO}_2\text{-BaO-BaCl}_2$  glasses.

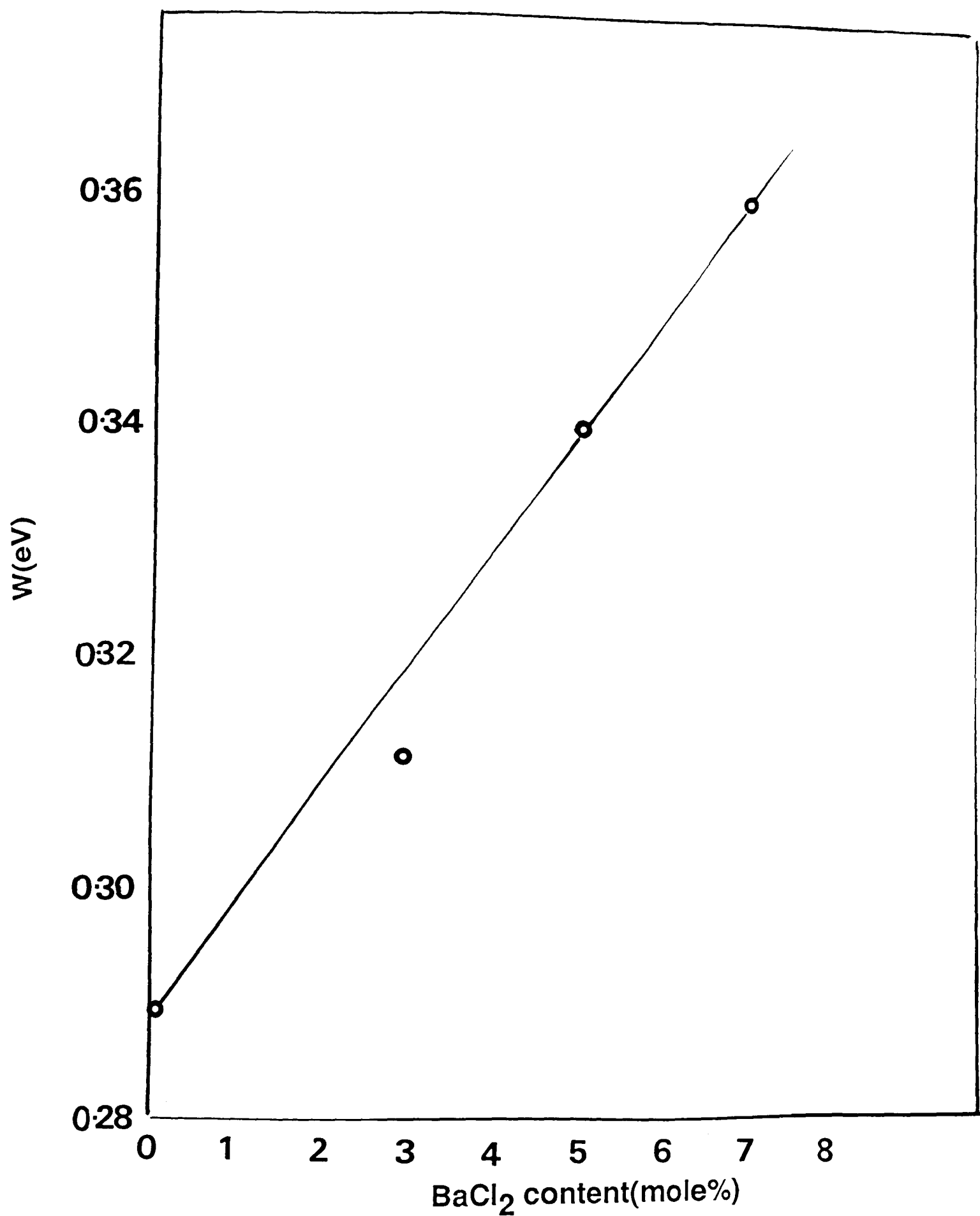


Figure(6.7)- Electrical conductivity as a function of reciprocal temperature for  $\text{TeO}_2\text{-BaO-V}_2\text{O}_5$  glasses.

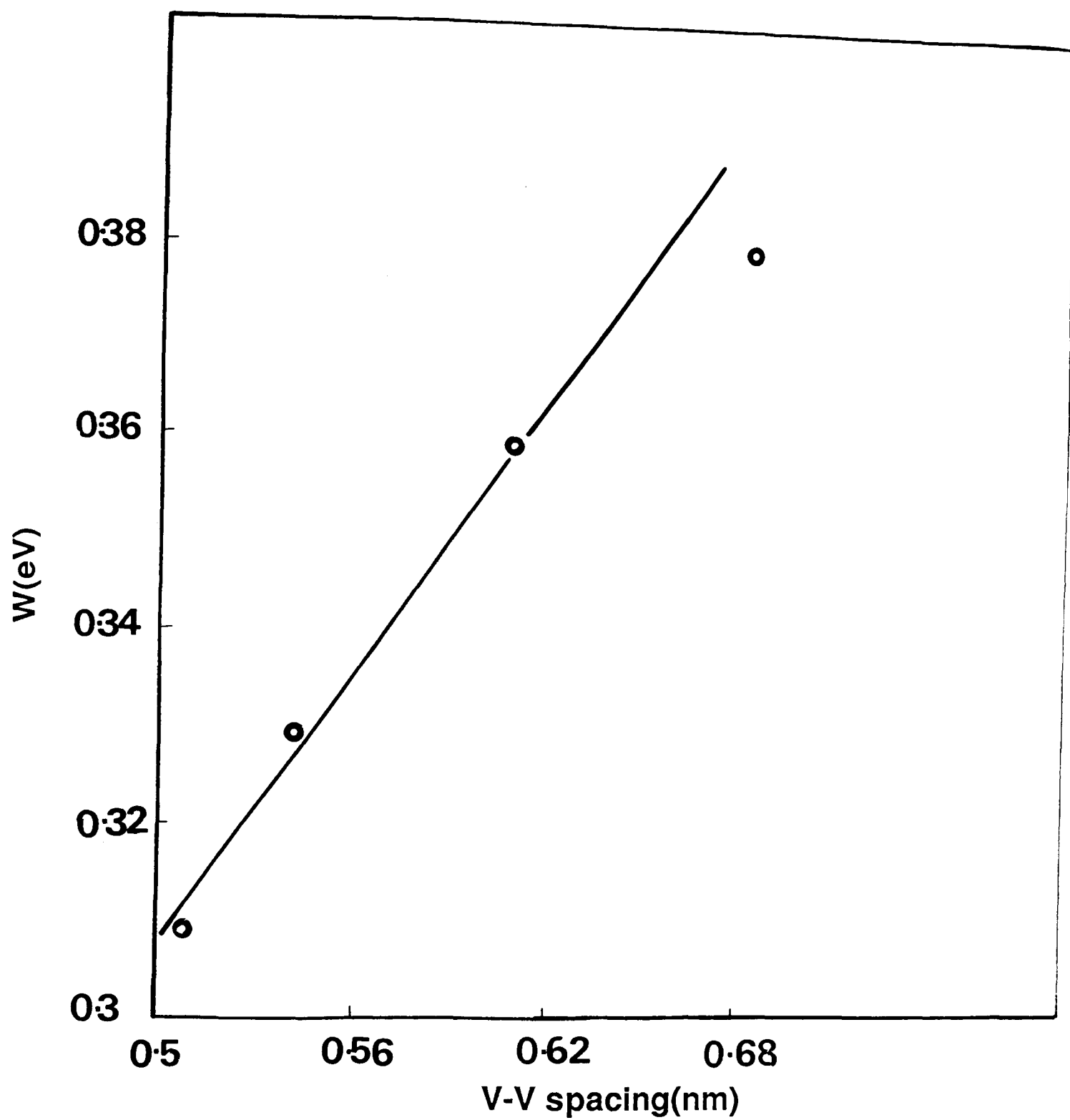




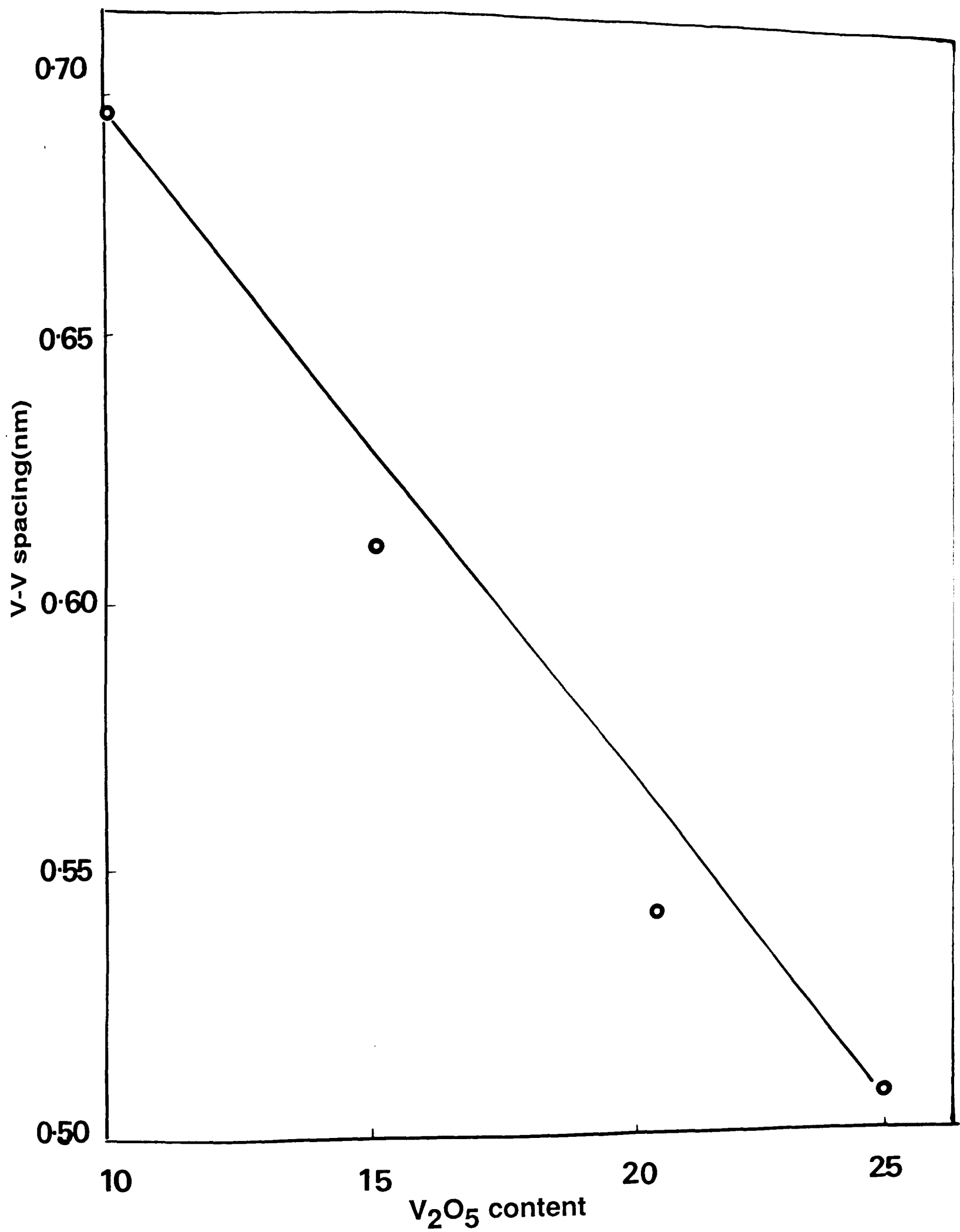
Figure(6.8)-Activation energy of  $TeO_2$ - $BaO$ - $V_2O_5$  glasses as a function of  $V_2O_5$  content.



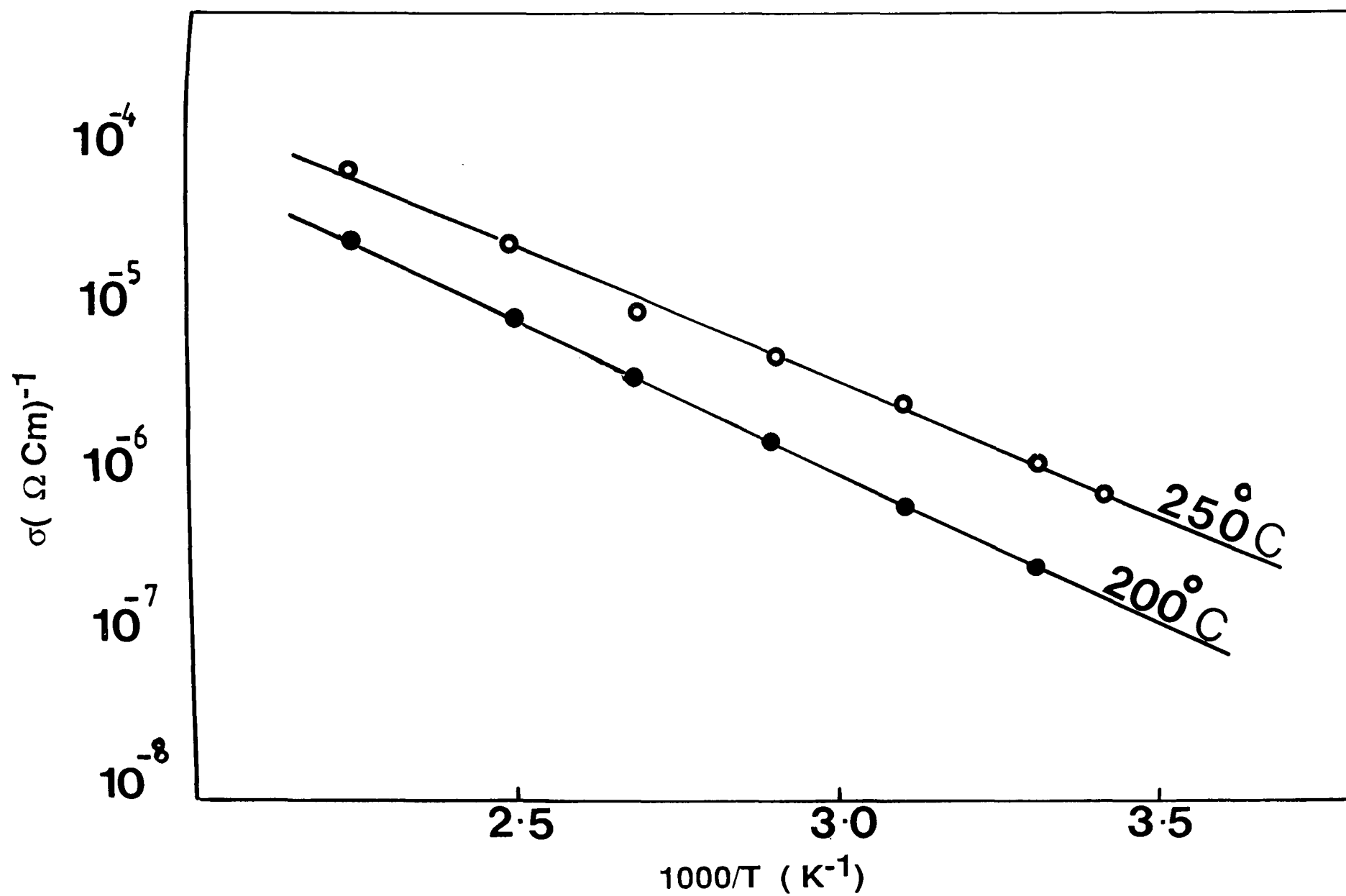
Figure(6.9)-Activation energy of  $\text{TeO}_2$ - $\text{BaO}$ - $\text{BaCl}_2$  glasses as a function of  $\text{BaCl}_2$  content .



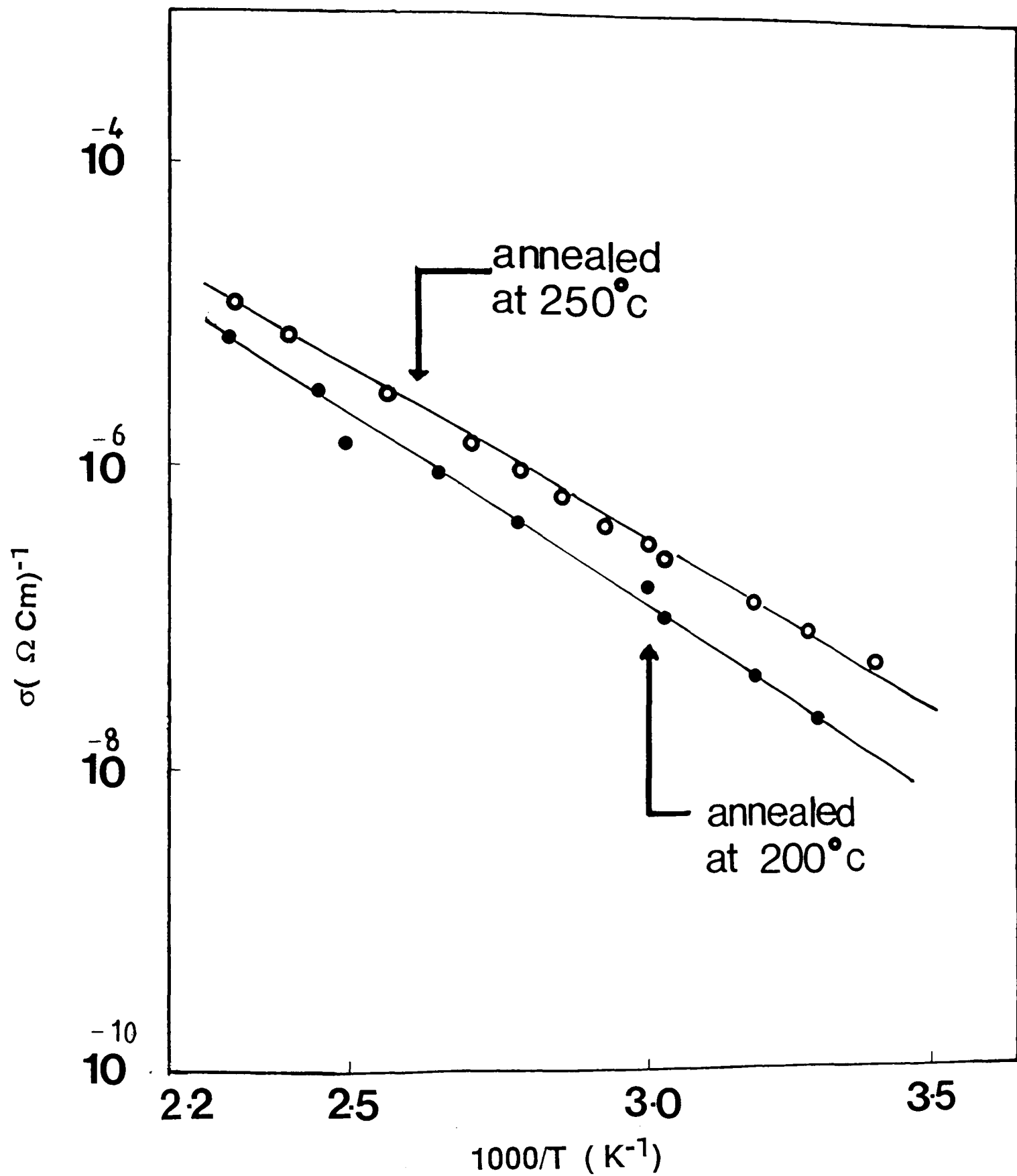
Figure(6.10)Activation energy as a function of V-V spacing(nm).



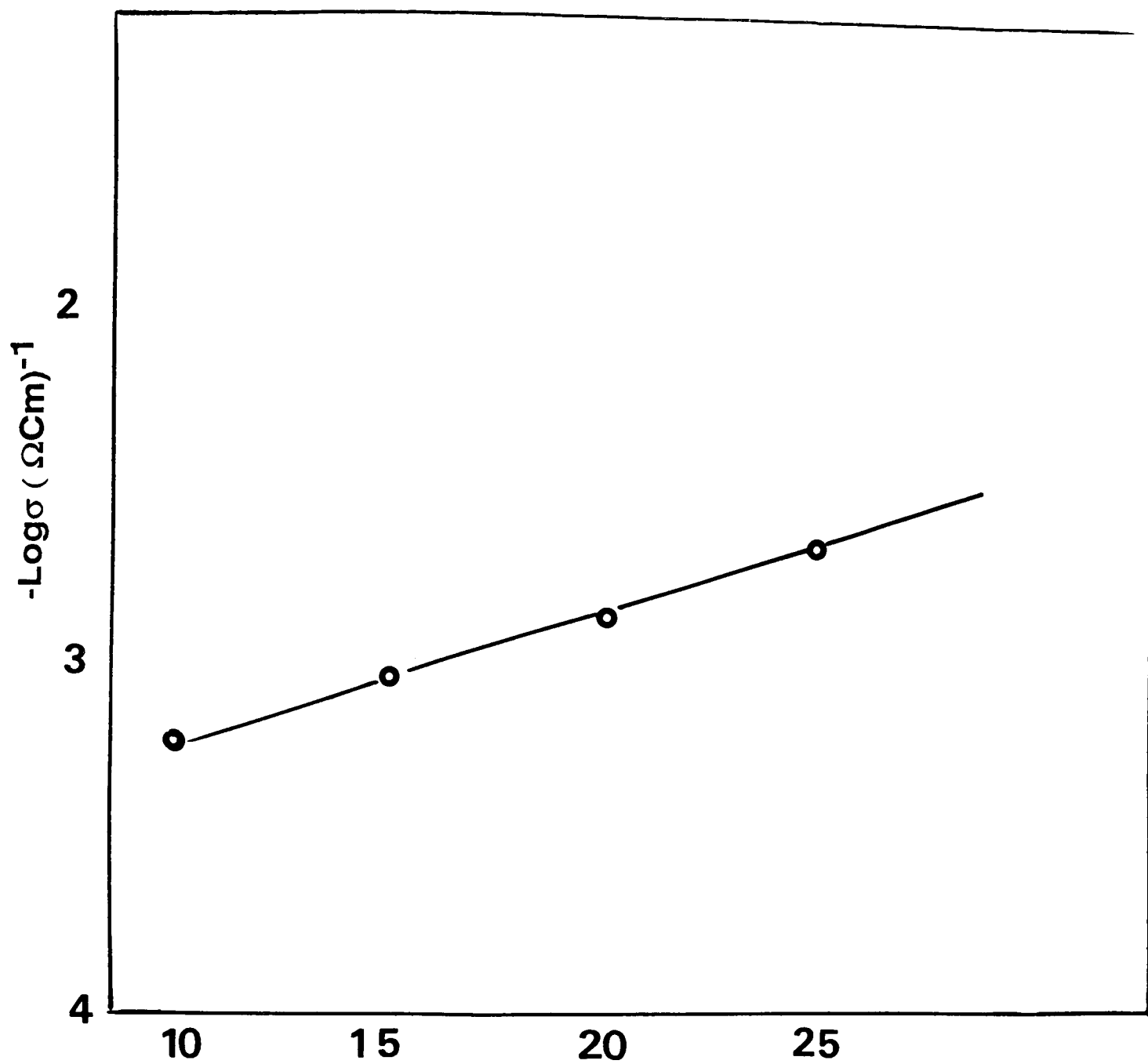
Figure(6.11)-The variation V-V spacing as a function of vanadium content in TeO<sub>2</sub>-BaO-V<sub>2</sub>O<sub>5</sub> glasses.



Figure(6.12)- Electrical conductivity as a function of reciprocal temperature for 65%  $\text{V}_2\text{O}_5$ -25%  $\text{BaO}$ -10%  $\text{BaCl}_2$  glasses, annealed for 2 hours at  $200^\circ\text{C}$  and  $250^\circ\text{C}$ .

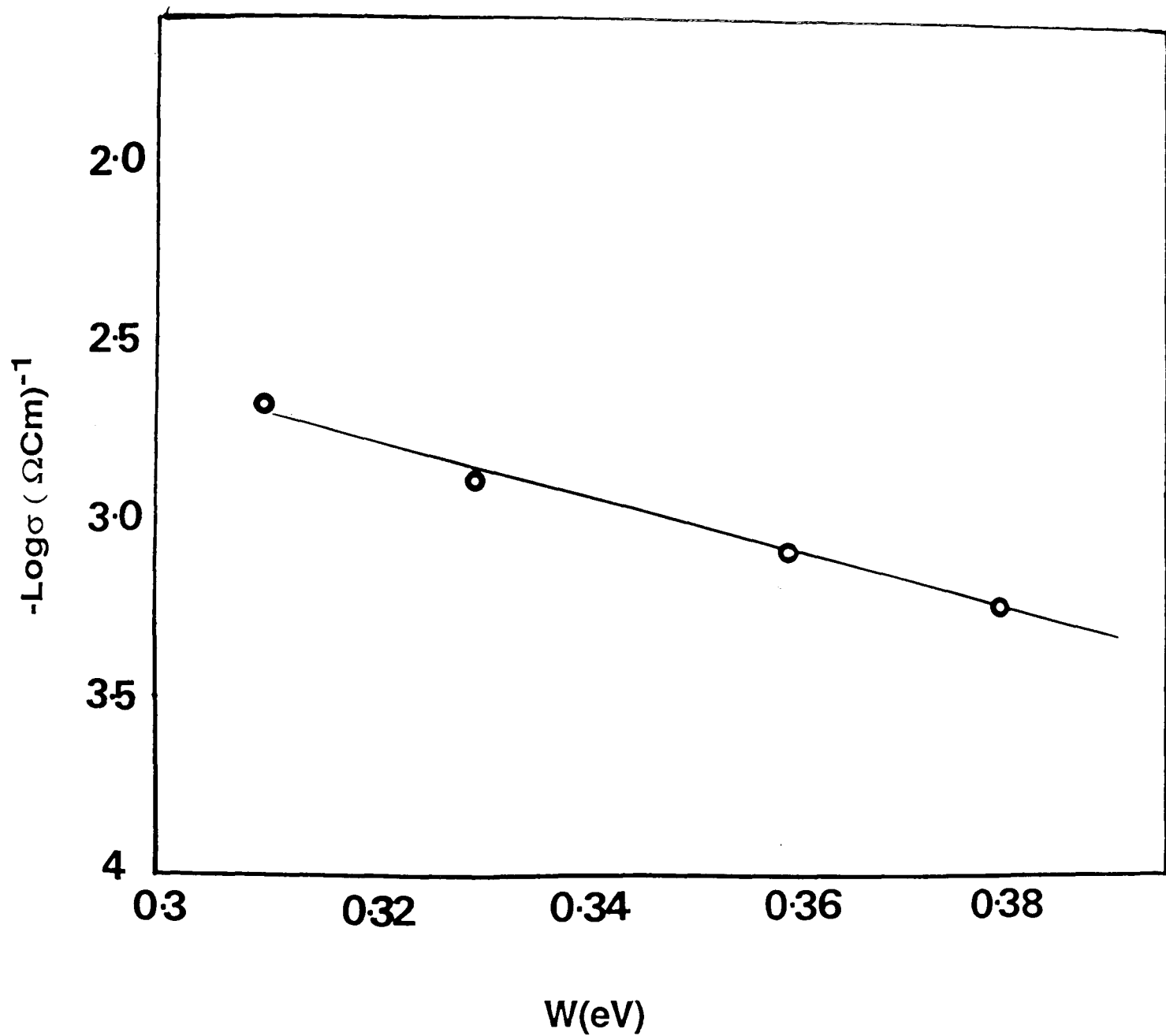


Figure(6.13)- Electrical conductivity as a function of reciprocal temperature for 65%  $\text{V}_2\text{O}_5$ -28%  $\text{BaO}$ -7%  $\text{BaCl}_2$  glasses, annealed



$\text{V}_2\text{O}_5$  content(mole%)

Figure(6.14)-Logarithmic plot of conductivity against  $\text{V}_2\text{O}_5$  content for  $\text{TeO}_2\text{-BaO-V}_2\text{O}_5$  glasses(conductivity measured at  $100^\circ\text{C}$ ).



Figure(6.15)-Logarithmic plot of conductivity against high temperature activation energy for  $\text{TeO}_2\text{-BaO-V}_2\text{O}_5$  glasses (conductivity measured at  $100^\circ\text{C}$ ).